Coral Reef Ecosystem Monitoring Report For The Pacific Remote Islands Marine National Monument

2000–2017

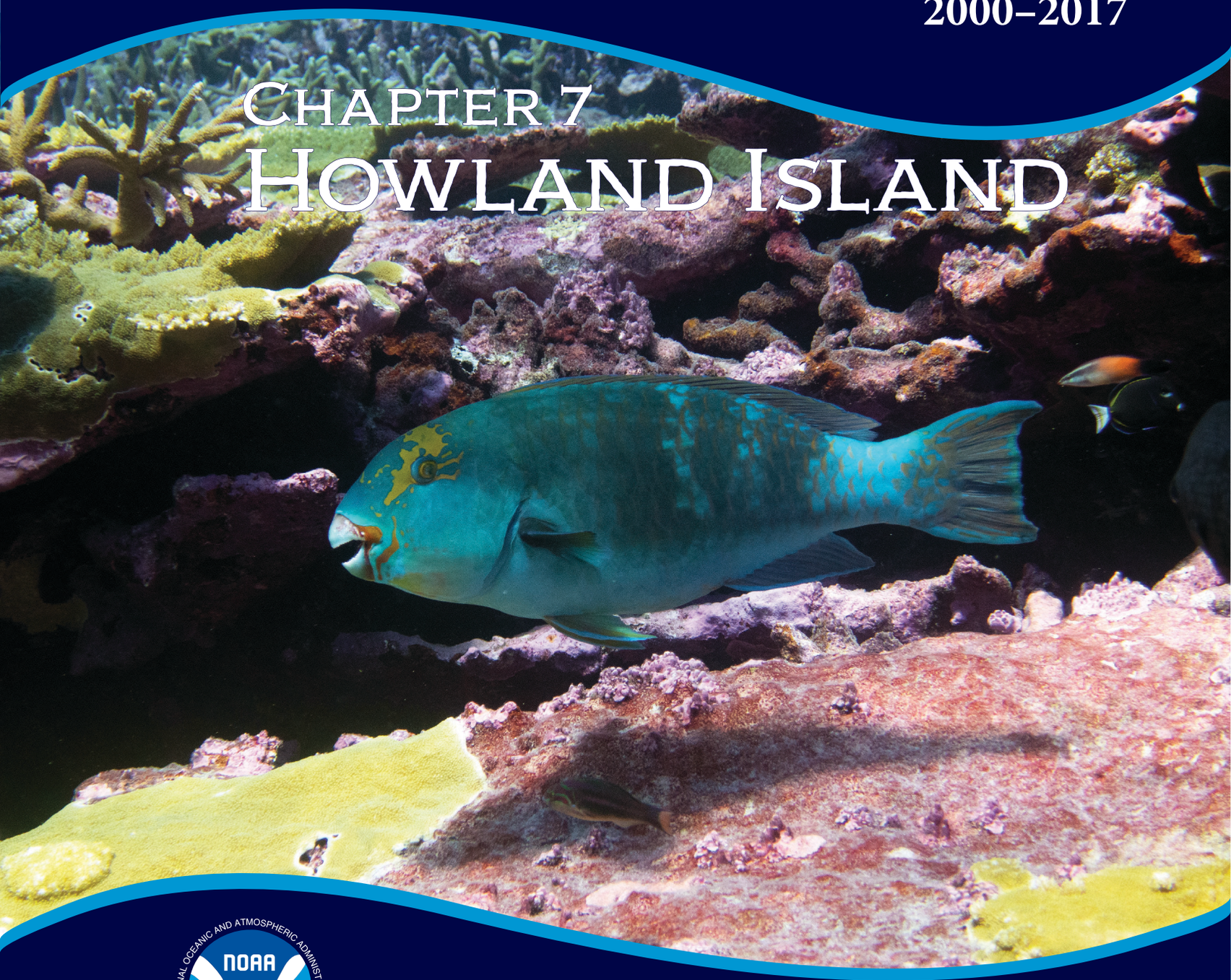

Chapter 7
Howland Island

NOAA FISHERIES

Ecosystem Sciences Division

Pacific Islands Fisheries Science Center

Coral Reef Ecosystem Monitoring Report for the Pacific Remote Islands Marine National Monument 2000–2017

Chapter 7: Howland Island

Authors

Brainard, Russell E.[1]; Acoba, Tomoko[2]; Asher, Megan A.M.[2]; Asher, Jacob M.[2]; Ayotte, Paula M.[2]; Barkley, Hannah C.[2]; DesRochers, Annette[2]; Dove, Dayton[2]; Halperin, Ariel A.[2]; Huntington, Brittany[2]; Kindinger, Tye L.[2]; Lichowski, Frances[2]; Lino, Kevin C.[2]; McCoy, Kaylyn S.[2]; Oliver, Thomas[1]; Pomeroy, Noah[2]; Suka, Rhonda[2]; Timmers, Molly[2]; Vargas-Ángel, Bernardo[2]; Venegas, Roberto M.[2]; Wegley Kelly, Linda[3]; Williams, Ivor D.[1]; Winston, Morgan[2]; Young, Charles W.[2]; Zamzow, Jill[2]

[1]National Oceanic and Atmospheric Administration, Pacific Islands Fisheries Science Center
[2]University of Hawaii, Joint Institute for Marine and Atmospheric Research
[3]San Diego State University

PIFSC Special Publication SP-19-006g
2019

United States Department of Commerce, National Oceanic and Atmospheric Administration, National Marine Fisheries Service, Pacific Islands Fisheries Science Center

NOAA Inouye Regional Center
Attn: NMFS/PIFSC/Ecosystem Sciences Division
1845 Wasp Boulevard, Building 176
Honolulu, Hawaii 96818 U.S.A.

This report is a deliverable for the NOAA Coral Reef Conservation Program's National Coral Reef Monitoring Program (NCRMP) Data, Reports, and Information Products for Management, Project ID 31186. It also contributed to the NOAA Pacific Islands Fisheries Science Center (PIFSC) Milestone P19-ESD-05 and PIFSC Accomplishment P19-ESD-36. The data used to generate this report are described in the NOAA Fisheries Enterprise Data Management tool, InPort, at the following link: https://inport.nmfs.noaa.gov/inport/item/53206. In addition, all monitoring data are archived with the NOAA National Centers for Environmental Information and most benthic habitat mapping data and products are available on the PIFSC Ecosystem Sciences Division's Pacific Islands Benthic Habitat Mapping Center website, unless otherwise specified in the InPort record.

Citations

This report as a whole may be referenced in the following manner:

Brainard RE, Acoba T, Asher MAM, Asher JM, Ayotte PM, Barkley HC, DesRochers A, Dove D, Halperin AA, Huntington B, Kindinger TL, Lichowski F, Lino KC, McCoy KS, Oliver T, Pomeroy N, Suka R, Timmers M, Vargas-Ángel B, Venegas RM, Wegley Kelly L, Williams ID, Winston M, Young CW, Zamzow J (2019) Coral Reef Ecosystem Monitoring Report for the Pacific Remote Islands Marine National Monument 2000–2017. Pacific Islands Fisheries Science Center, PIFSC Special Publication, SP-19-006. 820 p.

This chapter may be referenced in the following manner:

Brainard RE, Acoba T, Asher MAM, Asher JM, Ayotte PM, Barkley HC, DesRochers A, Dove D, Halperin AA, Huntington B, Kindinger TL, Lichowski F, Lino KC, McCoy KS, Oliver T, Pomeroy N, Suka R, Timmers M, Vargas-Ángel B, Venegas RM, Wegley Kelly L, Williams ID, Winston M, Young CW, Zamzow J (2019) Chapter 7: Howland Island. In: Coral Reef Ecosystem Monitoring Report for the Pacific Remote Islands Marine National Monument 2000–2017. Pacific Islands Fisheries Science Center, PIFSC Special Publication, SP-19-006g. 93 p. doi:10.25923/7k72-t460

For more information or to download a copy of this publication:

http://go.usa.gov/xpRRx

Front Cover: Parrotfish (*Chlorurus frontalis*) at Howland Island. Photo: Jacob Asher, NOAA Fisheries.

Back Cover: Butterflyfish (*Chaetodon meyeri)* at Howland Island. Photo: Ariel Halperin, NOAA Fisheries.

Table of Contents

Executive Summary

The work presented within the *Coral Reef Ecosystem Monitoring Report for the Pacific Remote Islands Marine National Monument 2000–2017* is a direct result of nearly 20 years of research in the U.S. Pacific Remote Islands Marine National Monument (PRIMNM) conducted over hundreds of field days aboard National Oceanic and Atmospheric Administration (NOAA) ships by dozens of contributors from NOAA, University of Hawaii–Joint Institute for Marine and Atmospheric Research, and partner scientists. For their efforts, we are eternally grateful and appreciative of their work.

Here, we examine seven islands and atolls within the PRIMNM, using a variety of methods across multiple disciplines in order to gauge how these unique ecosystems have fared through time. In brief, this report describes and highlights the spatial patterns and temporal trends of marine ecosystems associated with Johnston Atoll, Howland Island, Baker Island, Jarvis Island, Palmyra Atoll, Kingman Atoll, and Wake Atoll, along with cross-comparative assessments among the islands, reefs, and atolls of the PRIMNM and other island areas of the U.S. Pacific Islands region in "Chapter 9: Pacific Remote Islands Marine National Monument in the Pacific-wide Context."

Each island, reef, and atoll chapter, along with the Pacific-wide chapter, is constructed as follows: Introduction, Benthic Characterization, Ocean and Climate Variability, Coral Reef Benthic Communities, Cryptofauna Biodiversity (in the Pacific-wide chapter only), Microbiota, Reef Fishes, Marine Debris, and Ecosystem Integration.

Key Findings

- Given the wide geographic extent and large variance in oceanographic conditions experienced across the PRIMNM, it is more informative to consider the PRIMNM as three groupings: the northernmost oligotrophic islands of Johnston and Wake Atolls, the central transition islands of Kingman Reef and Palmyra Atoll, and the equatorial upwelling islands of Howland, Baker, and Jarvis Islands.
- Due to the combined effects of equatorial and locally-intense topographic upwelling of the eastward-flowing subsurface Equatorial Undercurrent, Jarvis Island, and to a lesser extent Howland and Baker Islands, are subject to noticeably cooler mean sea surface temperatures (SSTs) than their nearest neighbors (Palmyra Atoll and Kingman Reef). The upwelling routinely experienced by these islands further results in the highest chlorophyll *a* (chl-*a*) concentrations and associated biological productivity measured across the PRIMNM. In contrast, the lower chl-*a* concentrations observed at Wake and Johnston Atolls are similar to concentrations within the Mariana Archipelago and American Samoa, which are located in the oligotrophic gyres of the North Pacific and South Pacific.
- Higher aragonite saturation values correspond to the greater availability of carbonate ions, and thus favor the growth of corals, crustose coralline algae, and other marine calcifiers. The PRIMNM's northernmost oligotrophic islands (Johnston and Wake Atolls) retained two of the lowest average carbonate accretion rates in the U.S. Pacific Islands, indicating low reef growth over time.

- Jarvis Island experienced a massive decline in coral cover in response to acute thermal stress associated with the 2015–2016 El Niño warming event; Jarvis has shown no substantial recovery in coral cover since. Coral cover at Baker Island and Kingman Reef also declined from 2015 to 2018, reflecting a 13% decline over 3 years at both islands.
- Calcifiers comprised approximately half of the benthic communities at Howland Island, Kingman Reef, and Baker Island. Despite Jarvis's catastrophic decline in coral cover in 2016, the recent proportion of calcifiers at Jarvis Island remains high, likely due to a marked increase in cover of crustose coralline algae (CCA) observed in 2018.
- Across the PRIMNM, the crown-of-thorns sea star (*Acanthaster planci*, COTS) was consistently observed only at Kingman Reef and Johnston Atoll, though densities at these islands fluctuated across survey years. Localized outbreaks that were synchronized in timing across central Pacific reefs appeared to be genetically independent, rather than spread via the planktonic larvae released from a primary outbreak source.
- Mean reef fish biomass varied by a factor of >15 among all U.S. Pacific islands surveyed. The equatorial upwelling and central transition islands of the PRIMNM were among the islands that retained the highest biomass, especially of piscivores and planktivores, although Wake Atoll was an exception to this trend.
- The PRIMNM has also been notable for supporting larger abundances of species listed by the Endangered Species Act (ESA), including the greatest densities of the green sea turtle (*Chelonia mydas*) observed in the U.S. Pacific.

Scientists are increasingly recognizing the magnitude of ongoing and projected effects from global warming and ocean acidification on coral reef ecosystems. As such, this report provides an essential scientific foundation for informed decision making for the long-term conservation and management of the coral reef ecosystems within the PRIMNM. By summarizing trends in ecosystem response across space and time, this report is the first step towards assessing ecosystem resilience and identifying potential underlying drivers that impede or promote such resilience. Understanding these trends can inform the prioritization among candidate areas for management, as well as among the various types of policies and management actions themselves. In conclusion, the individual island, reef, atoll and Pacific-wide comparison chapters give resource managers and policymakers an unprecedented scale of spatial status and temporal trends to examine each ecosystem throughout the PRIMNM, with the hope of protecting and conserving these unique resources for generations to come.

Acknowledgements

We would like to give credit to all National Oceanic and Atmospheric Administration (NOAA) Pacific Islands Fisheries Science Center (PIFSC) and Research Corporation of the University of Hawaii/Joint Institute for Marine and Atmospheric Research (JIMAR) scientists and staff, and the numerous partners who provided support to the Pacific Reef Assessment and Monitoring Program (Pacific RAMP) during 2000–2017, and contributed to the development of this report. We extend a special thanks to the officers and crews from the NOAA Ships *Townsend Cromwell*, *Oscar Elton Sette*, and *Hi'ialakai* who provided field support for the Pacific RAMP surveys. We further express our sincere appreciation to PIFSC, JIMAR, the NOAA Coral Reef Conservation Program (CRCP), and Pacific Islands Regional Office (PIRO) for funding and providing collaborative resources throughout these efforts.

We specifically acknowledge Malia Chow as PIRO branch chief for the Essential Fish Habitat-Pacific Marine National Monuments, along with PIRO's Heidi Hirsh and Richard Hall for their collaboration, reviews, and inputs throughout this report's genesis, along with their participation in associated workshops. We would like to recognize the United States Fish and Wildlife Service Pacific Islands Refuges and Monuments Office for their partnership throughout Pacific RAMP history and their participation in the workshops associated with the report. In addition, we appreciate their reviews and those of PIRO interns, Jesi Bautista and Savannah Smith of Kupu Hawaii, who collectively provided valuable inputs toward the "History and Human Influences" sections for each island, reef, and atoll chapter. We further extend our thanks to the United States Air Force, 611th CES/CEIE, Joint Base Pearl Harbor, Hawaii for their collaborative efforts at Wake Atoll and inputs toward the report and at workshops.

We would like to recognize PIFSC Editorial Services, in particular, Jill Coyle, Katie Davis, and Hoku Johnson for their inputs throughout the editorial process, Donald Kobayashi, PIFSC, for his extensive time and insights in conducting chapter technical reviews, and PIFSC Director Michael Seki and PIFSC ESD Director Frank Parrish for their support and reviews. In addition, we wish to express our gratitude to the CRCP Coral Reef Information System and JIMAR data managers for their efforts to manage and make Pacific RAMP data publicly accessible and compliant with the Public Access to Research Results requirements.

Lastly, we are appreciative of Tom Hourigan and Dale Brown of NOAA Fisheries, two of the earliest visionaries in the establishment of the first Pacific long-term, integrated ecosystem-based monitoring program.

PIFSC has been fortunate to work with many partners who contributed to Pacific RAMP and associated efforts, and while this list is by no means comprehensive, we sincerely thank each and every one of you. Your contributions helped make this report possible, and as a result, we have collectively provided valuable inputs to the management and conservation of the coral reef ecosystems of the Pacific Remote Islands Marine National Monument.

Coral Reef Ecosystem Monitoring Report for the Pacific Remote Islands Marine National Monument 2000–2017

Chapter 7: Howland Island

NOAA drop-off of a U.S. Fish and Wildlife Service field team at Howland Island with sign and Earhart Light day beacon (named after Amelia Earhart) in the background. Photo: Tate Wester, NOAA Fisheries.

7.1 Introduction

Report Overview

The *Coral Reef Ecosystem Monitoring Report for the Pacific Remote Islands Marine National Monument 2000–2017* provides an overview of key spatial patterns and temporal trends of the environmental and oceanographic conditions, biological resources, and composition of coral reef ecosystems across the seven islands, atolls, and reefs of the Pacific Remote Islands Marine National Monument (PRIMNM). The data compiled for this report are from Pacific Reef Assessment and Monitoring Program (Pacific RAMP) research surveys conducted over the period from 2000 through 2017, by the National Oceanic and Atmospheric Administration (NOAA) Pacific Islands Fisheries Science Center (PIFSC) Ecosystem Sciences Division (ESD) and external collaborating scientists.

This report represents one of many installments of ESD's ongoing efforts to bring resource managers and interested stakeholders the best available, ecosystem-based data to help them make informed decisions about the sustainable use and conservation of the resources they manage, in this case, coral reef ecosystem in the PRIMNM. The information herein serves three main purposes:

- Provide snapshots of the status and condition of coral reef resources around each of the islands, atolls, and reefs in the PRIMNM over the course of the survey periods.
- Provide a foundation of knowledge regarding ecosystem conditions in the PRIMNM for ongoing monitoring of temporal changes to the ecosystem.
- Serve as a resource for stakeholders and resource managers for understanding marine areas of interest and formulating evolving management questions about how to best manage and conserve marine resources in the face of climate and ocean changes.

The report consists of nine chapters. In addition, attached to "Chapter 9: Pacific Remote Islands Marine National Monument in the Pacific-wide Context" are Appendix A, "Total Generic Richness of Hard Corals in the PRIMNM," and Appendix B, "Reef Fish Encounter Frequency in the PRIMNM." For more background information on the report as a whole, operational background, Pacific RAMP methods, and Public Access to Research Results, refer to "Chapter 1: Overview."

Chapter Overview

Howland Island is a small 4.50 km^2 (1,112 acres), uninhabited coral island, of the Phoenix Islands group, located just north of the equator in the central equatorial Pacific Ocean at 0°48′N, 176°36′W. Made up of a coral reef platform on top of a Cretaceous volcano, approximately 120–75 million years old (Hein et al. 2005), Howland Island has 6.4 km (4 miles) of low-lying, sandy coastline and is surrounded by a narrow fringing reef with a slightly raised central area and no lagoon (Figure 1). The highest point is about six meters above sea level with no remaining man-made features besides a crumbling navigational day beacon.

Figure 1. **Satellite image of Howland Island, October 13, 2011. (© DigitalGlobe Inc. All rights reserved)**

This chapter consists of sections on "Benthic Characterization," "Ocean and Climate Variability," "Coral Reef Benthic Communities," "Microbiota," "Reef Fishes," and "Marine Debris" to assist natural resource managers in making informed decisions relating to Howland Island and its coral reef ecosystems. Information from these sections is then tied together in the "Ecosystem Integration" section at the end of the chapter to provide a better understanding of the interactions and relationships among the various ecosystem components at Howland.

To aid discussions about the spatial patterns of ecological and oceanographic observations that appear throughout this chapter, four geographic regions, hereafter referred to as georegions, were defined for Howland Island (Figure 2). Most map-based figures throughout this chapter use the basemap template as shown in Figure 2, which includes georegions, land, and the 30 m and 100 m depth contours (isobaths).

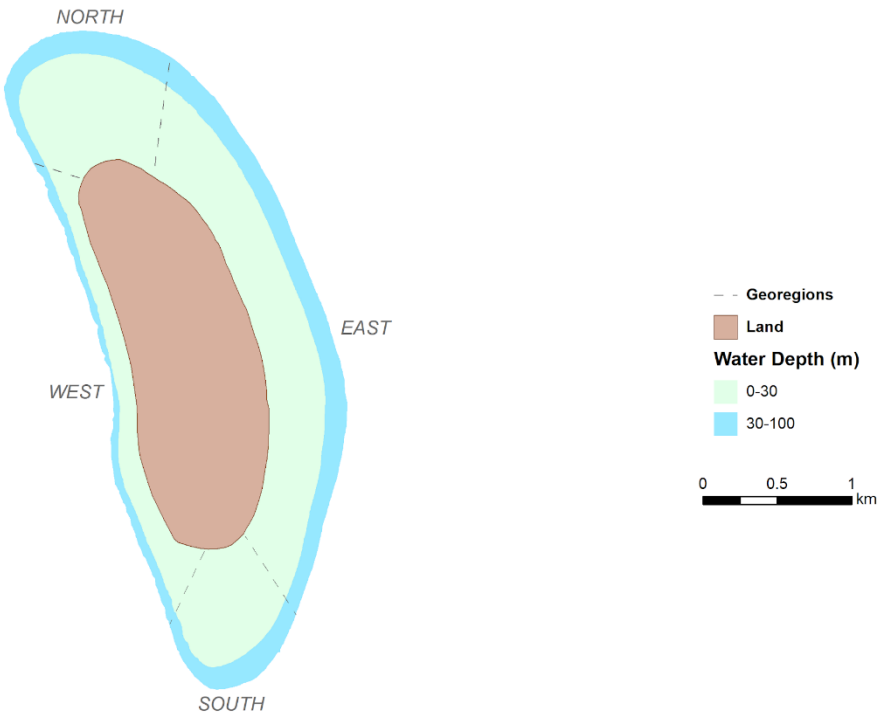

Figure 2. The four geographic regions, or georegions, for Howland Island: North, South, East, and West.

History and Human Influences

Sparse remnants were found on Howland Island, including a canoe, relics, excavations, trails, and other artifacts that indicate early Polynesian presence. Several American whaling ships hunting in the area sighted and charted the island as early as 1822. In 1842, Captain George E. Netcher, aboard the New Bedford whaleship *Isabella,* named the island Howland. Captain Netcher then formed the United States (U.S.) Guano Company and sent a vessel to exploit the guano on Howland in 1859 under the U.S. Guano Islands Act of 1856. However, the American Guano Company (mining guano on nearby Baker and Jarvis Islands) was already in operation on Howland and occupied the island before the United States Guano Company could take formal possession. In 1865, the dispute between the two companies was settled in court and both companies were allowed to mine the island's guano. These guano-mining enterprises ended in 1878, when the deposits were depleted.

In 1935, colonists from the American Equatorial Islands Colonization Project, also called the Hui Panala'au Project, arrived on the island to establish a permanent United States presence in the Central Pacific. The Project began with a rotating group of four male alumni and students from the Kamehameha School in Honolulu, Hawaii (Kamehameha Schools 2014). The recruits had signed on as part of a scientific expedition and were expected to spend their 3-month assignment collecting botanical and biological samples. A settlement named Itascatown, after the U.S. Coast Guard Cutter *Itasca,* was formed on Howland. The colonists of Itascatown made regular trips between the other equatorial islands during that era. Itascatown consisted of a half-dozen small, wood-framed structures and tents near the beach on the island's western side.

Ground was cleared for a rudimentary aircraft landing area during the mid-1930s, in anticipation of a stopover for commercial trans-Pacific air routes and to further U.S. territorial claims in the region. In 1937, three unpaved runways were built and prepped for Amelia Earhart so she could use Howland Island as a refueling station on her quest to circumnavigate the globe. The colonists also built the Earhart Light as a day beacon or navigational landmark. Unfortunately, Earhart and navigator Fred J. Noonan never reached Howland.

A Japanese air attack on December 8, 1941 killed two of the colonists and damaged the three airstrips. A Japanese submarine and bomber airplane later shelled what was left of the colony's few buildings into ruins. The two Hui Panala‘au Project survivors were finally evacuated by the U.S.S. *Helm* in 1942. Howland Island was then occupied by a battalion of the U.S. Marine Corps from 1943 until May 1944. No aircraft is known to have ever landed at Howland, and all attempts at habitation were abandoned after 1944.

In 1974, Howland Island National Wildlife Refuge was established and included the land, waters, as well as submerged and emergent lands, from the mean low tide water lines out to 3 nm. In 2009, President George W. Bush established the PRIMNM to protect and preserve the marine environment from 0 to 50 nm around Baker, Howland, and Jarvis Islands, Wake, Johnston, and Palmyra Atolls, and Kingman Reef, for the proper care and management of the historic and scientific objects therein (Federal Register 2009). As part of the PRIMNM designation, the Refuge boundaries were extended to include the waters and submerged lands from 0–3 nm to 12 nm. The monument waters and submerged and emergent lands from 0 to 50 nm are cooperatively managed by the U.S. Fish and Wildlife Service and NOAA.

The island habitat has suffered from the presence of multiple invasive exotic species. One of the first was the Polynesian rat, introduced in 1854 and eradicated in 1983 by feral cats introduced the year before. The cats were then eradicated by humans in 1986 due to their destructive predation on the island’s seabird and shorebird species (US Fish and Wildlife Service 2018).

Geology and Environmental Influences

Howland Island has a tropical desert climate that consists of little rainfall and intense equatorial sunshine. Temperatures are moderated by consistent easterly trade winds blowing across relatively cool upwelled waters. There are no natural freshwater resources on Howland. Scattered grasses, vines, low-growing *Pisonia* trees, and shrubs are the only vegetation. Howland is a nesting, roosting, and foraging habitat for seabirds and shorebirds. The waters surrounding Howland are biologically productive due to the combined effects of equatorial upwelling and topographic upwelling as the subsurface Equatorial Undercurrent encounters the western flanks bringing cool, nutrient-rich waters to the nearshore waters around the island.

Healthy reef at Howland Island.
Photo: Kevin Lino, NOAA Fisheries.

Benthic Characterization

7.2 Benthic Characterization

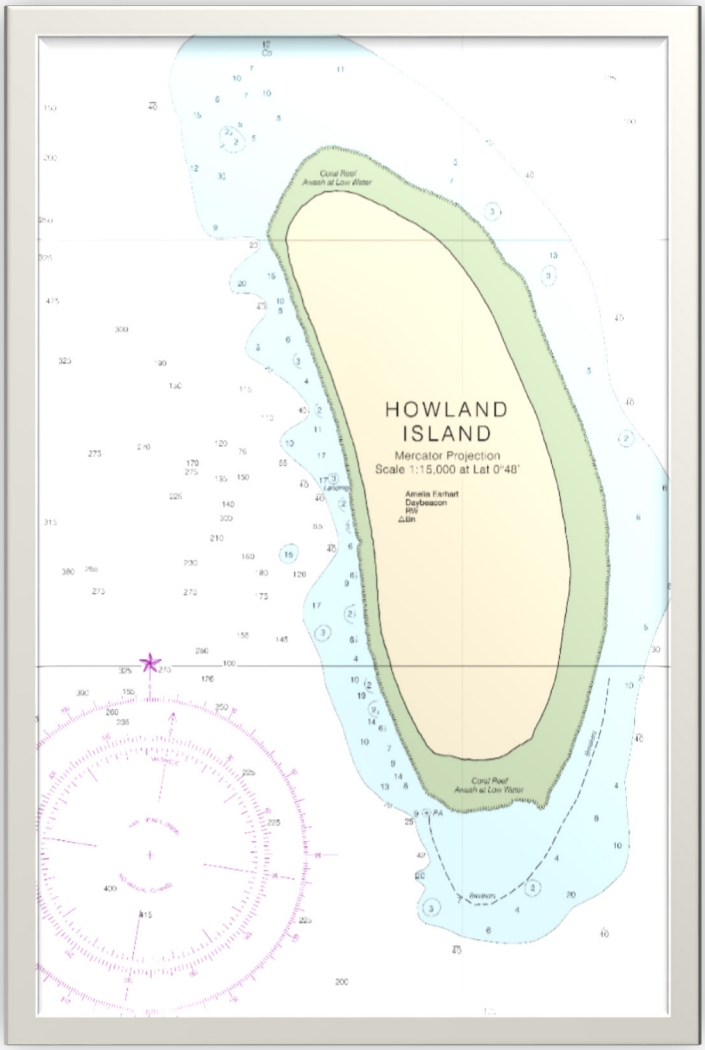

NOAA Nautical Chart of Howland Island.
Source: NOAA, 5th Ed., Sep. 2006.

In this section, the benthic habitats of Howland Island are characterized for the depth range from 0 to 1,000 m using integrated and synthesized data from numerous sources.

Survey Effort

NOAA has been collecting benthic habitat mapping data for the nearshore areas around Howland Island since 2006, using a variety of methods as described in the "Benthic Characterization Methods" section of "Chapter 1: Overview." These methods include multibeam bathymetric and backscatter surveys, single-beam surveys for depth validation, and towed-camera surveys for habitat validation.

Multibeam Surveys

Mapping surveys were conducted around Howland Island during the 2006 Pacific RAMP research cruise using multibeam sonar systems aboard the NOAA Ship *Hi'ialakai* (Simrad EM 300 and EM 3002D) and R/V *AHI* (Reson 8101-ER). Bathymetric and backscatter data were collected for depths between approximately 10 and 4,500 m, and used to derive mapping products covering a total area of approximately 221 km^2. Approximately 1.9 km^2 of the area between 0 and 30 m depths remained unmapped, because the shallower areas around the island were inaccessible to survey with vessel-mounted multibeam systems.

Two of the resulting gridded bathymetric products are a 5 m high-resolution grid of the reefs, banks, shelf, and slope habitats to allow for the identification of fine-scale features to a depth of 300 m and a coarser 40 m mid-resolution grid that includes the full extent of the multibeam bathymetric data collected (Figure 3). The data and supporting documentation are available on the Howland Bathymetry page of the Pacific Islands Benthic Habitat Mapping Center (PIBHMC) website.

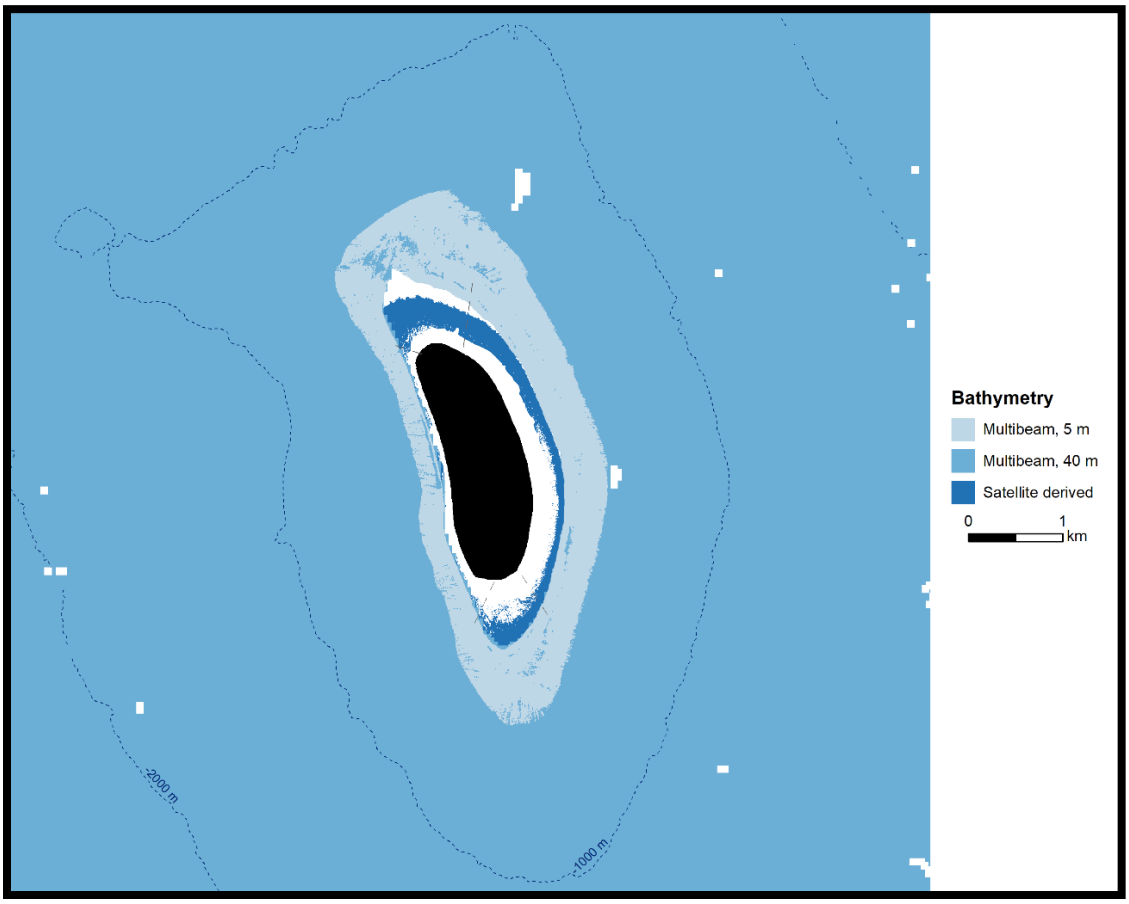

Figure 3. Bathymetric coverage map for Howland Island showing extent of available high- (5 m) and mid-resolution (40 m) gridded multibeam data acquired by Ecosystem Sciences Division (ESD) in 2006 (lighter blues), and estimated bathymetry derived by ESD from satellite imagery (dark blue). The dotted dark blue lines represent 1,000 m interval depth contours. Gaps in bathymetric coverage are shown in white and land features in black. Satellite-derived bathymetry is discussed later in this section.

The backscatter data from the shallower surveys conducted using the R/V *AHI* were gridded at 1 m resolution, while the data from the deeper surveys conducted using the *Hi'ialakai* were gridded at 5 m resolution. Acoustic backscatter intensities reveal characteristics of the seabed around Howland Island that are related to topography and slope. While these data are useful for geomorphology and habitat interpretation, both the shallow and deeper backscatter data have quality issues, including high-noise levels and patchiness in the coverage. The data and supporting documentation are available on the Howland Backscatter page of the PIBHMC website.

Single-beam Surveys

Single-beam sonar data were acquired around Howland Island from depths between 2 and 243 m in 2012, between 2 and 423 m in 2015, and between 1 and 1,179 m in 2017 (Figure 4). As ocean conditions varied each year and new survey equipment was introduced in 2017, the errors associated with the three years of data also varied. Soundings error was found to be significantly greater in 2012 (1.53 m) and 2017 (1.49 m) compared with 2015 (0.26 m); therefore, the data collected in 2012 and 2017 were filtered to exclude depths deeper than 100 m as shown in Figure 4.

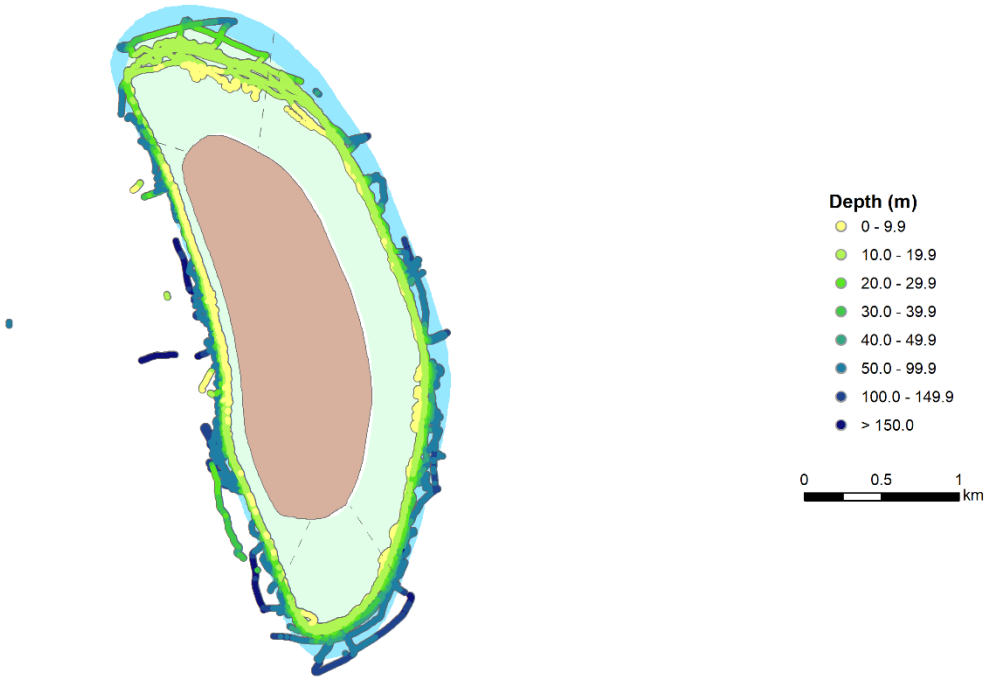

Figure 4. Depth validation data for Howland Island collected by Ecosystem Sciences Division in 2012, 2015, and 2017. Soundings >100 m were excluded from the 2012 and 2017 surveys due to data quality concerns.

Towed-camera Surveys

Habitat validation data in the form of underwater video and still photographs were acquired in the North and South georegions of Howland Island from depths between 20 m and approximately 400 m by ESD in 2002 and 2004 using the towed optical assessment device

(TOAD). A subset of the TOAD images collected was classified into substrate types (e.g., sand, rubble, boulder), biological cover type (e.g., coral, macroalgae, coralline algae), and coral growth morphology (e.g., branching, columnar, encrusting) to produce a map of percent cover for observed scleractinian coral at the image collection point. The data and supporting documentation are available on the Howland Optical Validation page of the PIBHMC website.

Habitat Characterization

Satellite-derived Bathymetry

ESD derived estimated depths from WorldView-2 satellite imagery acquired in 2011 to fill gaps in the nearshore shallow-water bathymetric coverage around Howland Island. Depth soundings collected in 2015 (Figure 4) were used to validate the satellite-derived depths, resulting in 75% average agreement between the overlapping soundings and estimated depths. The data and supporting documentation are available on the Howland Bathymetry page of the PIBHMC website. Though these estimated depths provide useful information for areas with little or no bathymetric measurements, the low depth accuracy limits the use of these data. See Figure 3 for the extent of satellite-derived depths generated by ESD that partially filled the bathymetric coverage gap around Howland.

Integrated Bathymetry

ESD's multibeam bathymetry and satellite-derived depths were combined to produce an integrated bathymetric map for Howland Island (Figure 5).

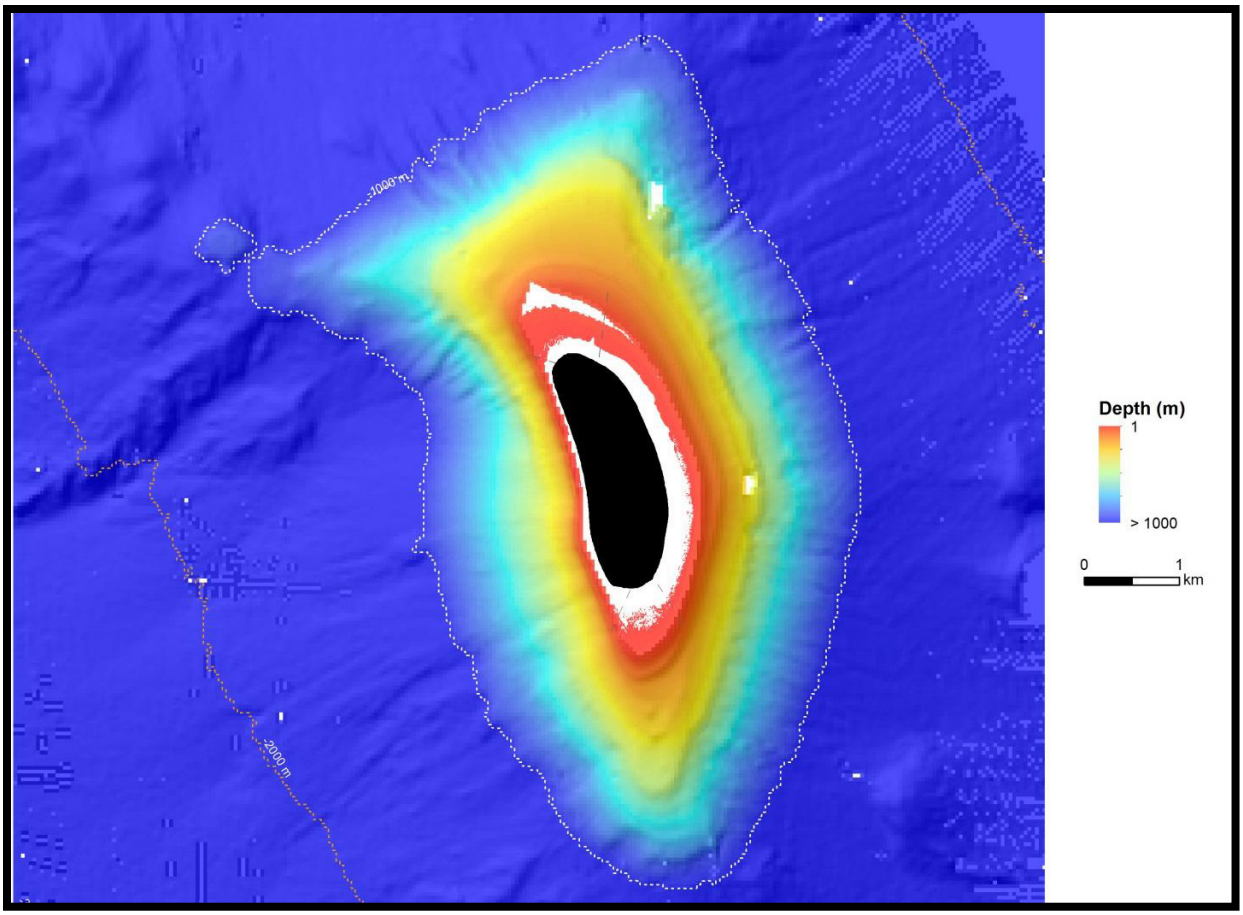

Figure 5. **Integrated bathymetric map showing depths from 0 m to ~1,000 m for Howland Island, with gaps in bathymetric coverage shown in white and land features in black. The dotted lines represent the 1,000 m (white) and 2,000 m (orange) depth contours.**

The bathymetric data around Howland Island's north-south elongated shape are characterized by shallow fringing reefs, extremely steep slopes, and a small terrace system. Both the East and West georegions of the island have near-vertical relief.

Bathymetric Derivatives

Several geomorphological layers derived from ESD's multibeam bathymetric grids were developed for Howland Island, including slope (i.e., the rate of change in elevation between a location and its surroundings, usually expressed in degrees), rugosity (a measure of the roughness or complexity of the seafloor surface), and bathymetric position index (BPI) zones and structures (i.e., a measure of where a location with a defined elevation is relative to the overall landscape, classified into broad scale and fine scale features, respectively). Similar to the bathymetric grids, each of these layers is available as high- (5 m) and mid-resolution (40 m) gridded products on the Howland Seafloor Characterization page of the PIBHMC website. The mid-resolution slope and BPI zones maps are presented here.

Slope

Nearshore 40 m resolution gridded slope values around Howland Island reflect the steep (~30–40°) vertical slopes or drop-offs in the East and West georegions of the island (Figure 6). The narrow forereef terraces located at various depths in the South georegion and along the northeast and northwest rift zones in the North georegion indicate possible previous sea level stands. The North and South georegions show steep drop-offs beyond the small terrace system as well. Mass-wasting features are apparent beyond the 1,000 m isobath around the entire island, especially beyond the East georegion as shown in Figure 6 (Maragos et al. 2008). Mass wasting—also referred to as submarine mass movement—is the structural failure of the seafloor (e.g., from a submarine landslide along a steep slope) that causes mass movement of sediment deposits.

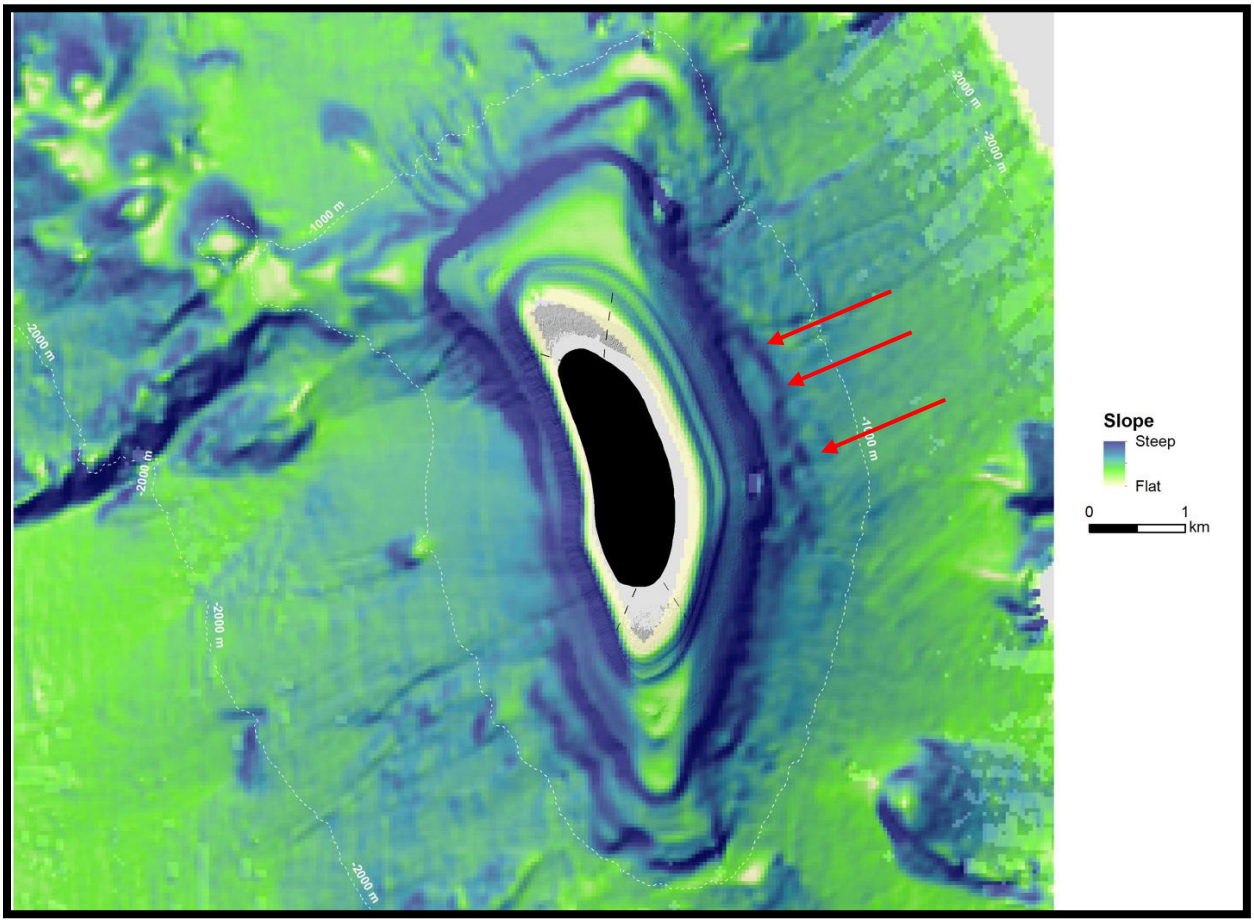

Figure 6. Slope map for Howland Island with data gaps shown in grey and land features in black. The dotted white lines represent 1,000 m interval depth contours. Red arrows indicate an example of a mass-wasting area.

Rugosity

A 40 m resolution gridded rugosity map (not shown) is available for Howland Island. Rugosity, along with a range of other bathymetric derivatives, was tested in the analysis conducted to derive seafloor substrates (discussed later in this section); however, it was highly spatially correlated with slope and therefore did not provide unique information to inform the substrate predictions.

Bathymetric Position Index (BPI)

The 40 m resolution gridded BPI zones map for Howland Island shows the seafloor landscape around the island was predominantly made up of broad crests (red areas) in the shallower depth ranges and slopes (blue areas) in the deeper depth ranges (Figure 7). The northeast, northwest, and south rift zones are apparent from the crest features in the North and South georegions beyond the nearshore depths. There are few topographic depressions (green areas) around the island with the exception of the West georegion where there are extensive depressions at the base of the steep slopes along the northwest rift zone. Considering the steepness of the island, there are no flats.

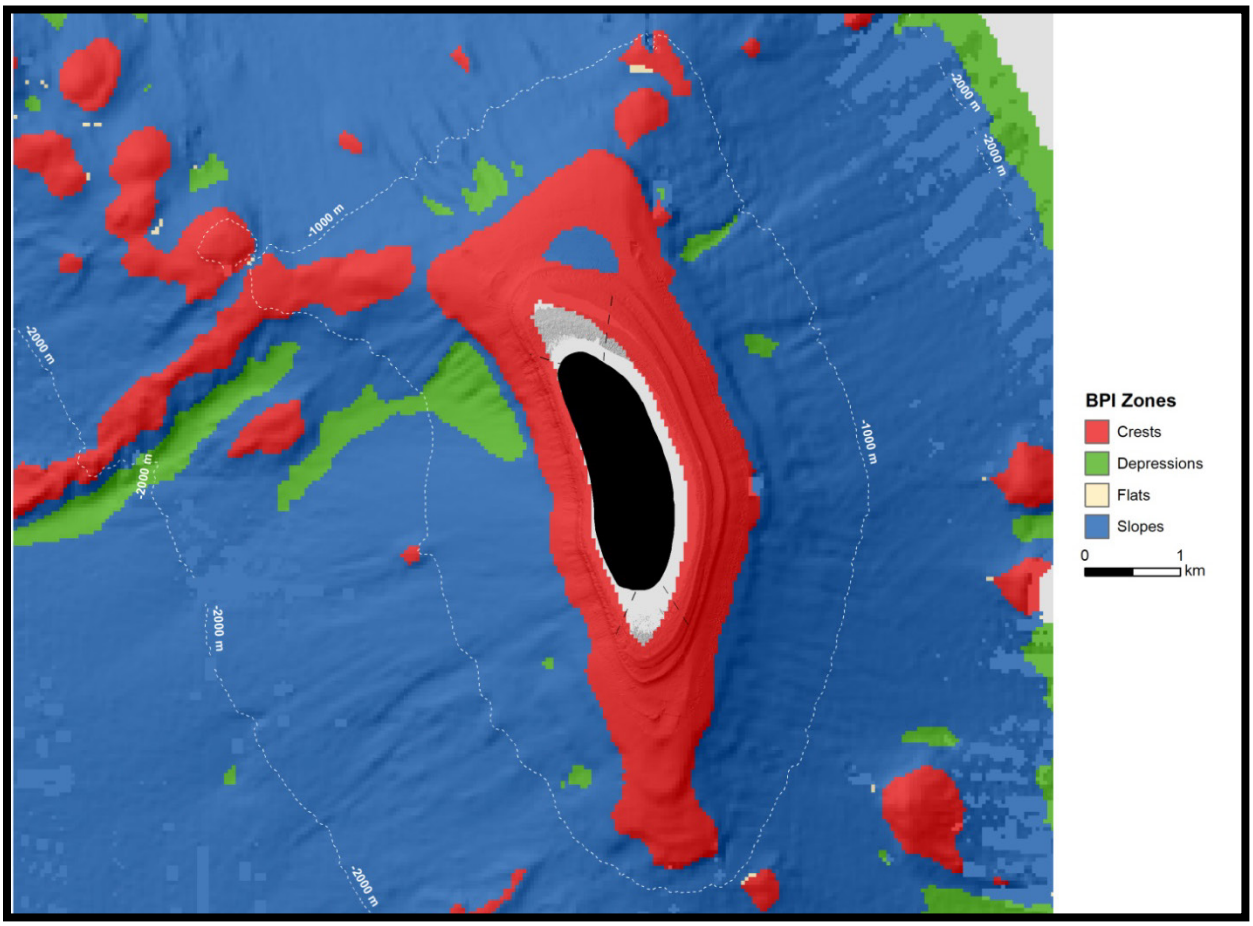

Figure 7. Map of bathymetric position index (BPI) zones for Howland Island, with data gaps shown in grey and land features in black. The dotted white lines represent 1,000 m interval depth contours.

The 40 m resolution gridded BPI structures map for Howland Island (not shown) shows the finer-scale details of each major BPI zone.

Seafloor Substrate

ESD generated predicted seafloor substrates (i.e., hard or soft bottom) for Howland Island in 2018 (Figure 8). The source data used to produce the substrate map for Howland for water depths to 1,000 m include multibeam bathymetric and backscatter data from the 2006 *Hi'ialakai*

surveys and satellite imagery acquired in 2011 (WorldView-2). The data and supporting documentation are available on the Howland Seafloor Characterization page of the PIBHMC website.

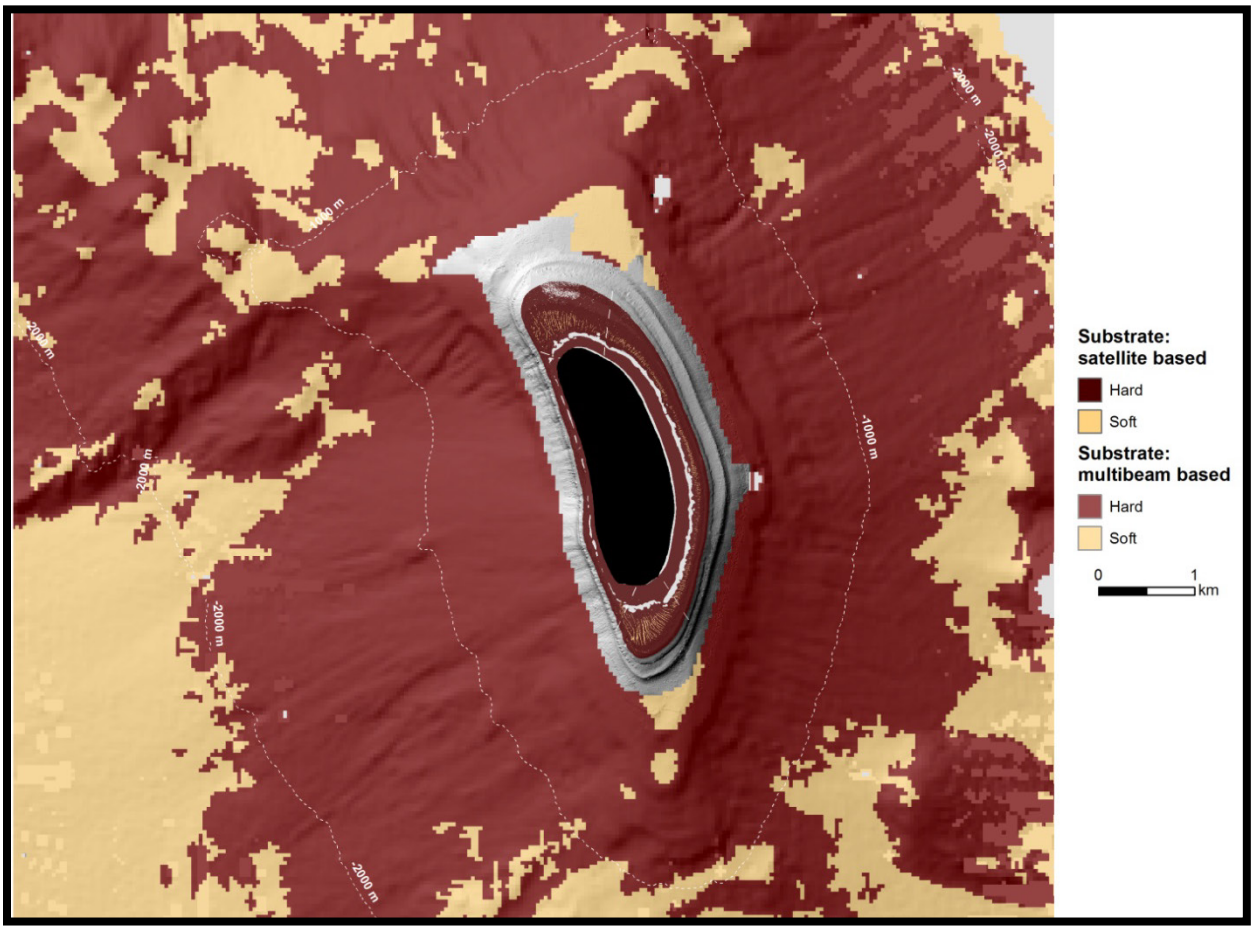

Figure 8. Seafloor substrate map of Howland Island showing hard- and soft-bottom habitats. Depths from ~0 to 30 m were derived from WorldView-2 satellite imagery and depths >30 m were based on gridded multibeam bathymetric and backscatter data (40 m and 5 m resolution, respectively). The dotted white lines represent 1,000 m interval depth contours. Gaps in substrate coverage are shown in grey and land features in black.

Analyses indicate that due to the poor quality backscatter data at Howland Island, the bathymetric data more significantly influenced the substrate predictions. The seafloor surrounding Howland is predominantly hard substrate with only relatively small patches of soft-bottom habitat for water depths to 1,000 m. The limited presence of soft-bottom habitats around the island is likely due to the steepness of the slopes and to the limited number of flat terraces. In shallower depths to approximately 15 m, spur-and-groove habitats are apparent in the North, East, and South georegions from the alternating pattern of hard and soft features as shown in Figure 9, which compares the predicted substrate map (*left*) with a satellite image (*right*) for the forereef terrace in the South georegion.

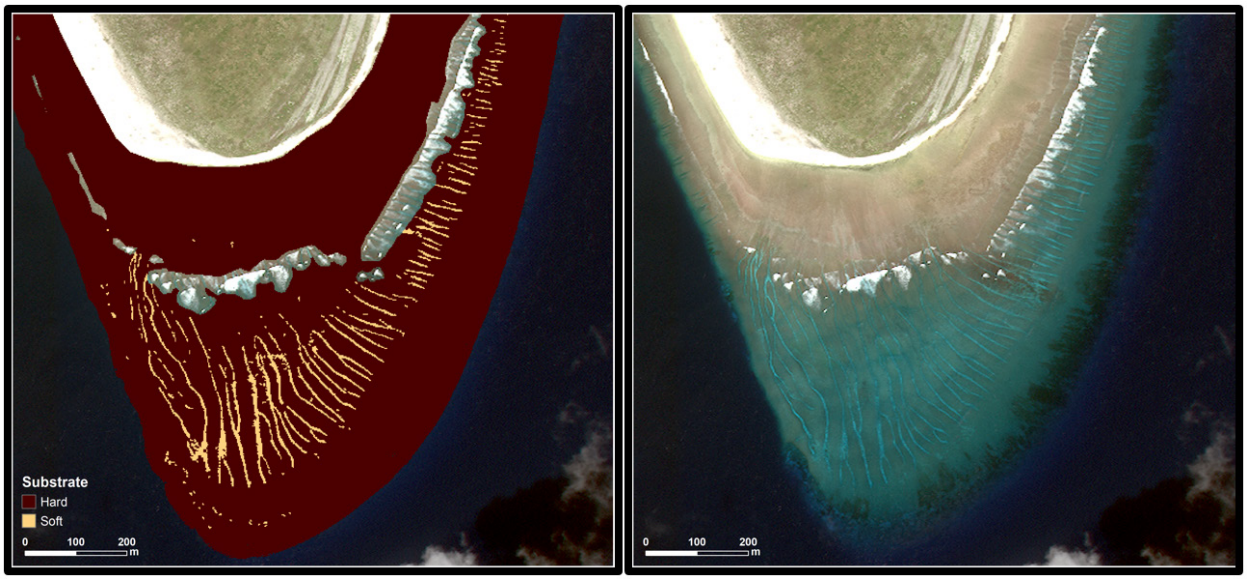

Figure 9. Satellite-derived substrate predictions (left) compared with a satellite image of the same area (right), demonstrating how the predicted substrates accurately delineate features, such as spur-and-groove habitat, at Howland Island.

Maps to Inform the Coral Reef Fish and Benthic Monitoring Survey Design

Many biological communities are structured by depth and habitat (i.e., reef zone), often due to differences in associated environmental parameters, such as light, temperature, salinity, and wave energy. The current Pacific RAMP stratified-random survey design restricts monitoring surveys to hard-bottom habitats in the 0 to 30 m depth range, stratified by both depth and reef zone.

Depth Strata

The integrated bathymetry shown in Figure 5 has been used to classify depth bins (Figure 10) from 0 to 1,000 m. For the Pacific RAMP surveys, depth strata have been defined as shallow (>0–6 m), mid (>6–18 m), and deep (>18–30 m). Estimated seafloor areas for each of the depth strata are included in Table 1. These area statistics enable calculation of pertinent population abundance statistics.

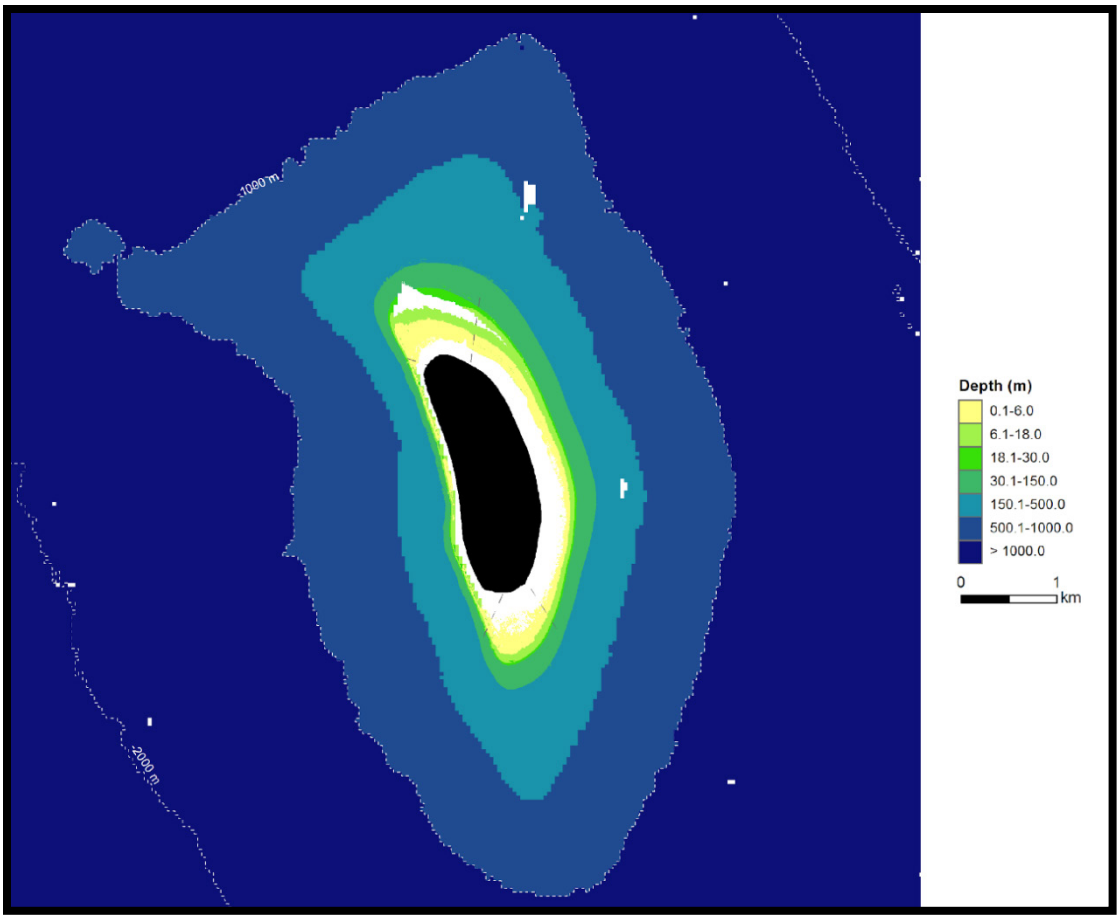

Figure 10. Depth strata map for Howland Island from 0 to 1,000 m, with gaps in bathymetric coverage shown in white and land features shown in black. The dotted white lines represent 1,000 m interval depth contours.

The shallow-water bathymetric data gap at Howland Island precluded derivation of 6 m or 18 m isobaths; therefore, the estimated seafloor area for the three shallowest depth strata (>0–6 m, >6–18 m, and >18–30 m) have been combined in Table 1. At Howland, 56% of the seafloor between 0 and 30 m depths was mapped, leaving an approximately 1.1 km^2 gap. The map of the seafloor from 30 m to 1,000 m depths was spatially complete.

Table 1. Land and seafloor area by depth strata from 0 m to 1,000 m depths for Howland Island. Seafloor area statistics include actual mapped area (km^2) and estimated seafloor area (km^2) based on the integrated bathymetric map for Howland. Land area is 1.8 km^2.

Depth (m)	Estimated Seafloor (km^2)	Mapped Seafloor (km^2)
>0–6	–	0.7
>6–18	–	0.5
>18–30	–	0.2
Subtotal: >0–30	**2.5**	**1.4**
>30–150	1.5	1.5
>150–500	7.5	7.5
>500–1,000	19.0	19.0
Total: >0–1,000	**30.5**	**29.4**

Reef Zones

To support the stratified-random design for Pacific RAMP monitoring surveys, reef zones have been delineated for Howland Island, including forereef, reef crest/reef flat, and land (Figure 11). Satellite imagery was primarily used to manually digitize the zones. Reef crests/reef flat areas include the shoreline out to and encompassing breaking waves; however, the date of the satellite image may influence the accurate delineation of the reef crest (i.e., due to seasonal changes in wave action).

Only forereef habitats have been surveyed around the island, because these habitats most commonly occur in coral reef areas. Therefore, results from surveys at Howland can be compared with results from surveys across all coral reefs of the U.S. Pacific Islands. Moreover, hazards from emergent reef in the shallow reef crest/reef flat areas precluded surveys in these habitats at Howland.

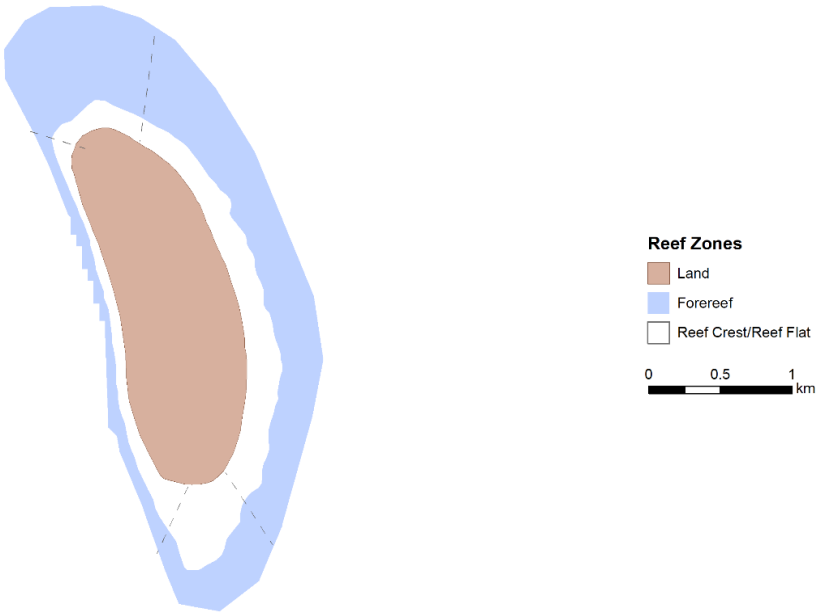

Figure 11. **Reef zones for Howland Island.**

Substrate

Only hard-bottom substrates were targeted for stratified-random reef fish and benthic monitoring surveys of Pacific RAMP. However, at the time the survey strata were established for Howland Island, no substrate information existed. As previously discussed, predicted seafloor substrates have since been developed for Howland and will be incorporated into the survey strata in advance of the Pacific RAMP surveys at Howland scheduled for 2021. In general, the majority of the seafloor area around the island is hard bottom with patches of soft-bottom substrates in the spur-and-groove habitat areas around the island (Figure 9).

Survey Strata

To date, the survey strata used for the stratified-random fish and benthic surveys were based on depth only (Figure 10). A cursory assessment of the new substrate and reef zone data together with the depth strata indicate approximately 1.3 km^2 of surveyable seafloor is available within forereef, hard-bottom habitats in the 0 to 30 m depth range at Howland Island.

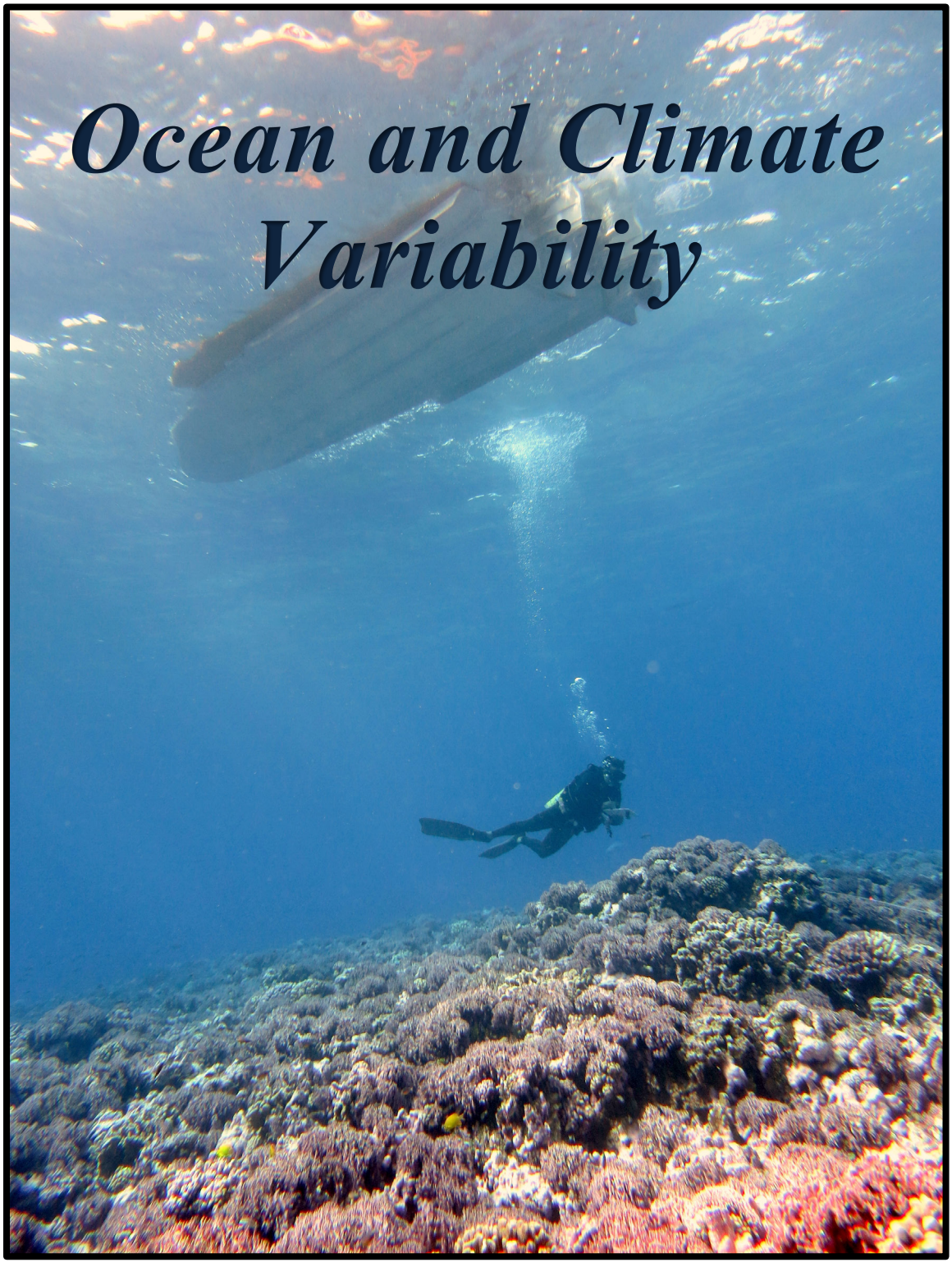

Scoping out a survey site at Howland Island.
Photo: Andrew Gray, NOAA Fisheries.

7.3 Ocean and Climate Variability

Installing a subsurface temperature recorder at Howland Island.
Photo: NOAA Fisheries.

Survey Effort and Site Information

Located just north of the equator in the central Pacific, Howland Island sits directly in the path of both the westward-flowing South Equatorial Current (SEC) at the surface and the opposing eastward-flowing subsurface Equatorial Undercurrent (EUC). Both wind-driven equatorial

upwelling and topographic upwelling as the EUC encounters the steep western slope of the island bring cool, low-pH, and nutrient-rich waters to the surface where photosynthesis drives unusually high biological productivity that bathes the coral reef ecosystems surrounding Howland. The strength of the EUC and trade winds that drive the intensity of topographic and equatorial upwelling at Howland vary with the interannual variability in the El Niño Southern Oscillation (ENSO). During La Niña years, strong trade winds drive increased equatorial upwelling, and a strong EUC drives intense localized upwelling on the west side of Howland, both resulting in anomalously cool temperatures and high productivity. During El Niño events, both a weaker EUC and weaker trade winds result in reduced upwelling, which results in warmer temperatures and reduced productivity (Maragos et al. 2008).

ENSO-driven fluctuations in nearshore ocean conditions affect the health and function of coral reef ecosystems at Howland Island. These environmental oscillations are occurring on a backdrop of global climate change, as concentrations of carbon dioxide in the atmosphere are altering the temperatures and chemistry of the ocean environments that influence coral reef habitats. Episodic high temperatures, largely driven by El Niño events, have led to increases in the frequency and intensity of coral bleaching in the past few decades. In addition, the dissolution of carbon dioxide in ocean surface waters sets off a chain of chemical reactions that decrease seawater pH and make it more difficult for corals and calcifying reef organisms to grow. Understanding the shifts in ocean conditions that are occurring and the sensitivity of coral reef ecosystems to these changes is critical for projecting their survival under 21st century climate change.

Since 2000, Pacific RAMP efforts have monitored the oceanographic environments of coral reef ecosystems in the PRIMNM. These efforts have collected data on key parameters using: (1) a diverse suite of moored instruments, (2) nearshore conductivity, temperature, and depth (CTD) vertical profiles of water column structure, (3) discrete water samples to assess dissolved nutrients, chlorophyll-*a*, and carbonate chemistry, and (4) estimates of calcium carbonate accretion and coral growth and skeletal density to examine the balance between production and removal of calcium carbonate on the reef (Figure 12, Figure 13, Figure 14, Figure 15, Figure 16). A summary of the environmental survey efforts around Howland Island from 2001 to 2017 is shown in Table 2. Refer to “Chapter 1: Overview” for oceanographic instrumentation specifics and water sample collection methodologies.

Field data collection efforts have been complemented with satellite remote sensing data and oceanographic model outputs to provide the large-scale climate and oceanographic context for the in situ observations. Specifically, the Oceanic Niño Index (ONI, the standard index of ENSO activity), sea surface temperature (SST) anomalies from the Optimum Interpolation SST data set, the Degree Heating Week (DHW) thermal stress index from NOAA’s Coral Reef Watch, chlorophyll *a* (chl-*a*, a proxy for primary productivity) anomalies from the Sea-Viewing Wide Field-of-View Sensor and Moderate Resolution Imaging Spectroradiometer Aqua, and global WaveWatch III model output are provided to examine and discuss multi-decadal variability in ocean conditions influencing reef health at Howland Island.

Table 2. **Summary of the ocean and climate survey efforts at Howland Island by year, from 2001 through 2017. The following instruments were deployed: sea surface temperature (SST) buoy, subsurface temperature recorder (STR), calcification accretion unit (CAU), and autonomous reef monitoring structures (ARMS). Diurnal monitoring suites included moored conductivity, temperature, depth (CTD) measurements, and discrete water samples. CTD casts, both shallow (near reef) and deep (offshore), have corresponding discrete water samples. Coral cores of *Porites* spp. were collected by either a pneumatic or hydraulic drill. Numbers indicate the quantity of instruments deployed (D) and retrieved (R) as D/R, water samples and diurnal suite collections, CTD casts, and coral cores per year. Instruments that were deployed and never retrieved were lost in the field.**

	Instruments				CTD Casts		Water Samples		Coral Cores
Year	SST	STR	CAU	ARMS	Shallow	Deep	Shallow	Deep	*Porites* spp.
2001	–	–	–	–	27	–	–	–	–
2002	1/-	–	–	–	16	–	–	–	–
2004	1/-	4/-	–	–	23	–	–	–	–
2006	–	3/2	–	–	29	12	28	60	–
2008	–	4/4	–	9/-	22	7	16	35	–
2010	–	5/4	25/-	9/9	13	16	10	40	–
2012	–	6/5	25/24	-/9	5	32	10	80	4
2015	–	6/6	20/22	–	8	–	9	–	–
2017	–	2/2	–	–	4	–	7	–	–
Total	**2/-**	**30/23**	**70/46**	**18/18**	**147**	**67**	**80**	**215**	**4**

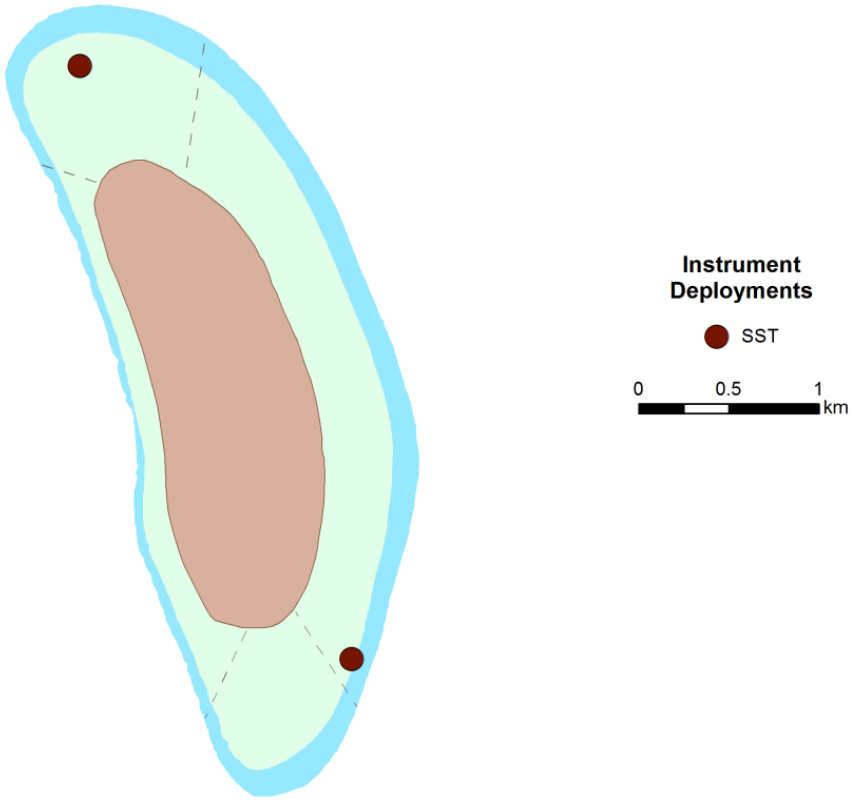

Figure 12. **Deployment locations of sea surface temperature (SST) buoys around Howland Island.**

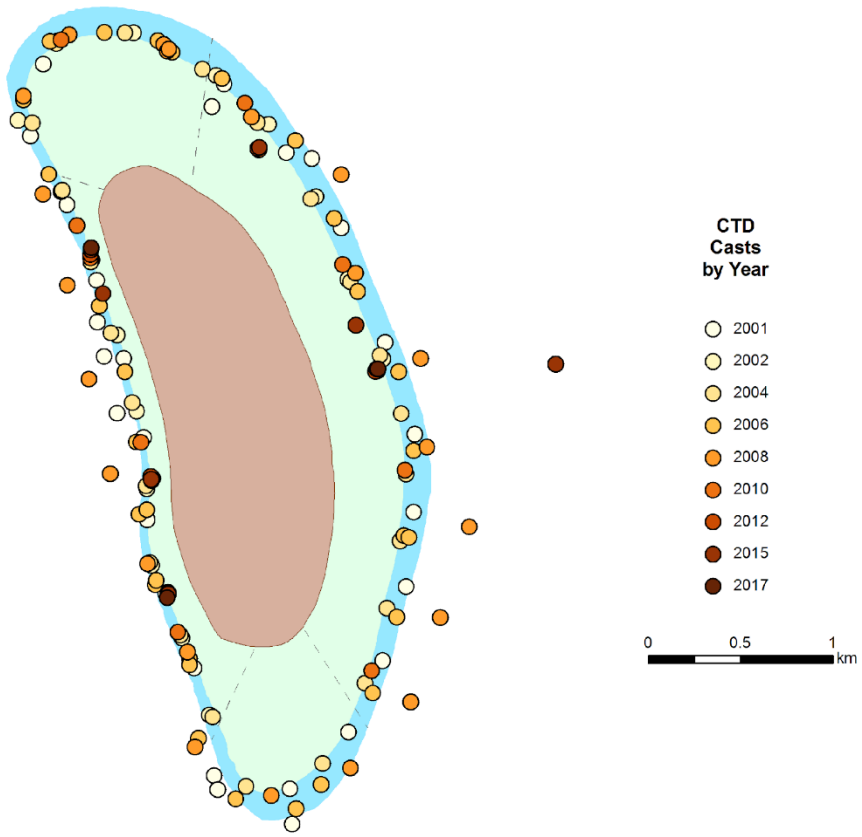

Figure 13. **Locations of nearshore conductivity, temperature, depth (CTD) hydrocasts, measuring water column salinity and temperature from the ocean surface to the seafloor around Howland Island. Hydrocasts at the same location over multiple years have been plotted adjacent to one another and organized around their shared location on the map. Casts in earlier years (2001–2010) prioritized sampling the entire perimeter of the Howland reef, while later efforts (2012–2017) focused on permanent instrumentation sites (sites with subsurface temperature recorders and/or calcification accretion units).**

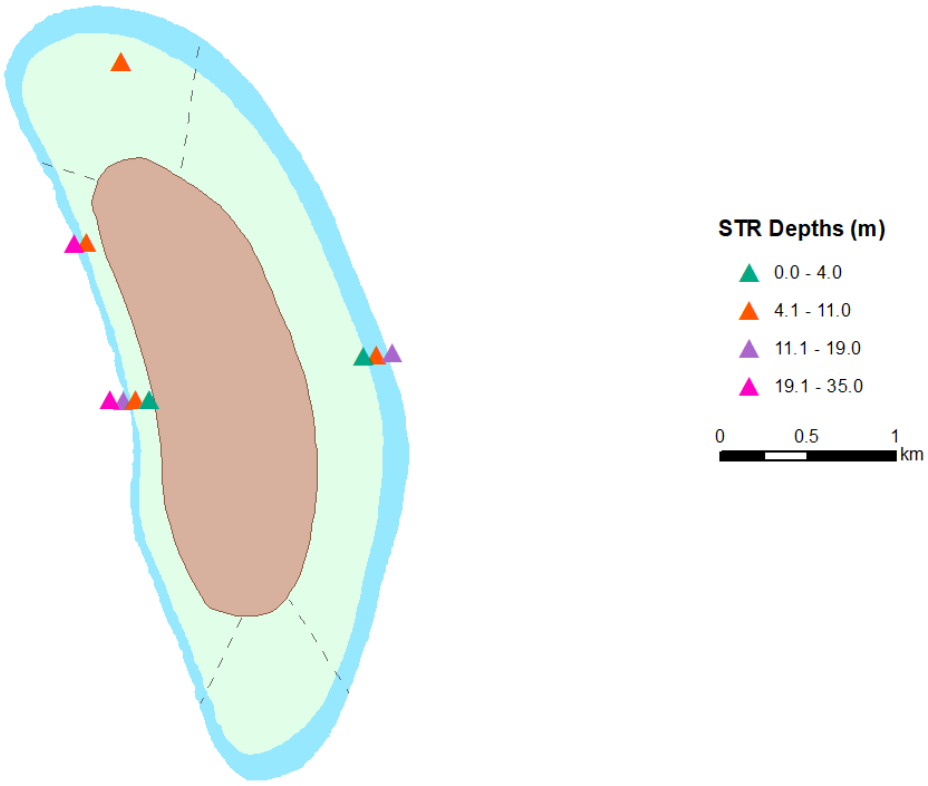

Figure 14. Locations of subsurface temperature recorders (STR) deployed on the reef substrate in depths ranging from 1 to 30 m around Howland Island. Instrument deployments at the same location over multiple years have been plotted adjacent to one another and organized around their shared location on the map.

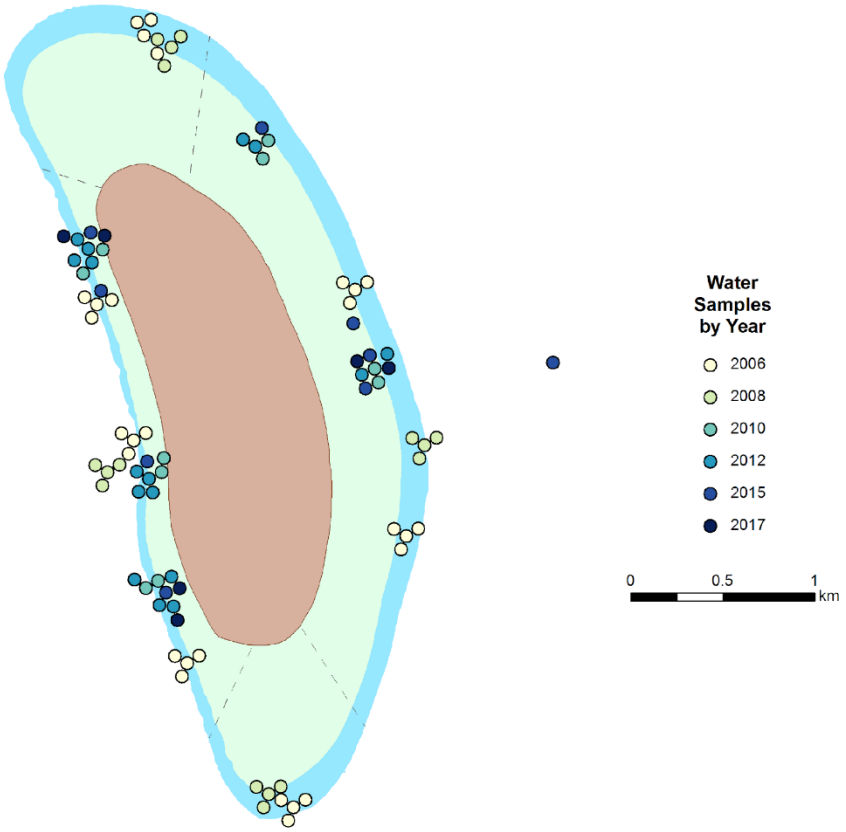

Figure 15. Locations of discrete seawater sample collections from 1 to 30 m depths around Howland Island. Samples evaluated for various analytes: dissolved inorganic carbon, total alkalinity, chlorophyll-*a*, and dissolved inorganic nutrients. Water samples collected at the same location over multiple years have been plotted adjacent to one another and organized around their shared location on the map. Water collections were largely focused on sampling permanent instrumentation sites (sites with subsurface temperature recorders and/or calcification accretion units).

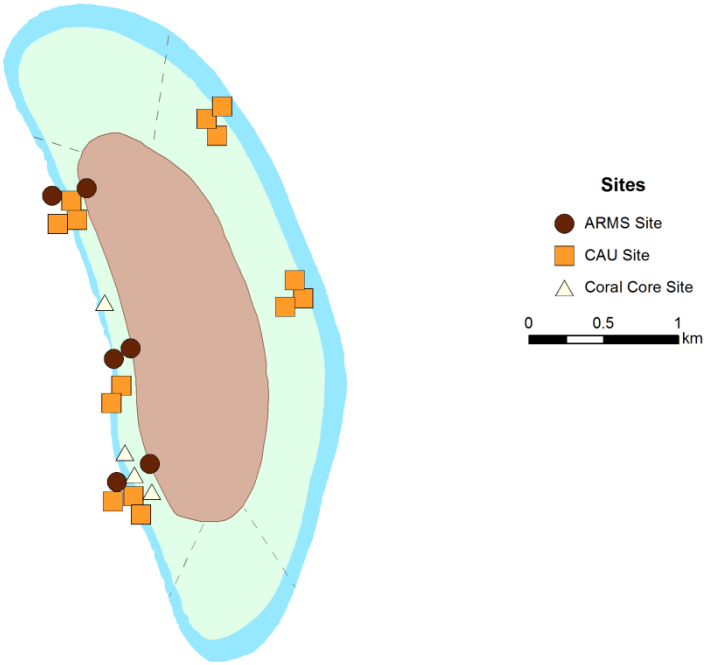

Figure 16. Locations of autonomous reef monitoring structures (ARMS, 3 per site) and calcification accretion units (CAUs, 5 per site) deployed on the reef at 15 m depths around Howland Island. Coral cores of *Porites* spp. collected opportunistically at depths from 5 to 15 m. Instrument deployments at the same location over multiple years have been plotted adjacent to one another and organized around their shared location on the map.

Oceanographic Observations

Oceanographic conditions around Howland Island show a strong relationship with ENSO variability. The ONI, SST anomalies, DHW, and chl-*a* anomalies in recent decades are shown in Figure 18. The ONI shows the variability and frequency of warm El Niño (positive ONI) and cool La Niña (negative ONI) thermal anomalies over the period 1981–2017, based on a threshold of ±0.5 °C [3-month running mean of SST anomalies in the Niño 3.4 region (5°N–5°S, 120°W–170°W)] (Figure 17; Figure 18a). While patterns in SST anomaly in the area immediately around Howland largely tracked variability in ENSO (Figure 17b), there were notable breaks from a strong correlation with these indicators. In particular, Howland experienced relatively low SST warm anomalies compared to the magnitude of the ONI during the extreme 1997–1998 and 2015–2016 El Niño events and relatively high SST warm anomalies during the more moderate 2009–2010 El Niño.

The coral reefs around Howland Island have experienced several episodes of ENSO-driven thermal stress over the period from 1985 to 2017, as indicated by DHW in Figure 17c. DHWs estimate the amount of thermal stress that has accumulated in an area over a 12-week period by summing and integrating the magnitude and duration of temperatures exceeding the local coral bleaching threshold defined as 1 °C above the maximum monthly mean. SST anomalies above this threshold can drive significant coral bleaching when sustained for several weeks to months, with moderate bleaching predicted when DHW >4 °C-weeks and severe bleaching expected when DHW >8 °C-weeks. The cumulative DHWs during this period related directly to strong

warming observed in the ONI (Figure 17a), with DHWs accumulated at Howland in response to El Niño events in 1987–1988, 1991–1992, 1994–1995, 2002–2003, 2006–2007, 2009–2010, and 2015–2016. The most severe thermal stress events for coral reefs at Howland occurred during the 1994–1995, 2002–2003, 2006–2007, 2009–2010, and 2015–2016 El Niño, during which DHW exceeded 10 °C-weeks (severe bleaching expected).

At Howland Island, an inverse relationship existed between ENSO-driven variability in SST and phytoplankton chl-*a* pigment concentration, where increased temperatures during the 1997–1998, 2002–2003, 2006–2007, 2009–2010, and 2015–2016 El Niño events were associated with decreased concentrations of chl-*a* (Figure 17d, Figure 18b). During La Niña, enhanced upwelling of anomalously cool, nutrient-rich, deeper water drove high chl-*a* concentrations and primary productivity. During El Niño conditions, anomalously weak easterly trade winds decreased equatorial upwelling, and an anomalously weak EUC suppressed topographic upwelling. The combined effects of decreased equatorial and topographic upwelling resulted in decreased chl-*a* concentrations and productivity during El Niños. Strong negative anomalies in chl-*a* were observed during the transitions from El Niño to La Niña in 2002–2003, 2006–2007, 2009–2010, and 2015–2016.

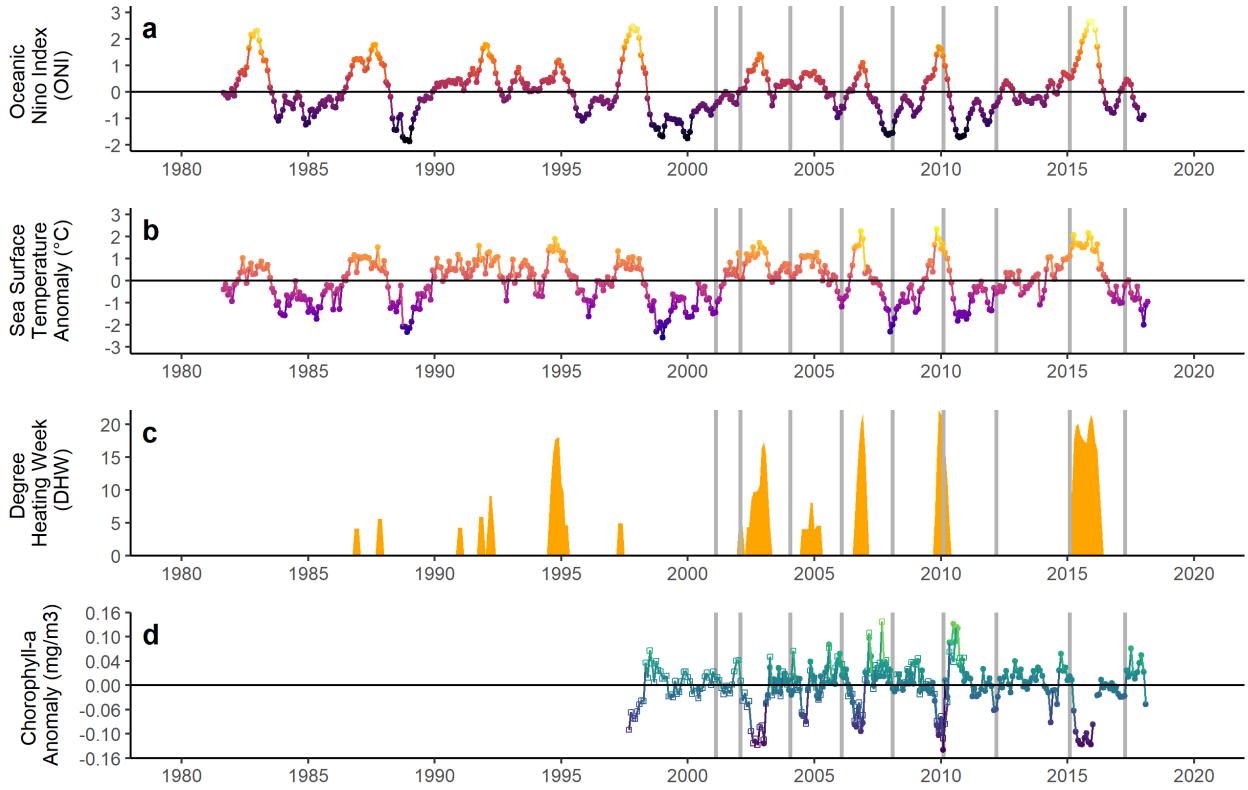

Figure 17. Time series of oceanographic conditions at Howland Island: (a) a 3-month rolling mean of Oceanic Niño Index (ONI) from September 1981 to April 2018 in the El Niño 3.4 region (5°N–5°S, 120°W–170°W), (b) sea surface temperature (SST) anomalies from September 1981 to April 2018, (c) Cumulative Degree Heating Week (DHW) from 1985 to 2017, and (d) phytoplankton chlorophyll *a* (chl-*a*) concentrations from 1997 to 2017. Available data for ONI, SST, DHW, and chl-*a* were extracted for a box around Howland Island (Latitude North: 0.699185 to 0.916334 and Longitude West: -176.716683 to -176.518939). Vertical bars show the dates of Pacific Reef Assessment Monitoring Program field data collection efforts.

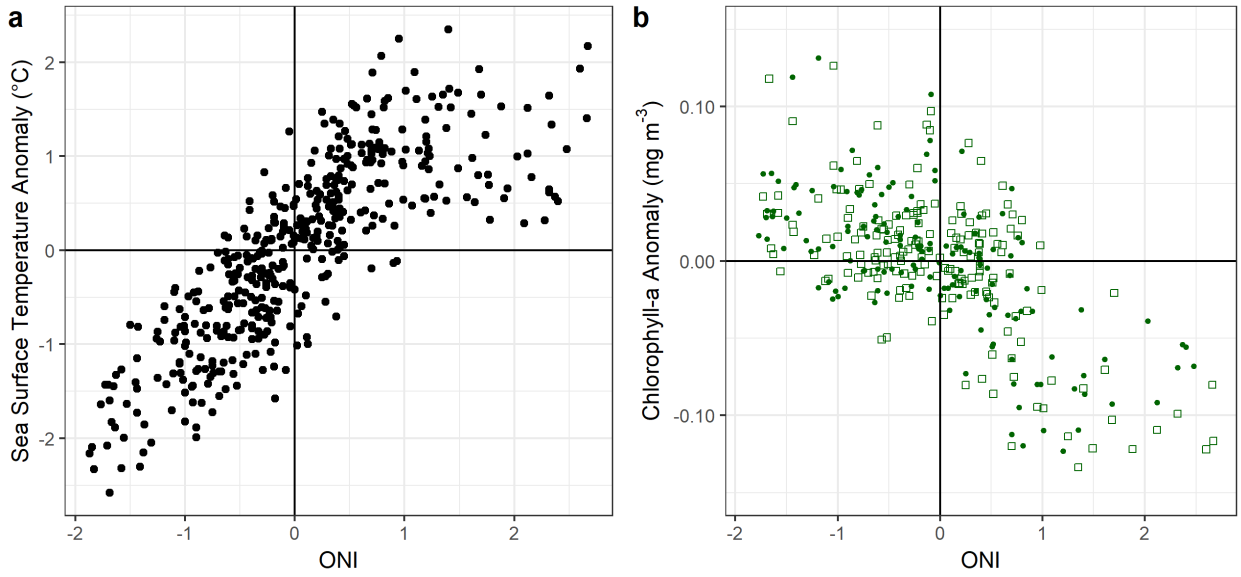

Figure 18. **Relationship between monthly-averaged oceanographic conditions at Howland Island: (a) Oceanic Niño Index (ONI) vs. sea surface temperature (SST) anomaly, and (b) ONI vs. satellite-derived chlorophyll *a* (chl-*a*, Sea-Viewing Wide Field-of-View Sensor in boxes and Moderate Resolution Imaging Spectroradiometer in circles) data. Available data for ONI, SST anomaly, and chl-*a* were extracted for a box around Howland Island (Latitude North: 0.699185 to 0.916334 and Longitude West: -176.716683 to -176.518939).**

Water Column Observations

The physical properties and stratification of Howland Island's water column varied both temporally with phases of ENSO and spatially around the exposed forereef. Figure 19 shows the location of shallow-water CTD casts conducted in the nearshore waters around Howland in January 2006 (29 casts) and February 2008 (22 casts). Cast data documented measurable differences in temperature, salinity, and density profiles between weak (2006) and moderate (2008) La Niña years. Temperatures in 2006 were about 1 °C warmer, and salinity and density were noticeably higher relative to 2008 (Figure 20). During both 2006 and 2008, the profiles show lower temperatures, higher salinities, and associated higher seawater densities on the western side of the island, which are interpreted to reflect active topographic upwelling of the subsurface EUC. In both years, there was little vertical stratification of water properties in the West and East georegions, though noticeable stratification in the North and South georegions, likely caused by surface currents and waves interacting with the relative shallow reef terraces (Figure 20).

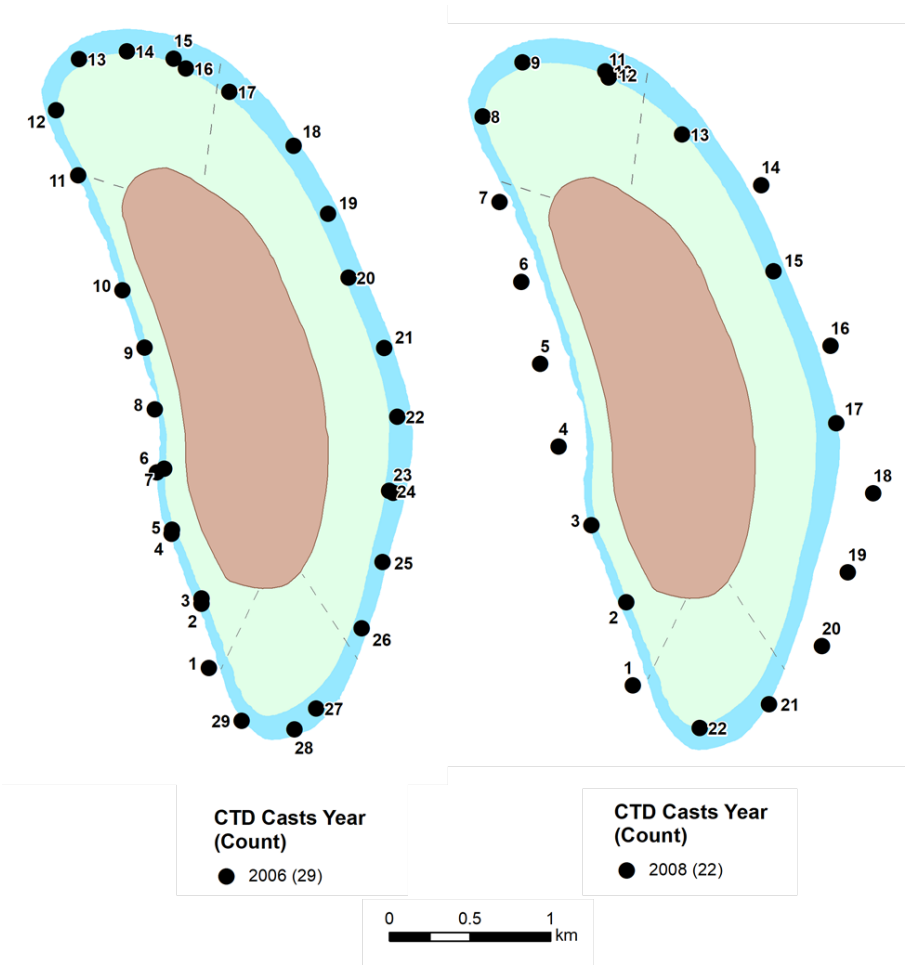

Figure 19. **Shallow-water conductivity-temperature-depth (CTD) sampling locations around Howland Island. CTDs were conducted during January of 2006 (29 casts), and February of 2008 (22 casts). The casts are numbered sequentially in a clockwise direction around the island from left to right.**

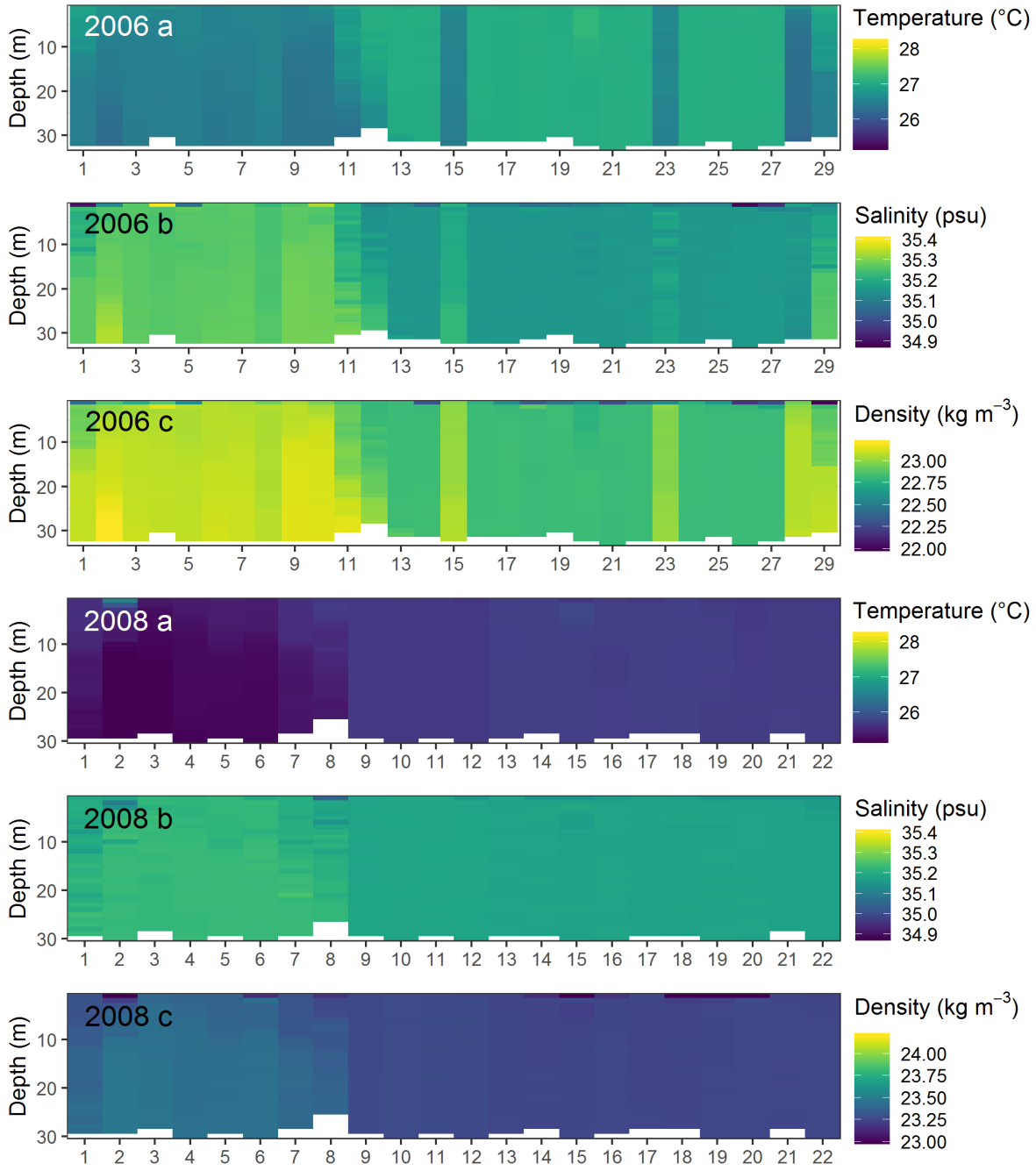

Figure 20. Profiles from shallow-water conductivity-temperature-depth casts around Howland Island in 2006 (top three panels) and 2008 (bottom three panels) for (a) temperature (°C), (b) salinity (psu), and (c) sigma-t density (density of seawater at atmospheric pressure in kg m^{-3} - 1,000), from the surface to depths of ~31 m. The casts are numbered sequentially in a clockwise direction around the island. The top three panels show profiles from 29 cast locations in January 2006, while the bottom three panels show profiles from 22 cast locations in February 2008.

Between 2004 and 2017, a total of 30 moored subsurface temperature recorders (STRs) collected temperature time series at depths between 1 and 31 m (locations shown in Figure 14). This suite of STRs provided in situ vertical thermal structure observations to characterize the temperature

regimes experienced by the coral reefs around Howland at smaller spatial scales and greater depths than is possible using only satellite SST observations at the surface. Interannual variability in temperature was large, particularly on the western side of the island that experiences localized topographic upwelling, where temperatures ranged from above 30 °C during El Niño warm events to temperatures as low as 24 °C during La Niña cool events (Figure 21). The West and East georegions experienced mostly vertically-mixed thermal conditions, though there were periods when vertical stratification was observed, i.e., warmer temperatures near the surface and cooler temperatures with depth.

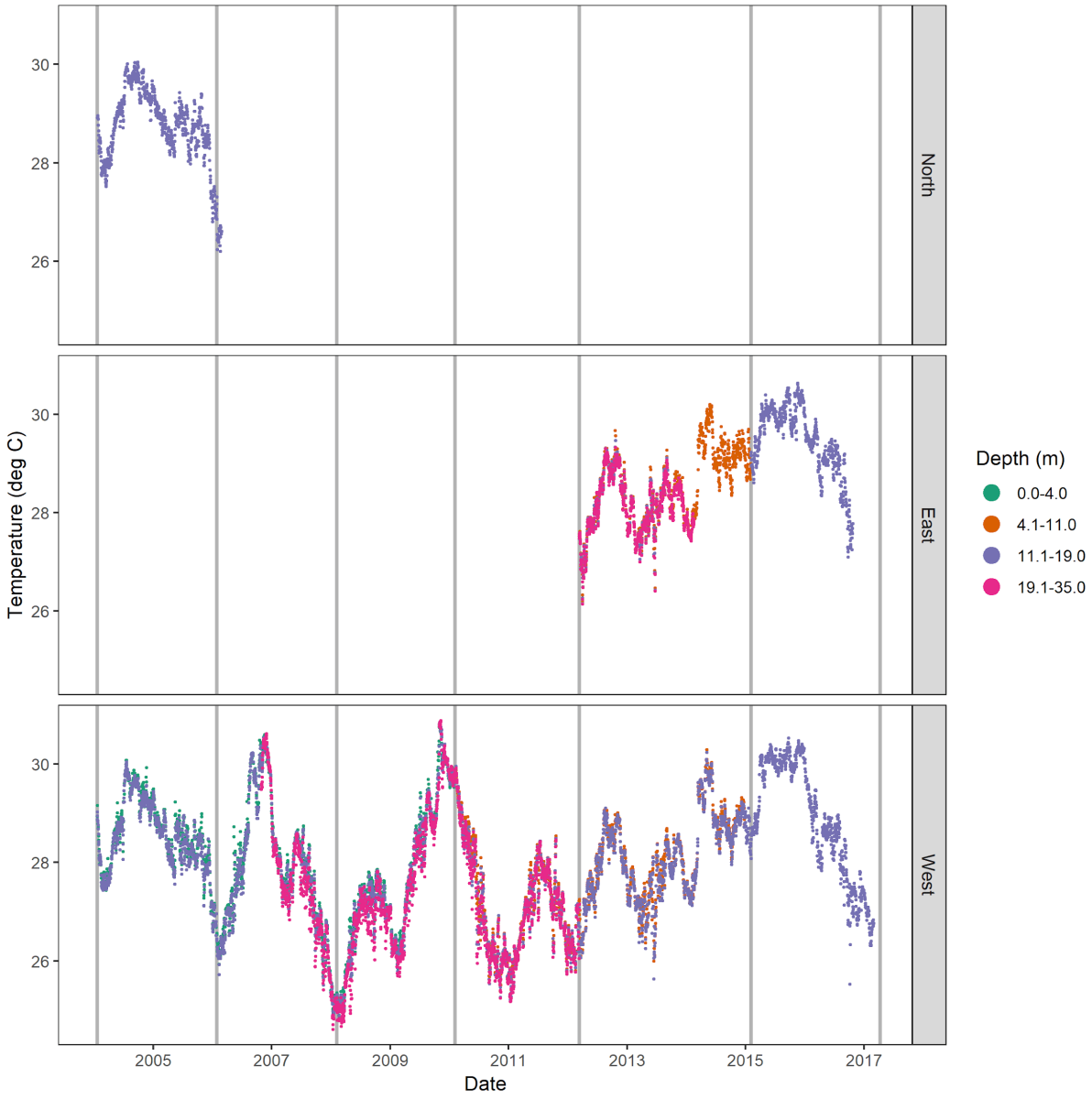

Figure 21. Daily subsurface temperature recorder time-series observations of temperature from 2004 to 2017, collected around Howland Island (North, East, and West). Four different depth ranges were defined at each of these locations: green (0–4 m), red (>4–11 m), blue (>11–19 m), and magenta (>19–35 m). Vertical bars show the dates of Pacific Reef Assessment and Monitoring Program field data collection efforts.

Wave Energy

Ocean wave dynamics strongly influence the environmental conditions of nearshore coastal and island habitats. The energy generated by ocean waves varies on seasonal and interannual time scales, and spatial differences in the direction, magnitude, and frequency of waves around an island or atoll can have significant impacts on the sub-island distribution of coral reef communities. Hourly wave model outputs for 2010–2016 are shown in Figure 22 and Figure 23. The northwest side of Howland Island experienced more waves that had a longer period (the length of time between crests) and greater height (vertical distance from trough to crest) over the winter period from December through February (Figure 22, left panels). During the period from July through September (Figure 22, right panels), the south and east sides were exposed to more waves with both a higher period and height from July through September, though wave heights were generally smaller and more evenly distributed around the island. The mean annual integrated wave power shows that the North, East, and South GeoRegions of Howland received the most wave power, while the West was relatively sheltered (Figure 23).

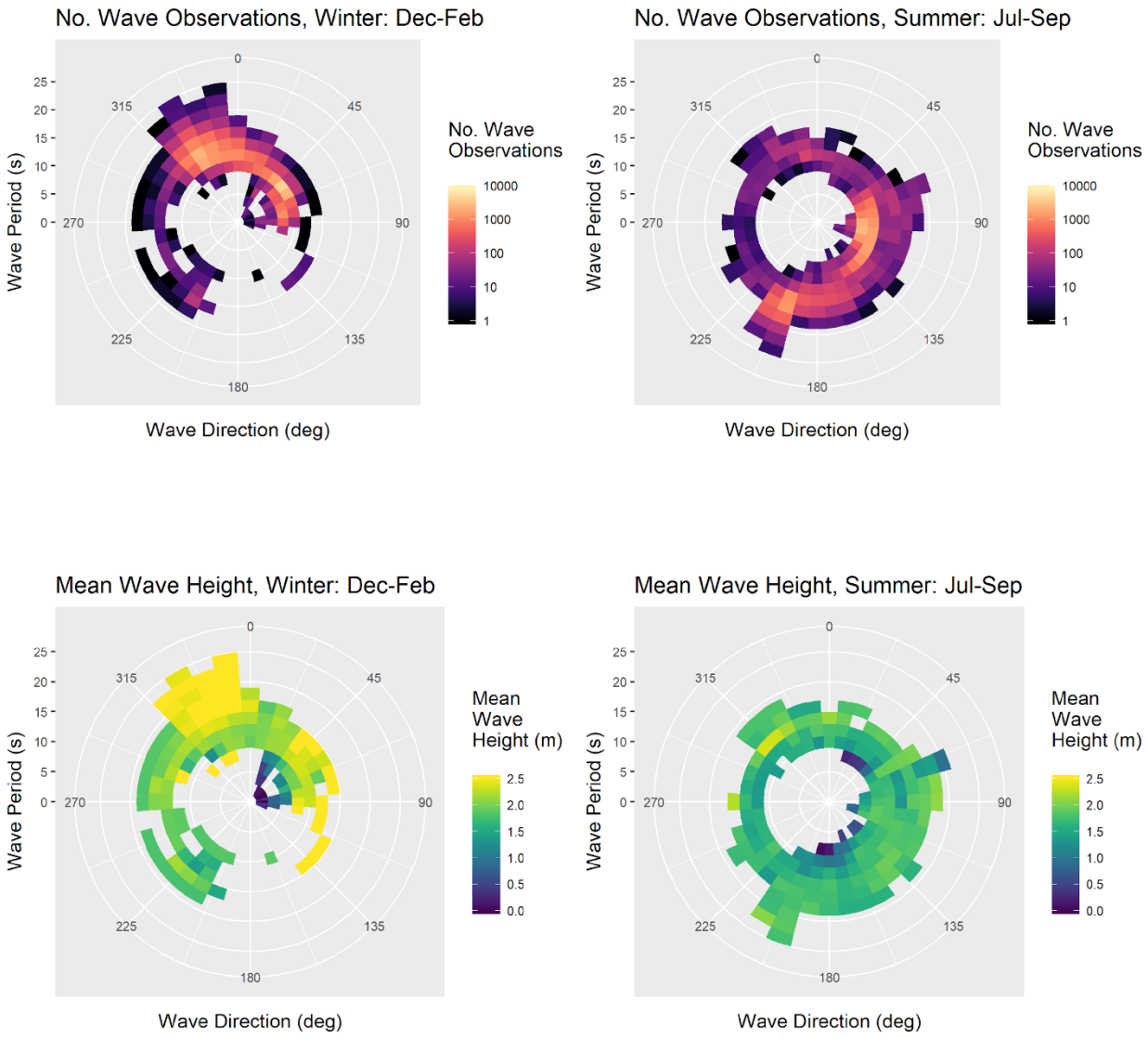

Figure 22. WaveWatch III model output from 2010–2016 for the region around Howland Island. Top panels: Polar plot of the percent of wave observations coming from different directions between December–February (left), and between July and September (right). Bottom panels: Polar plot of derived mean wave height between December and February (left), and between July–September (right). The position of wave data around the 360-degree circle (in 10-degree bins) displays the direction from which the waves hitting Howland travel. Zero degrees indicate that waves arrive from due north and 180 degrees from due south. The height of each directional bin from the center shows the wave period (greater distances from center represent longer wave periods), and the shading shows the number of hourly observations (top) and mean wave height (bottom) for each direction and period.

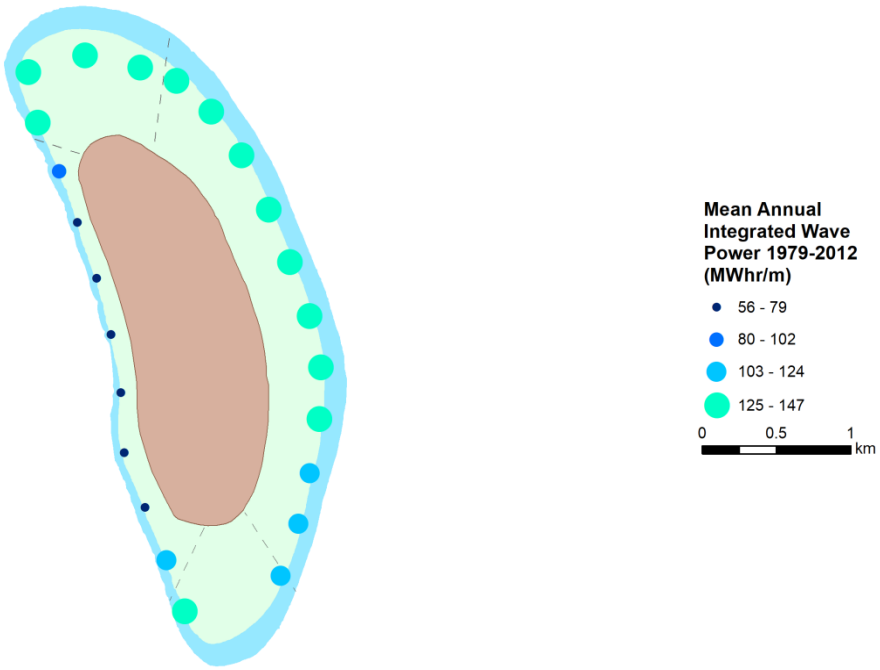

Figure 23. Mean annual integrated wave power (MWhr/m) at Howland Island. Data from 1979 to 2012 correspond to modified WaveWatch III by coastline shadowing using the incident wave swath method (Clark and Oliver, In prep).

Carbonate Chemistry

Aragonite saturation state (Ω_A) is a measure of the degree to which seawater is saturated with respect to the carbonate mineral aragonite, where Ω_A values above one indicate supersaturated conditions. Ω_A is often used as a more biologically-relevant alternative to pH because it reflects the availability of the carbonate ion (CO_3^{2-}) building blocks which calcifying organisms need in order to construct their calcium carbonate ($CaCO_3$) shells and skeletons. Greater values of Ω_A correspond to higher CO_3^{2-}concentrations and thus favor the growth of corals, crustose coralline algae (CCA), and other reef calcifiers. However, under the process of ocean acidification, with increased dissolution of carbon dioxide in seawater, the seawater pH, Ω_A, and concentrations of CO_3^{2-} all decrease. This makes it more difficult for corals and calcifying reef organisms to grow.

The presence of upwelling at Howland Island causes Ω_A values to be relatively low, especially on the western side of the island, and there is strong interannual variability in Ω_A related to ENSO (Figure 24). Of the three periods with carbonate chemistry observations to date (February 2010, March 2012, and February 2015), the overall highest values in Ω_A were measured during strong El Niño conditions in 2010, likely driven by the reduction of upwelling that usually brings deep, lower-Ω_A water to the surface and by coral bleaching, which likely decreased the biological drawdown of Ω_A present on a healthy reef and thus caused Ω_A to rise. Conversely, Ω_A values during more ENSO-neutral periods in 2012 and 2015 were much lower than those measured in 2010 (2015 data were collected just prior to the onset of warming associated with the 2015–2016 El Niño). Ω_A and pH values for the reef waters around Howland were higher (2010) and near or slightly below (2012 and 2015) the median of values observed by ESD across the U.S. Pacific Islands region (Figure 25).

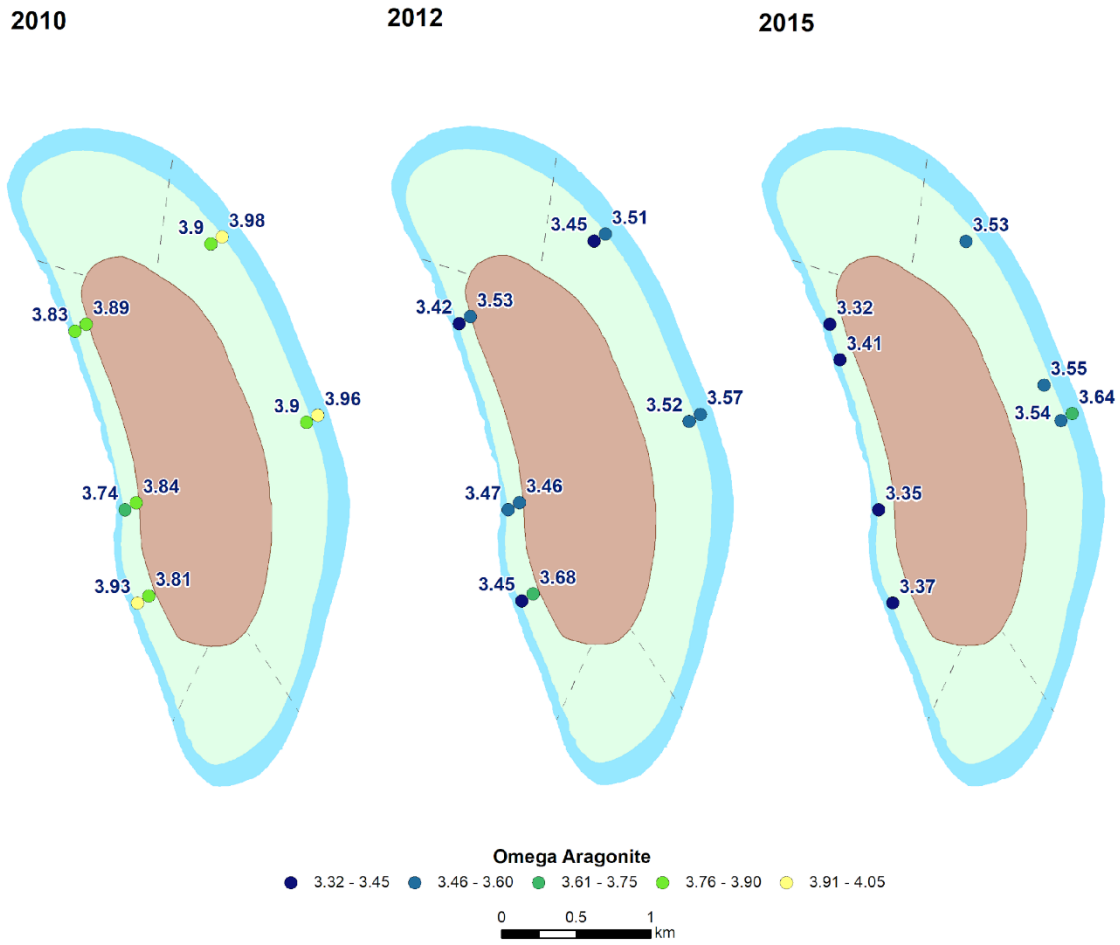

Figure 24. Spatial distribution of aragonite saturation state (Ω_A), observations during 2010, 2012, and 2015 around Howland Island.

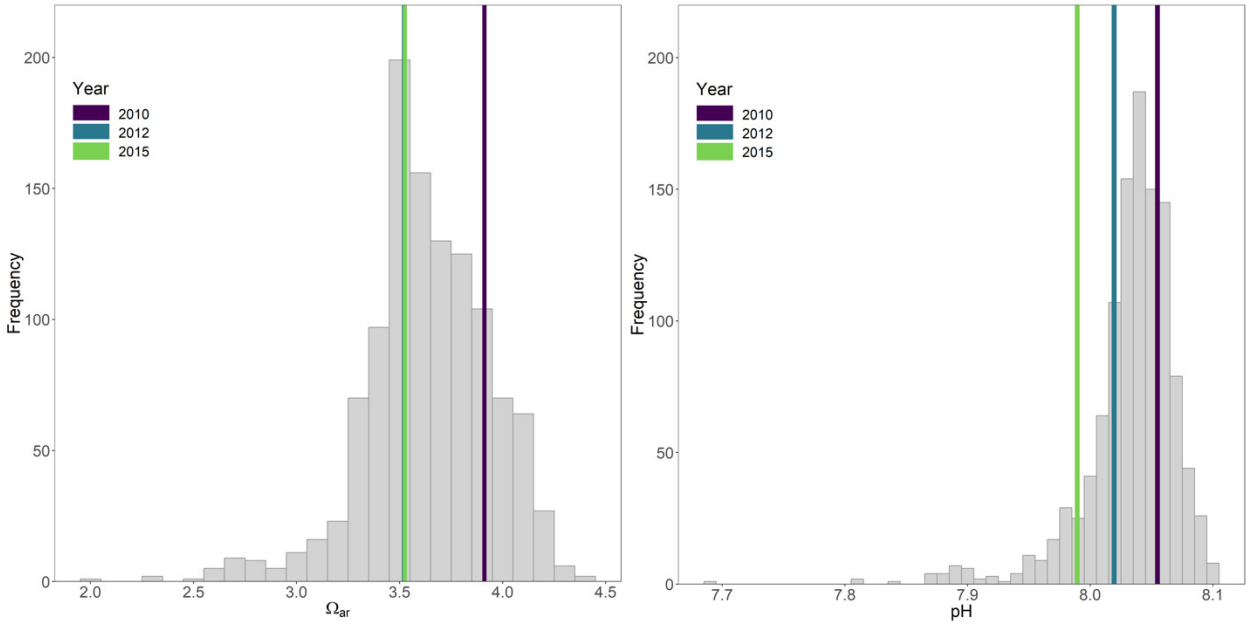

Figure 25. Histogram of all aragonite saturation state (Ω_A; left) and pH (right) values measured from discrete seawater samples across the U.S. Pacific Islands region. Howland Island median values from 2010 (purple), 2012 (blue), and 2015 (green) sampling are denoted as overlaid vertical bars. The 2012 and 2015 Ω_A medians are equivalent.

Net Carbonate Accretion

Calcification accretion units (CAUs) are simple, two-plate fouling structures that are staked to the reef substrate for 2–3 years and then analyzed for the total weight of $CaCO_3$ accreted by the calcareous organisms that recruit to the plates (largely, CCA and hard corals). CAUs provide a proxy for the net rate of $CaCO_3$ accretion that results from the competing processes of carbonate precipitation by calcifying organisms and the removal of material by physical (e.g., strong waves) and/or biological (e.g., parrotfish, burrowing bivalves) erosion. $CaCO_3$ accretion is essential for reefs because it builds the structural framework for coral reef ecosystems and provides essential habitat for reef organisms. However, accretion rates are strongly influenced by dynamic nearshore environmental conditions. In particular, calcification rates of corals and CCA are sensitive to changes in carbonate chemistry and decrease with decreasing pH and Ω_A (Pandolfi et al. 2011). Refer to "Chapter 1: Overview" for CAU-design specifics and deployment methodologies.

CAUs were deployed from 2010 to 2012 and from 2012 to 2015 around Howland Island to assess spatial and temporal variability in accretion rates. Carbonate accretion rates varied across deployment sites, and spatial patterns were not consistent across years (Figure 26). Only the CAUs at the southwestern site (HOW-11) had high accretion rates during both deployments. Overall, accretion rates were substantially higher in 2010–2012 than in 2012–2015 (Figure 24). La Niña conditions persisted during much of the period from 2010 to 2012, while 2012–2015 was marked by more ENSO-neutral years. It is likely that higher accretion rates during 2010–2012 could have resulted from the elevated nutrient concentrations and productivity brought about by strong upwelling associated with La Niña, which could have outweighed co-occurring lower pH and Ω_A also associated with deep-water upwelling.

Accretion rates at Howland were greater than at most locations surveyed throughout the rest of the Pacific (Figure 27). Median pH and Ω_A at Howland are generally near to or lower than values measured across the Pacific during non-El Niño years, so it is also possible that the relatively fast accretion rates observed were driven by high nutrient concentrations and primary productivity, as well as other environmental variables.

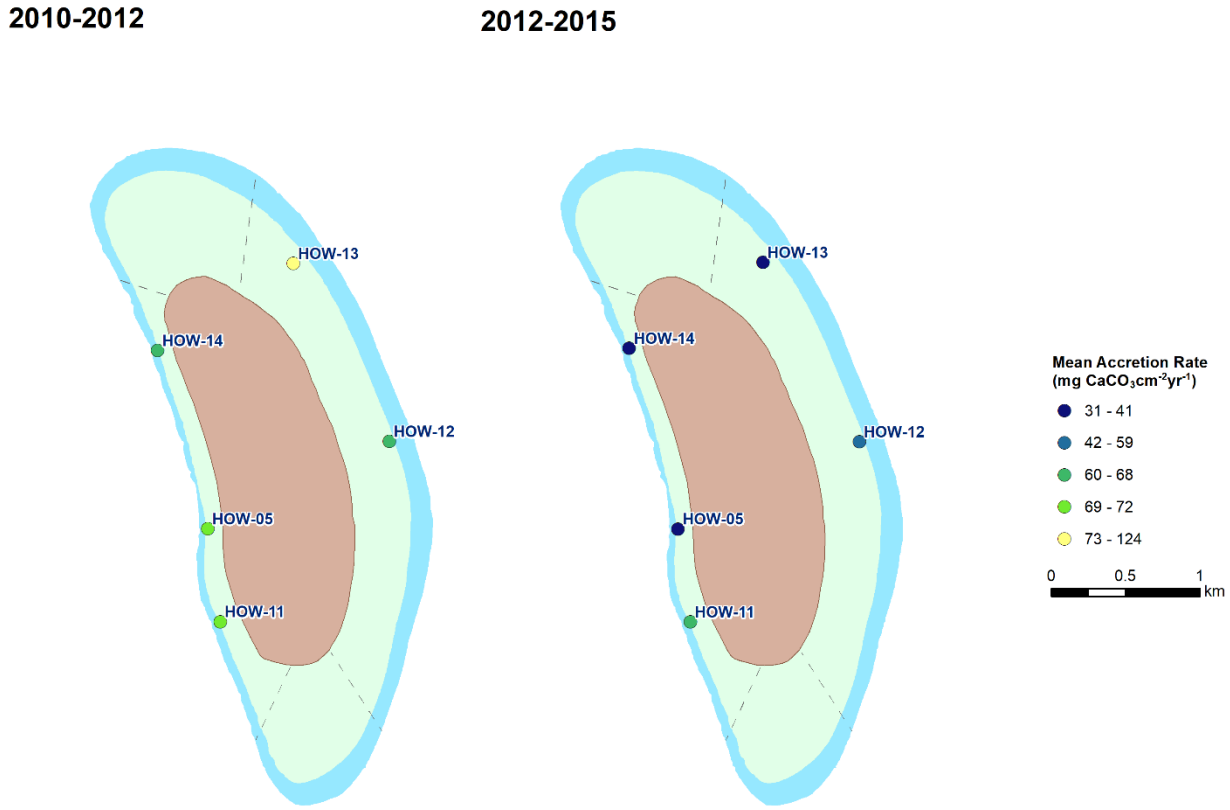

Figure 26. **Spatial distribution of mean carbonate accretion rate (mg $CaCO_3$ cm^{-2} yr^{-1}) at Howland Island during 2010–2012 (left) and 2012–2015 (right). The calcification accretion units are labeled by location code**.

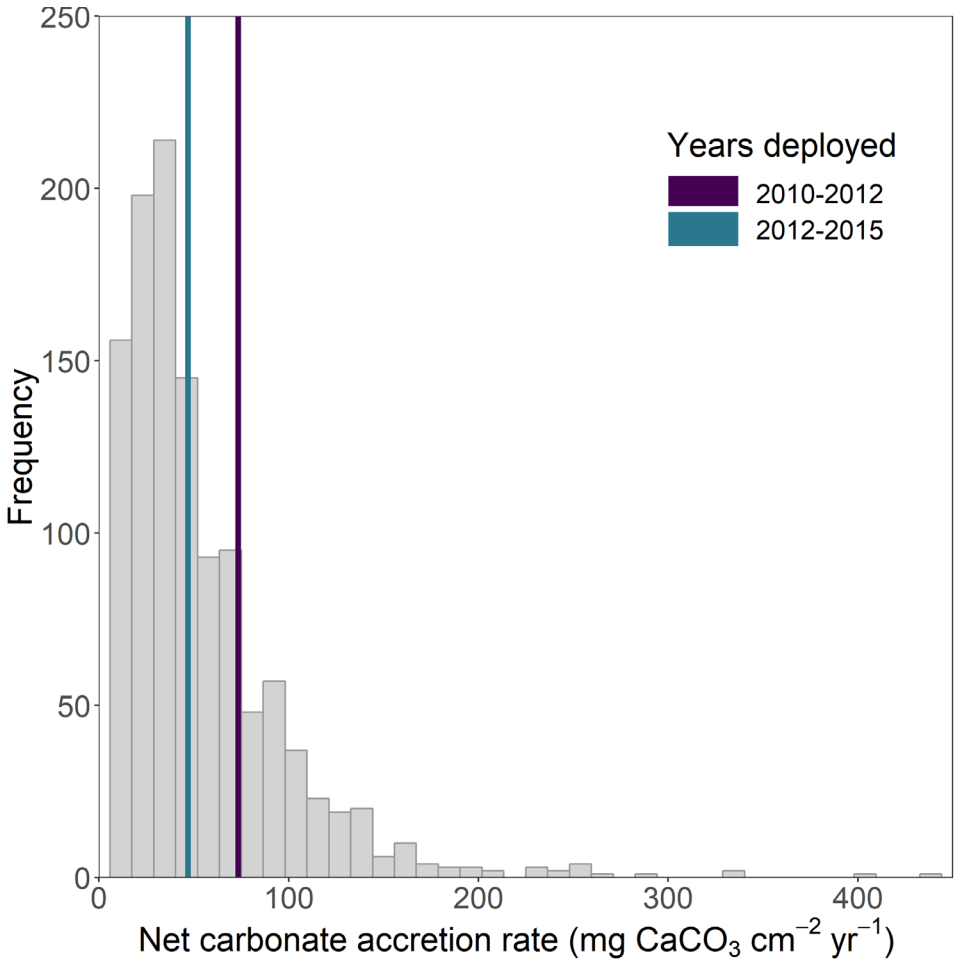

Figure 27. Histogram of all net carbonate accretion rates (mg $CaCO_3$ cm^{-2} yr^{-1}) measured by all calcification accretion units during the period 2010–2017 across the U.S. Pacific Islands region (gray). Median values for 2010–2012 (purple) and 2012–2015 (blue) samples for Howland Island are denoted as overlaid vertical bars.

Scientist Jeff Milisen takes photos of corals at Howland Island to help assess reef health. Photo: Louise Giuseffi, NOAA Fisheries.

7.4 Coral Reef Benthic Communities

Manta rays swim over reef at Howland Island.
Photo: Louise Giuseffi, NOAA Fisheries.

Survey Effort and Site Information

Data to characterize benthic habitats and the coral populations around Howland Island were collected using Rapid Ecological Assessment (REA) surveys and towed-diver surveys (TDS) during nine survey efforts conducted between 2001 and 2017 (Table 3). REA surveys at Howland were primarily performed at repeat sites at mid-depth (>6–18 m) through 2012, thereafter a stratified-random sampling (StRS) design was adopted to generate more statistically robust island-scale estimates of coral reef benthic communities. The use of a StRS study design allowed for an increased number of survey sites across multiple depth strata (shallow: >0–6 m; mid: >6–18 m; and deep: >18–30 m). The stratified-random sites were more widely and evenly distributed around the island than the former repeat sites (Figure 28). Benthic REA surveys implemented the line-point-intercept method (LPI) from 2006 through 2012 and the photoquadrat method from 2015 through 2017 to estimate percent cover of benthic communities. The belt-transect (BLT) method (2004–2017) was used to estimate the abundance, distribution, condition, and diversity of the coral populations (with progressive updates to the methods detailed in "Chapter 1: Overview"). Photoquadrat surveys were also conducted at fish REA sites

over the period 2015–2017, yielding a greater sample size to determine benthic cover. Benthic TDS were conducted primarily around the island perimeter at predominantly mid-depth forereef habitats to estimate the percent cover of benthic functional groups, the density of ecologically- or economically-important macroinvertebrates, and occurrences of potentially significant ecological events, such as widespread bleaching, outbreaks of disease, and abundance of invasive or nuisance species. Opportunistic benthic surveys were conducted in 2017 between the normal Pacific RAMP survey years (2015 and 2018) specifically to monitor the aftermath of the extreme 2015–2016 El Niño-induced mass coral bleaching event (Brainard et al. 2018). Due to time limitations during these opportunistic visits, benthic REA community surveys (i.e., photoquads) and TDS surveys were prioritized; no REA coral population data were collected in 2017.

Table 3. **The total number of Rapid Ecological Assessment (REA) survey sites and towed-diver survey (TDS) segments completed by year and strata (if applicable) at Howland Island. Numbers in parentheses (bold) indicate the number of surveys conducted at mid-depths (>6–18 m). *Note: In 2015, REA survey methodology shifted from repeat sites to stratified-random sampling (StRS). StRS sites are located across three depth strata: shallow (S), mid (M), and deep (D). Partial surveys in 2017 were opportunistically conducted to assess the impacts and recovery of coral bleaching experienced during the extreme 2015–2016 El Niño warm event.**

Year	TDS	REA	
		Coral Populations	Benthic Communities
2001	32 (**32**)	–	–
2002	37 (**37**)	–	–
2004	88 (**62**)	2	–
2006	53 (**31**)	5	6 (6)
2008	80 (**69**)	4	5 (4)
2010	116 (**101**)	8	8 (8)
2012	97 (**92**)	8	8 (8)
2015*	50 (**42**)	10 (S) 6 (M) 5 (D)	22 (S) 19 (M) 15 (D)
2017**	49 (**44**)	–	7 (S) 7 (M) 6 (D)

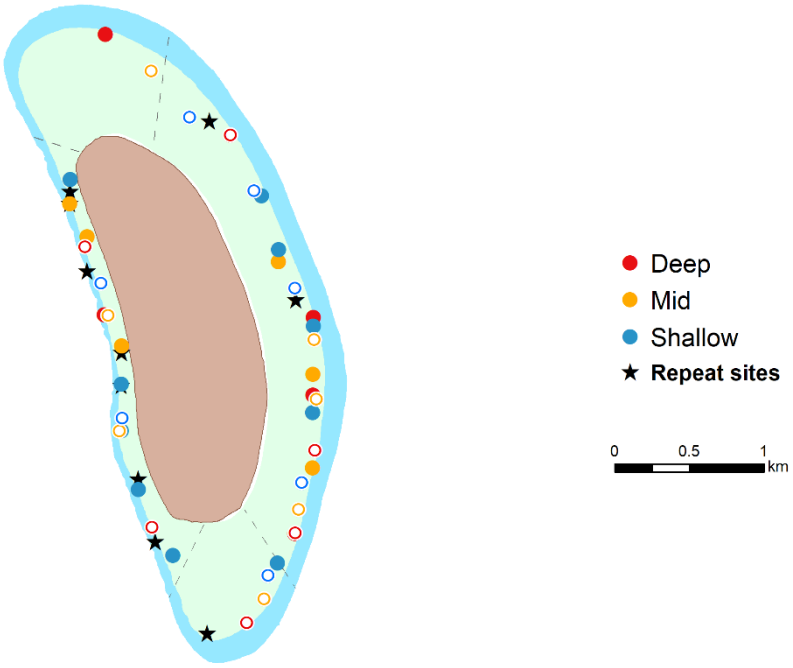

Figure 28. Howland Island benthic Rapid Ecological Assessment surveys locations. Repeat sites (stars) were sampled from 2004 through 2012 and stratified-random sampling (StRS) sites were sampled in 2015 and 2017 (blue, yellow, and red circles for shallow [>0–6 m], mid [>6–18 m], and deep [>18–30 m] depth strata). Photoquadrats for assessing benthic communities were collected at all StRS sites (open circle with white fill and solid circles). Coral population surveys were only conducted at sites indicated by solid circles.

Recent State of Benthic Cover

Of the three main benthic functional groups surveyed, hard coral was the dominant observed during mid-depth TDS around Howland Island in 2017 (mean = 28.3% ± 5.5 SE; Figure 29), followed by CCA (mean = 20.6% ± 3.5 SE) and macroalgae (including encrusting and calcified macroalgae; mean = 5.5% ± 2.2 SE). Combined, these three functional groups comprise approximately half of the benthic cover at Howland. As the cover of sand habitat was also low (1.1% ± 0.5 SE), the remainder of the benthos was likely a combination of pavement, rock, and rubble substrates and associated turf algae (though these categories were not quantified during the TDS). Overall, hard coral cover was high; it was observed during all TDS segments, with cover per 5-minute tow segment ranging from 8% to 56%. The majority of the TDS segments had more than 25% hard coral cover. Coral cover was highest in the East georegion, which was exposed to prevailing flow of the westward-flowing SEC and persistent trade wind swells. The lowest coral cover values were along the more sheltered West and North georegions.

Macroalgae cover ranged from 0.5% to 7.5%, but the majority of TDS segments (i.e., 84%) had cover values of 2.5% or less. CCA cover ranged between 2.5% and 35% throughout the island, with lower cover values (~2.5%) found predominantly along the North and South georegions and the southern end of the East georegion. Overall, higher CCA cover values were observed along the wind-exposed forereef habitats of the East georegion.

Steep forereef slopes characterize the West georegion; limited available substrate may be implicated in the low overall benthic cover levels of corals and CCA in this georegion. Also, bioerosion processes can eventually lead to coral colony dislodgement followed by corals tumbling downslope to suboptimal habitat depths; another driver likely underlying the lower levels of coral cover observed along the West georegion.

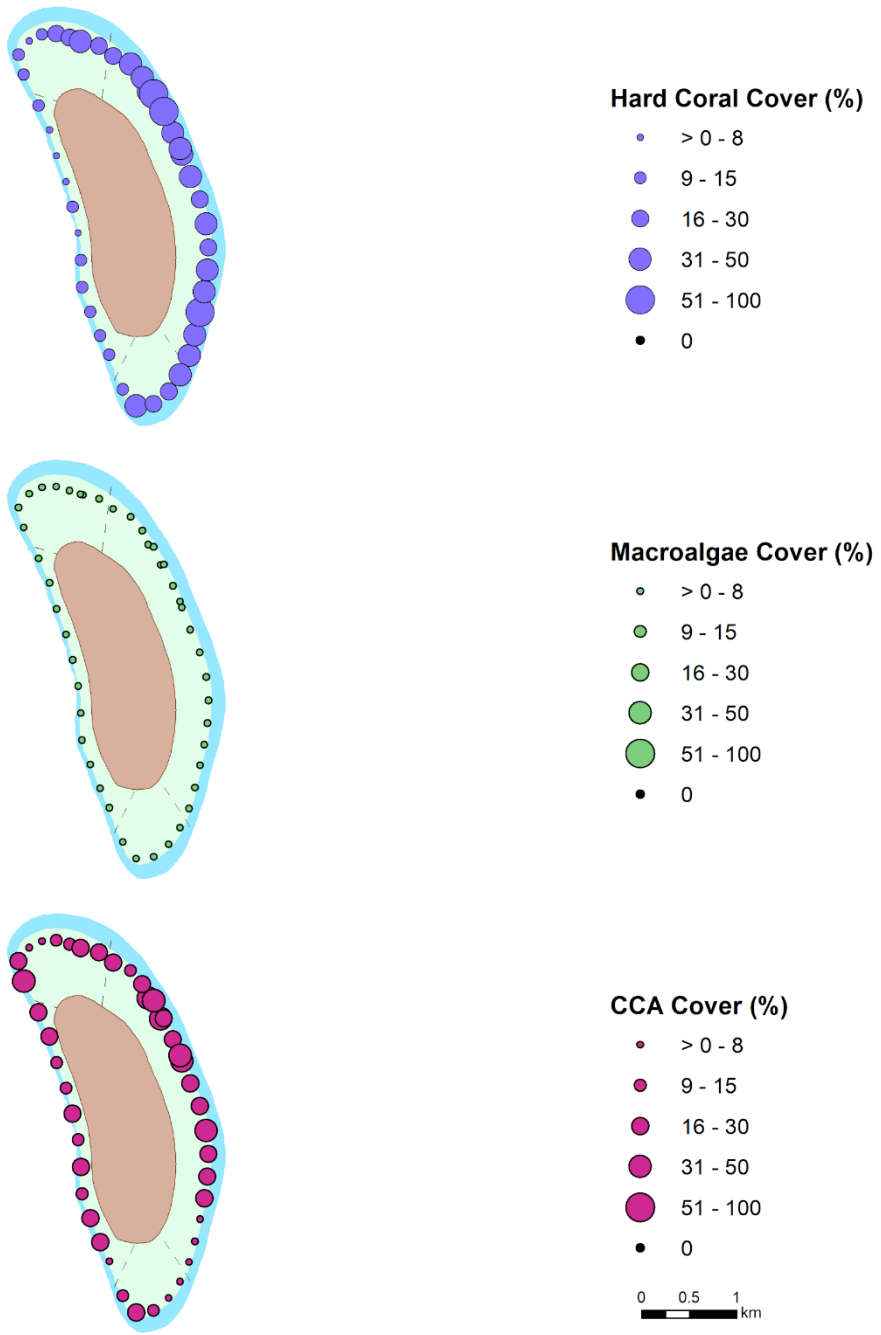

Figure 29. Visual estimates and spatial distribution of mid-depth (>6–18 m) hard coral, macroalgae, and crustose coralline algae (CCA) cover (%) at Howland Island from towed-diver surveys in 2017.

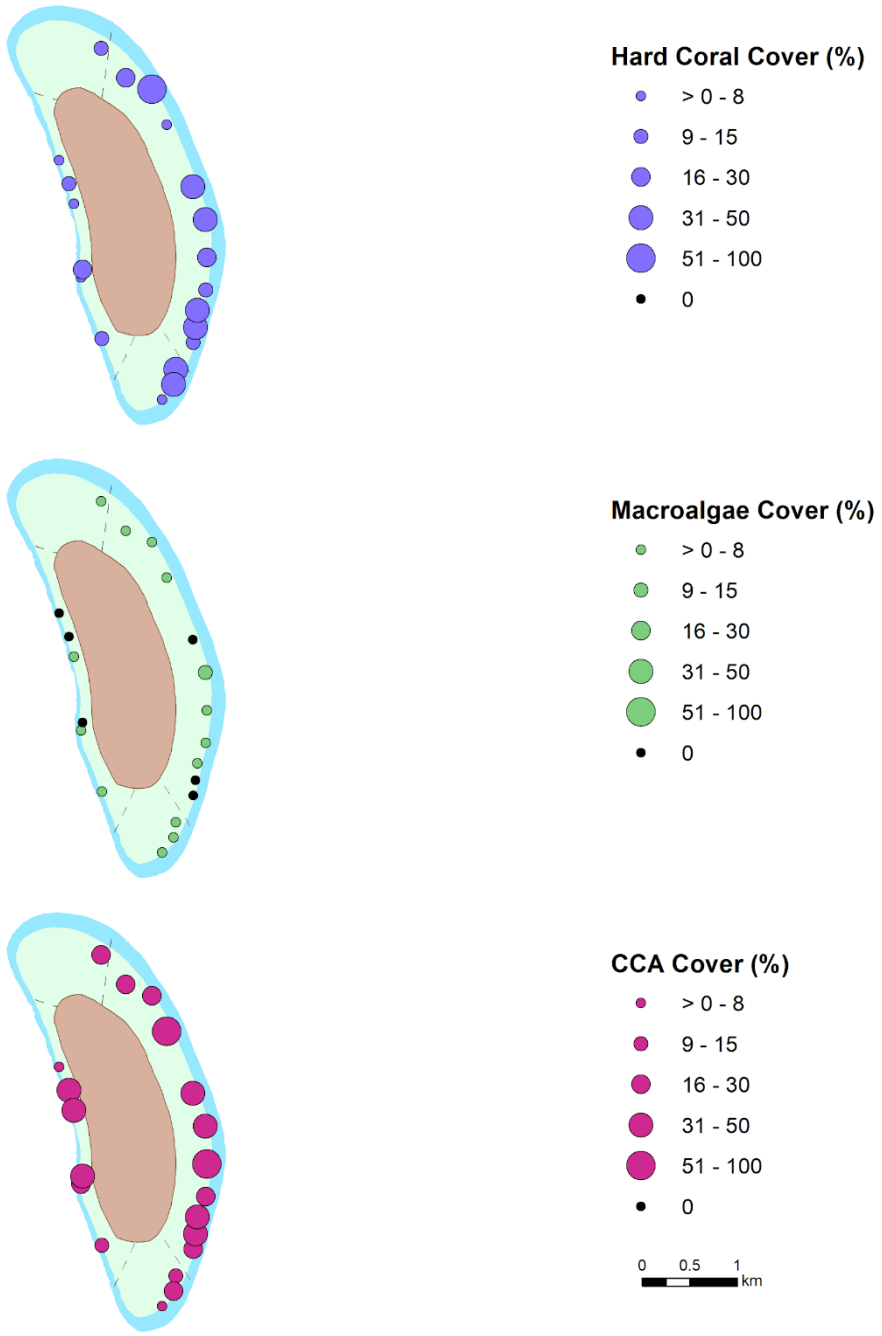

Figure 30. Site-level estimates of hard coral, fleshy macroalgae (excluding calcified and encrusting macroalgae), and crustose coralline algae (CCA) cover (%) at Howland Island from stratified-random sampling photoquadrat surveys conducted at all depth strata combined (>0–30 m) in 2017.

Site-specific benthic cover estimates from StRS photoquadrat surveys (Figure 30) showed that in 2017, CCA was the dominant functional group, followed by spatially variable coral cover and uniformly low macroalgae cover (Jimenez 2018). Island-wide, CCA cover ranged between 7% and 67% and was reported present on all survey sites, 80% of which reported relatively high

CCA cover (>15%). CCA cover was consistently high along the wind-exposed forereef habitats of the East georegion, and low along the South georegion and a couple of sites on the West georegion. Together with CCA, coral, and encrusting macroalgae, calcifying organisms represented more than 50% of the benthic cover at 90% of sites. High preponderance of calcifying vs. non-calcifying (i.e., fleshy macroalgae and turf algae) organisms tends to be common among healthy, resilient coral reef systems.

Hard coral was present at all StRS sites surveyed at Howland Island in 2017, and ranged from 0.3% to 55%, with nearly 50% of sites exhibiting hard coral cover greater than 20%, particularly sites in the East georegion. Cover of fleshy macroalgae (excluding calcified and encrusting macroalgae) was moderately low. Although it ranged from 0% to 10.7%, 90% of the survey sites exhibited less than 4% macroalgae cover. The site with the highest macroalgae cover was located in the East georegion.

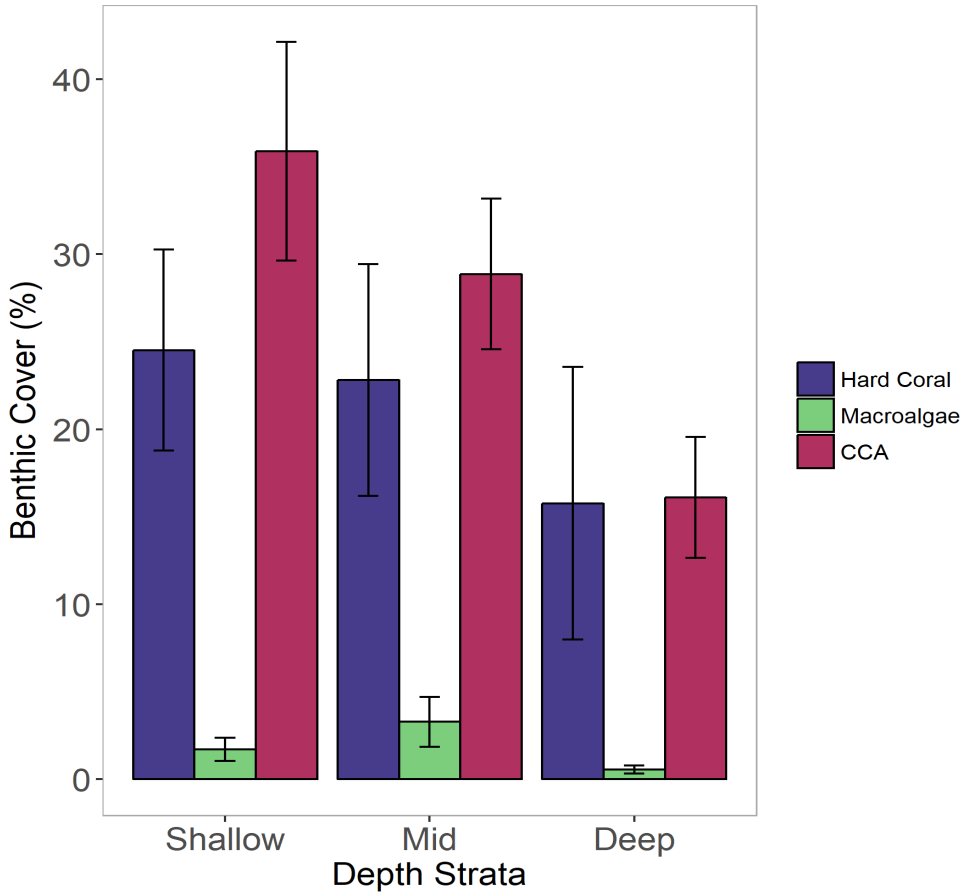

Figure 31. Strata-level mean benthic cover (± 1 SE) at Howland Island by benthic functional groups of hard coral, fleshy macroalgae (excluding calcified and encrusting macroalgae), and crustose coralline algae (CCA) for shallow (>0–6 m), mid (>6–18 m), and deep (>18–30 m) depth strata from stratified-random sampling photoquadrat surveys conducted in 2017.

Based on the 2017 photoquadrat surveys, of the three main functional groups studied, CCA and coral were dominant throughout all depth strata (Figure 31). The scales of difference among CCA and coral cover are small relative to the uncertainty in the data (represented by the errors bars). Mean hard coral cover was moderate (range = 16–25%), and together with CCA

contributed to over 50% of the live benthos in the shallow- and mid-depth strata. Cover of these two functional groups progressively decreased with depth, a common pattern likely driven by light availability declining with depth. Mean fleshy macroalgal cover was low overall and ranged between 0.6% and 3.3%. Compared to the other islands in the PRIMNM, mean macroalgae cover at Howland Island was intermediate: lower than at Jarvis Island, Wake Atoll, and Baker Island, but higher than the reef systems at Palmyra and Kingman Atolls in the PRIMNM.

Time Series of Benthic Cover

The time series of benthic cover in Figure 33 illustrate the variable nature of the coral cover at Howland Island over the period 2001–2017. Compared to the baseline collected by TDS, mean hard coral cover increased by approximately 30% between 2001 and 2002, and remained notably high (~42–52%) and stable (overlapping error bars) throughout the period 2002–2012. This same pattern was corroborated by the more spatially-limited LPI methodology for the survey years 2008–2012. Between 2006 and 2008, LPI surveys reported a 25% decrease in coral cover, which could be linked to positive SST anomalies that occurred during the moderate 2007 El Niño event registered by both the in-situ STRs and satellite SST records (Figure 17 and Figure 21). Later, in 2012, TDS detected an approximately 20% reduction in coral cover which is likely attributable to the 2009–2010 El Niño event, whereby 30–35% of corals at Howland were observed to be bleached (Vargas-Ángel et al. 2011).

Averaged across all survey years (2001–2017) and methods (TDS, LPI, and StRS), hard coral cover at Howland Island has remained relatively high along the East and North georegions and lower throughout the South and West georegions (Figure 32a). The decadal trend analysis presented in Figure 32b shows that over time coral cover losses, mostly less than 10%, were registered along the East, West, and North georegions, interspersed by a few focal areas of little or no change in the South, East, and North georegions. Interestingly, none of the 500 m^2 grid cells experienced decadal increases in coral cover. The observed coral cover declines were mostly recent (2012–2017, Figure 32c) and mainly occurred in the North and West georegions. The high level of spatial and temporal variability in coral cover, in addition to the method changes from LPI at repeat sites to image analysis of photoquadrats at random sites in 2015, obscures the elucidation of clear temporal trends.

In 2017, TDS and REA photoquadrat surveys were specifically conducted to assess the potential impacts of the extreme 2015–2016 El Niño warm event. While the REA photoquadrat survey revealed an approximately 28% reduction in coral cover at Howland Island (Figure 33), high variance among sites (visualized as SE bars in Figure 33) suggest this decline from 2016 to 2017 is not significant; TDS showed no decline in coral cover over this same time period. Concomitant surveys documented coral cover losses in the order of approximately 20% at the neighboring Baker Island, located 70 km away.

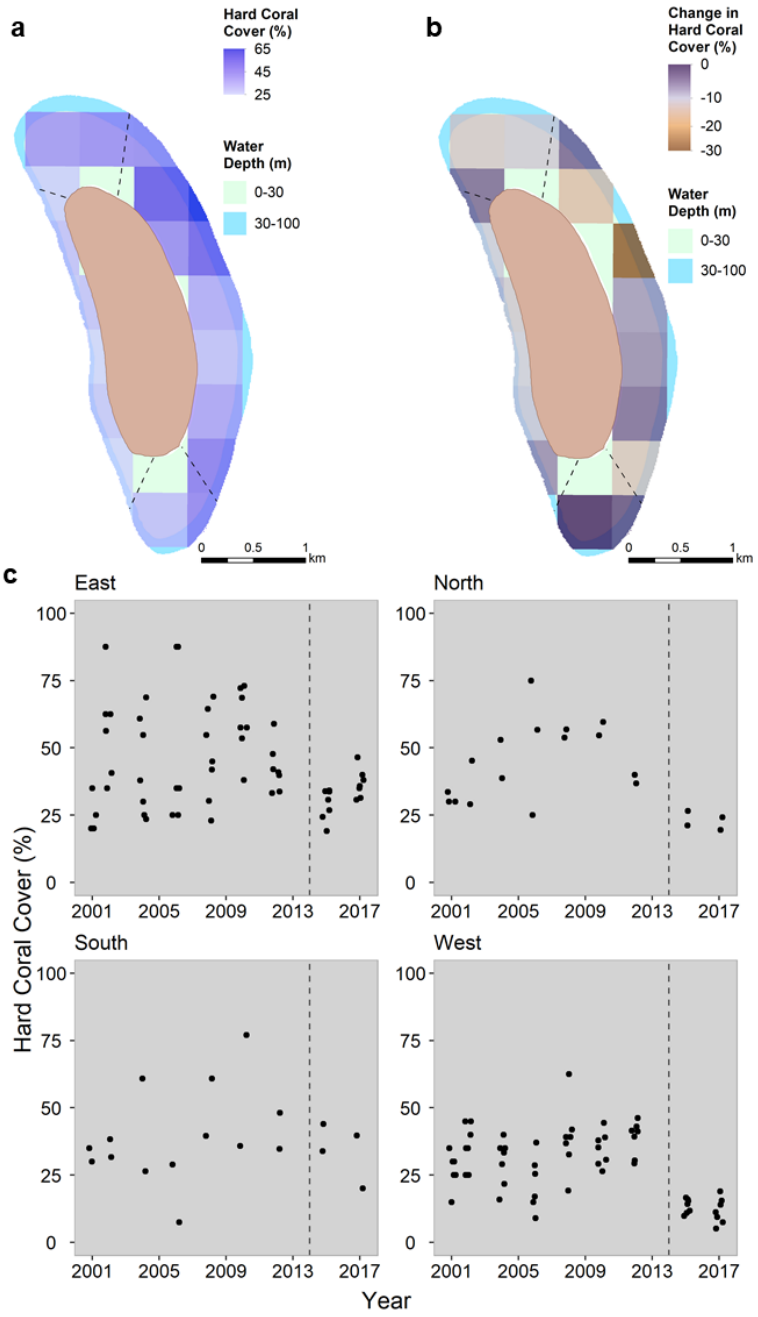

Figure 32. Spatial patterns and temporal trends of gridded (500 m × 500 m) mean coral cover at Howland Island across survey years (2005–2017) and methods (towed-diver surveys, line-point-intercept [LPI], and stratified-random sampling [StRS] benthic and fish photoquadrats). (a) Mean hard coral cover per 500 m by 500 m grid cell across all survey years; (b) temporal change in hard coral cover per 500 m by 500 m grid cell, only including cells with at least a 10-year span of data and at least 3 observation years; and (c) time series of hard coral cover by georegion. In 2014 (dashed line), Rapid Ecological Assessment survey methodology changed from LPI at repeat sites to photoquadrat surveys at StRS sites. See "Survey Methods for Coral Reef Benthic Communities" in "Chapter 1: Overview" for further details.

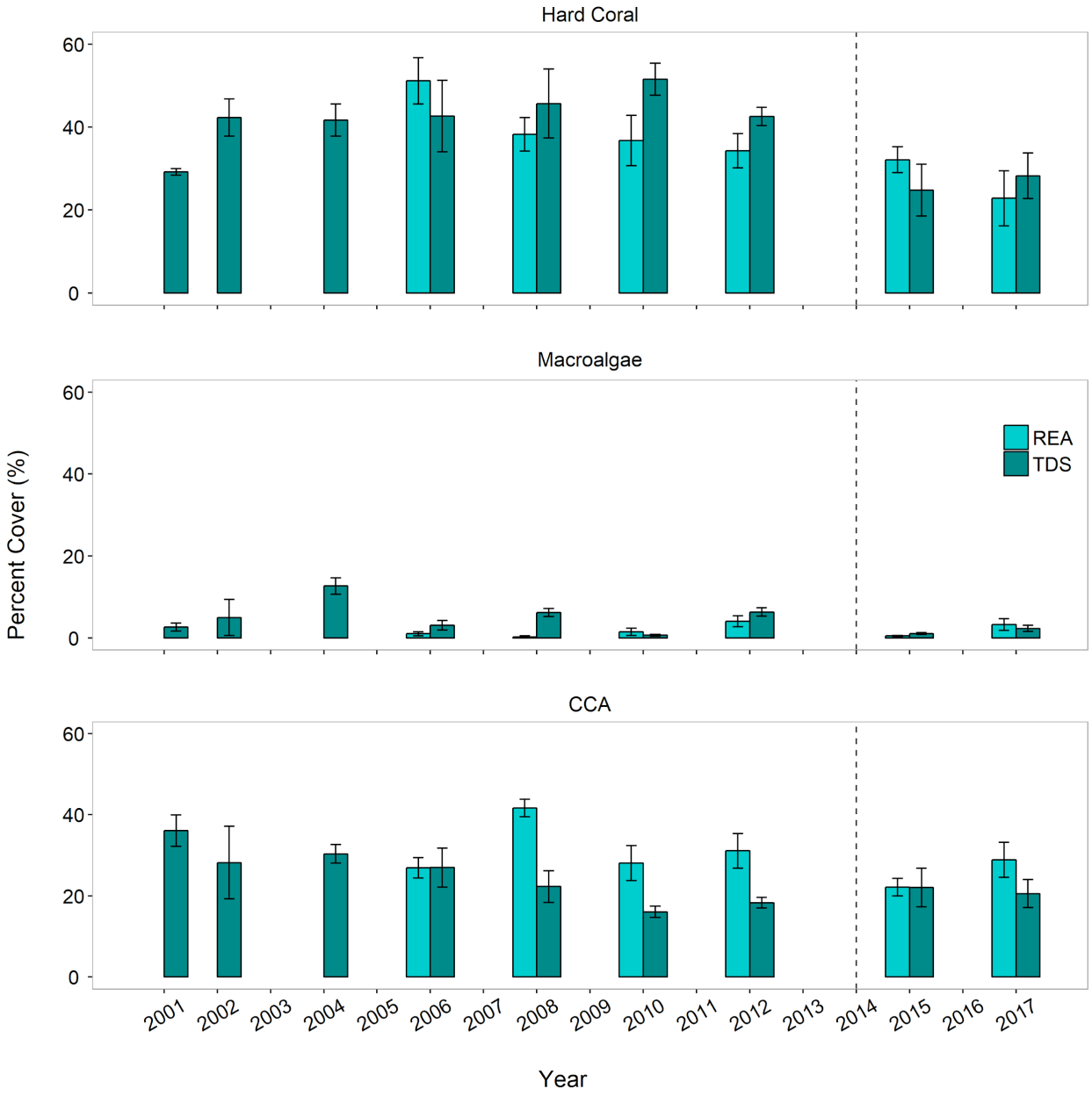

Figure 33. Time series of mean (± 1 SE) hard coral, macroalgae, and crustose coralline algae (CCA) cover (%) at Howland Island by survey method (Rapid Ecological Assessment [REA] and towed-diver survey [TDS]) conducted at the mid-depth stratum (>6–18 m) from 2001 through 2017. In 2014 (dashed line), REA survey methodology changed from line-point-intercept at repeat sites to photoquadrat surveys at stratified-random sampling sites. *Note: TDS macroalgae data include calcified and encrusting macroalgae; the REA macroalgae data exclude it.

Over time, mean cover of macroalgae was uniformly low at Howland Island (Figure 33); the TDS registered an approximately 45–60% increase between survey years 2001 and 2004, when cover peaked at 12.7%. This estimate was nearly four-fold the amount of macroalgae reported by the LPI surveys (3.1%). Higher macroalgae values were likely because turf algae were included in early TDS estimates of "macroalgae" from 2004 to 2006. Overall, TDS estimates of mean island-wide macroalgae cover tended to be greater than estimates acquired using the LPI and

photoquadrat methods, except for the years 2010 and 2017; surveys in both years occurred in the aftermath of the major El Niño events in 2009–2010 and 2015–2016.

Patterns of CCA cover were variable over time (Figure 33); the TDS method reported a steady, average reduction of approximately 20% from 2001 to 2010, when the lowest island-wide mean CCA cover was documented (16%). Following that decrease, CCA cover increased and stabilized in 2015. Comparatively, REA surveys exhibited a different temporal pattern, with intermittent cover increases registered in 2008, 2012, and 2017 (percent increase = 35%, 10%, and 23%, respectively). Interestingly, these increases occurred in the aftermath of warm or cold SST anomaly events that resulted in documented mass coral bleaching and related mortality in 2009–2010 and 2015–2016 (see the "Ecosystem Integration" section).

Time Series of Algal Disease

CCA disease occurrence index is the proportion of the number of disease cases relative to the CCA percent cover. Values close to or greater than 1 suggest high disease occurrence; numbers close to zero indicate low occurrence. At Howland Island, CCA disease occurrence was quite low and variable over time, with only one type of disease registered in two of the nine survey years: one case of coralline white band syndrome in 2008, and four cases in 2010 (Figure 34). Fast CCA growth and accretion rates may be implicated in the transient nature of these disease occurrences. Interestingly, in 2006, CCA diseases at Howland were conspicuously absent; this contrasts with reports of notably high levels of disease in Palmyra Atoll, Kingman Reef, and American Samoa during the same survey year (Vargas-Ángel 2010).

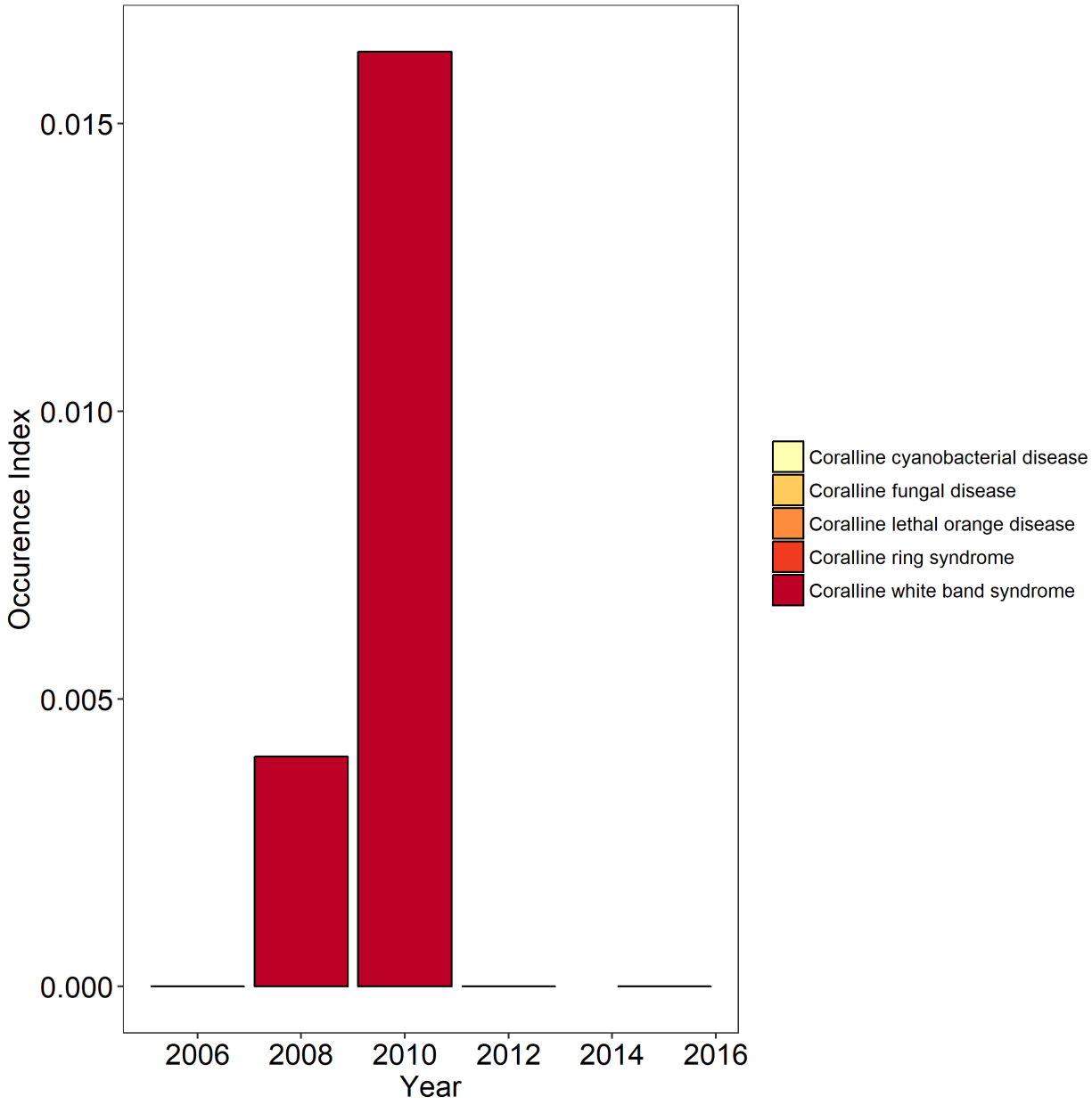

Figure 34. T**ime series of crustose coralline algae disease occurrences at Howland Island for all depth strata combined (>0–30 m) from Rapid Ecological Assessment surveys conducted from 2006 through 2015.**

Recent Coral Abundance

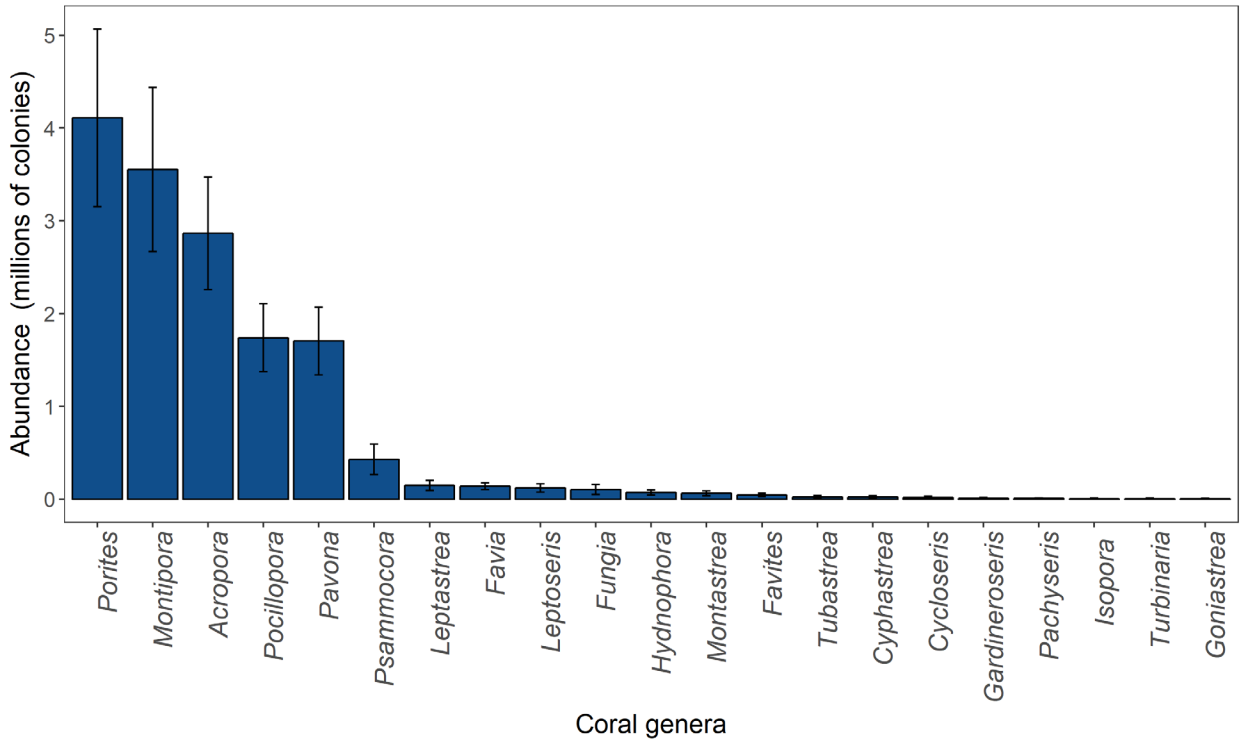

Figure 35. **Island-scale abundance (± 1 SE) estimates by coral genera for all depth strata combined (>0–30 m) at Howland Island from Rapid Ecological Assessment surveys conducted in 2015.**

Island-scale abundance estimates for coral genera were extrapolated from the REA transect colony densities over the area of hard bottom habitat found in the survey strata (0–30 m). In 2015, a total of 22 coral genera were enumerated at Howland and total abundance estimates indicated that *Porites* was the dominant taxon, and *Goniastrea* was the least abundant genus (Figure 35). Abundance estimates also indicated that *Porites*, *Montipora*, *Acropora*, *Pocillopora*, and *Pavona* together accounted for over 90% of all colonies.

Adult colonies dominated the coral community irrespective of depth; juveniles (colonies <5 cm) comprised approximately 20% of the coral population in each strata (Figure 36). For all genera combined, mean colony density of adults and juveniles decreased with depth. This pattern is likely driven by the density of *Porites*, *Montipora*, and *Acropora* combined. Contrastingly, this pattern was the inverse for other common coral taxa in the PRIMNM like *Pavona and Pocillopora*, whereby adult colony densities were greatest in the deep stratum (Figure 36).

Branching colonies of *Pocillopora* are typically fast growing and thrive in shallow, well-lit habitats. Low density of this taxon in the shallow stratum was probably due to space limitation by *Porites*, *Montipora*, and *Acropora*; this was likely the case for *Pavona* as well. *Acropora* sp. is also a sun-loving taxon; during the 2015 surveys, colony densities peaked in the mid-depth stratum with a mean density of 2.2 colonies/m^2 (± 0.4 SE). No juvenile *Acropora* sp. were found in the deep stratum (Figure 36).

Genus-specific differences indicate that community composition varied across survey depths in the forereef habitats around the island. These shifts likely reflect differences in the life histories of these genera, which impact their optimal depth range, as well as competitive abilities. However, the low colony densities of coral genera at various depths may also imply that larger colonies are present in these areas, not necessarily that the percent cover of coral is lower.

Sightings of the coral species *Acropora retusa*—listed under the Endangered Species Act (ESA) of 1973 (National Oceanic and Atmospheric Administration 2005)—were reported outside the BLTs during the 2015 surveys. One colony of the coral genus *Isopora* was reported on a BLT that same survey year. No further details are available regarding the sightings of these ESA-listed taxa. A table showing total generic richness of hard corals in the PRIMNM can be found in Appendix A of "Chapter 9: PRIMNM in the Pacific-wide Context."

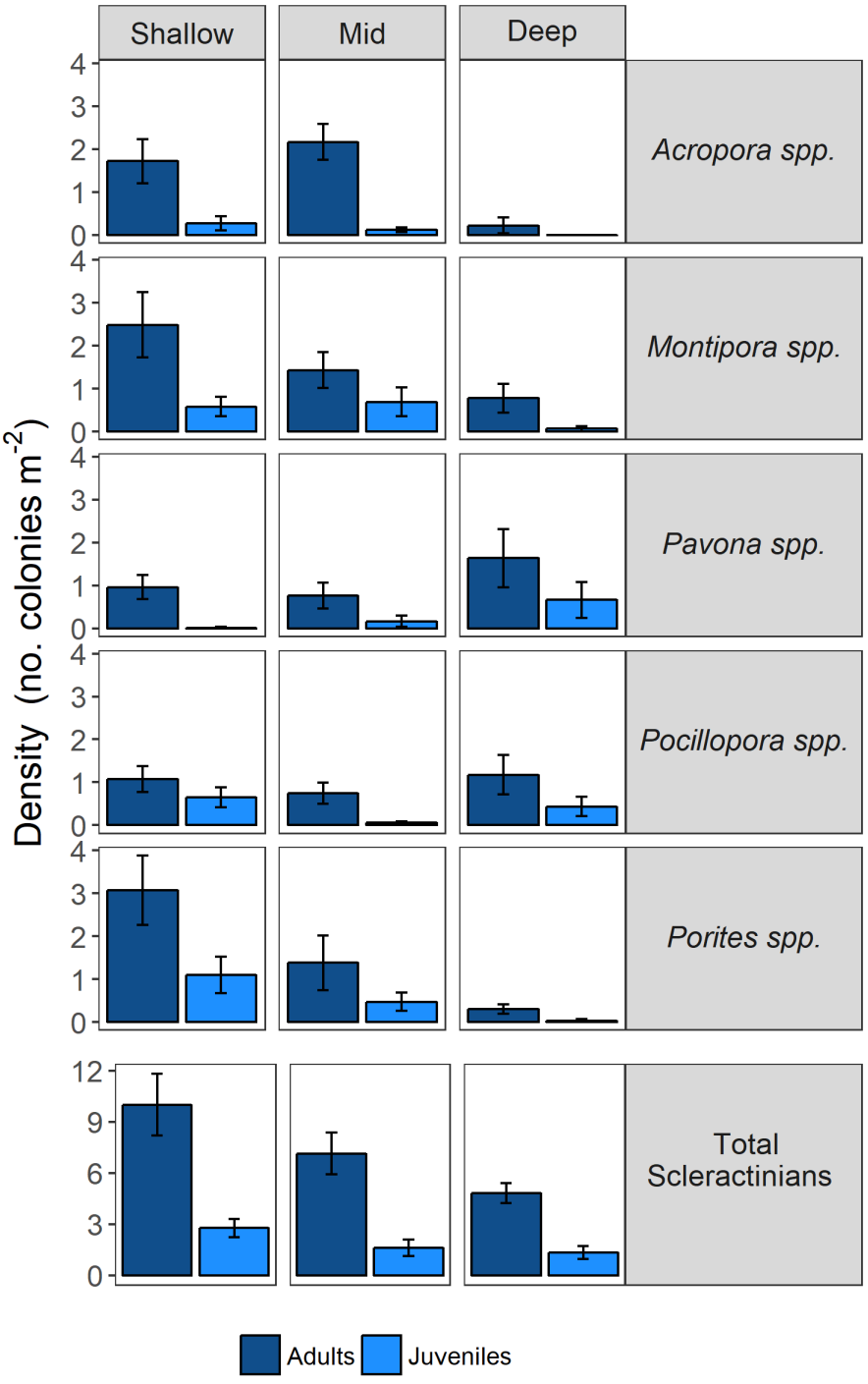

Figure 36. **Mean (± 1 SE) adult and juvenile colony density from Rapid Ecological Assessment surveys conducted at Howland Island in 2015 for shallow (>0–6 m), mid (>6–18 m), and deep (>18–30 m) depth strata for five coral genera generally abundant in the Pacific Remote Islands Marine National Monument (*Acropora* spp., *Montipora* spp., *Pavona* spp., *Pocillopora* spp., and *Porites* spp.) to facilitate comparison among islands.**

Time Series of Coral Abundance and Condition

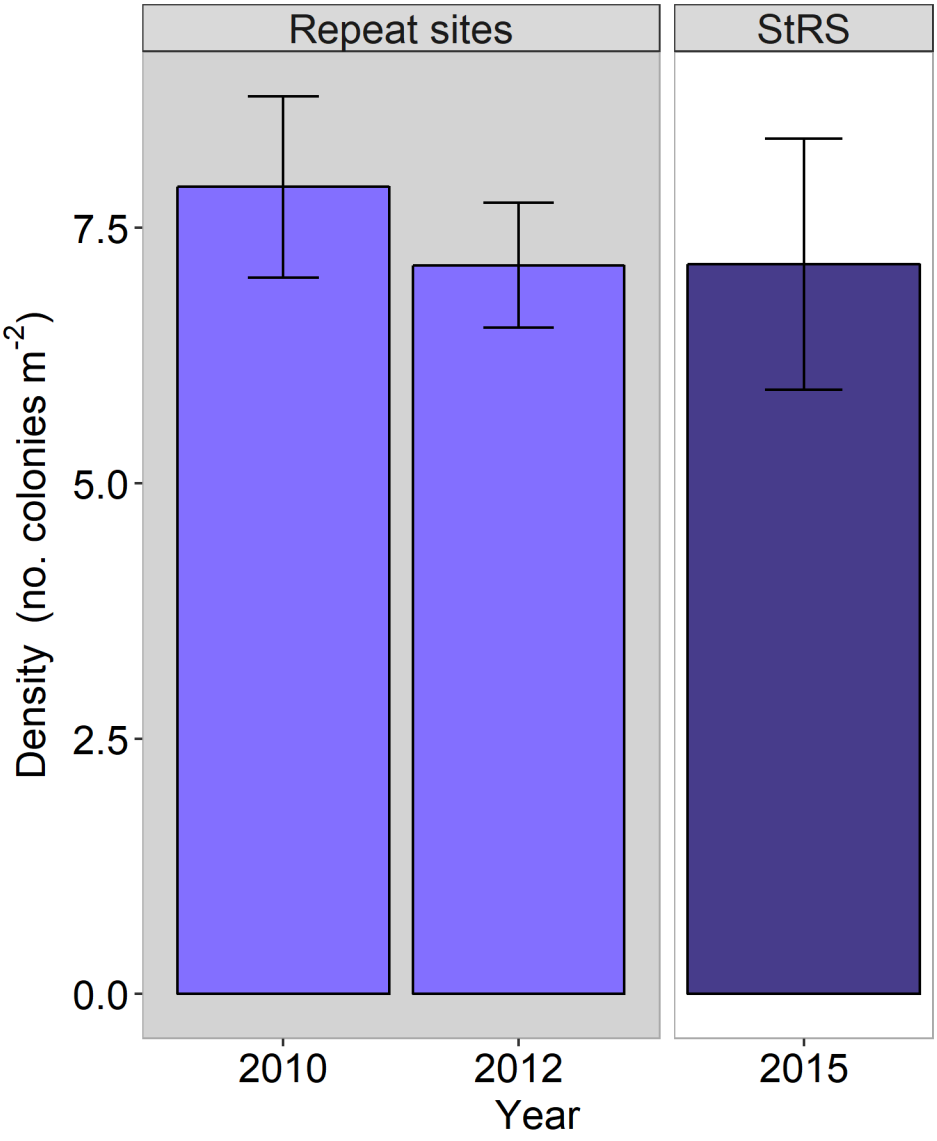

Figure 37. Time series of mean adult colony density (± 1 SE) at Howland Island, from mid-depth (>6–18 m) strata Rapid Ecological Assessment surveys by survey design, repeat sites or stratified-random sampling (StRS), conducted from 2010 through 2015.

From 2010 to 2015, mean coral colony density remained stable (Figure 37). Based on data collected at "repeat" sites, from 2010 to 2012 mean coral colony density decreased slightly (7.9 colonies/m^2 ± 0.9 SE; 7.1 colonies/m^2 ± 0.6 SE, respectively), but not ostensibly, as indicated by the overlapping error bars. Mean colony density remained stable between 2012 and 2015 (2015 mean = 7.1 colonies/m^2 ± 1.2 SE). While the difference in survey design necessitates caution when interpreting differences in data collected at repeat sites and StRS sites, the relatively comparable mean adult colony density across survey years suggests that in the recent past coral populations at Howland Island have remained relatively stable.

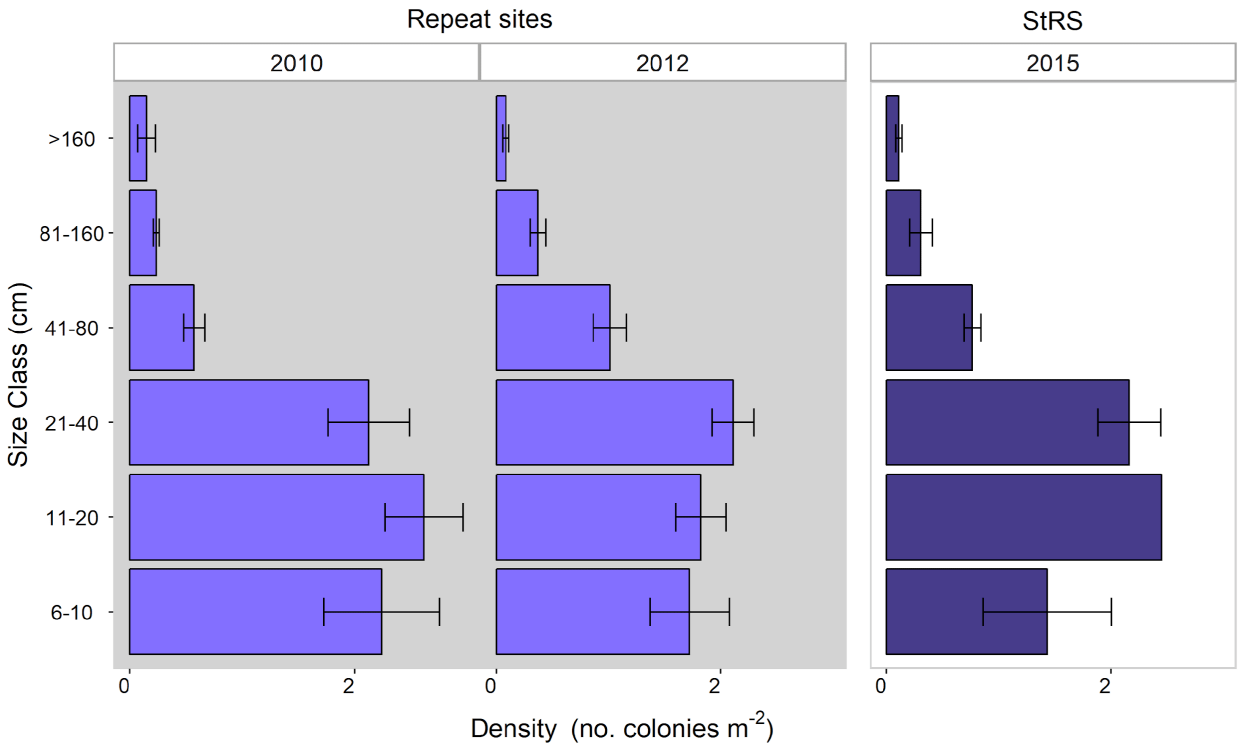

Figure 38. **Time series of mean adult colony density (± 1 SE) at Howland Island by size class from mid-depth (>6–18 m) strata Rapid Ecological Assessment surveys by survey design, repeat sites or stratified-random sampling (StRS), conducted from 2010 through 2015.**

Two main patterns are evident when reviewing the time series of adult colony densities illustrated in Figure 38. First, the coral size frequency distributions had a unimodal pattern where the majority of the colonies were in the moderate-size classes (11–40 cm); smaller (5–10 cm), presumably younger colonies were present together with a few large (>81 cm) colonies that have survived many decades. Furthermore, despite subtle variations, the unimodal pattern was consistent across years and survey methods. Importantly, coral size-frequency curves holding the above pattern (i.e., skewed to the larger/older colonies) are indicative of healthy coral populations (Bak and Meesters 1998). In addition, the fact that this pattern has held consistently since 2010 suggests some level of stability in the coral population.

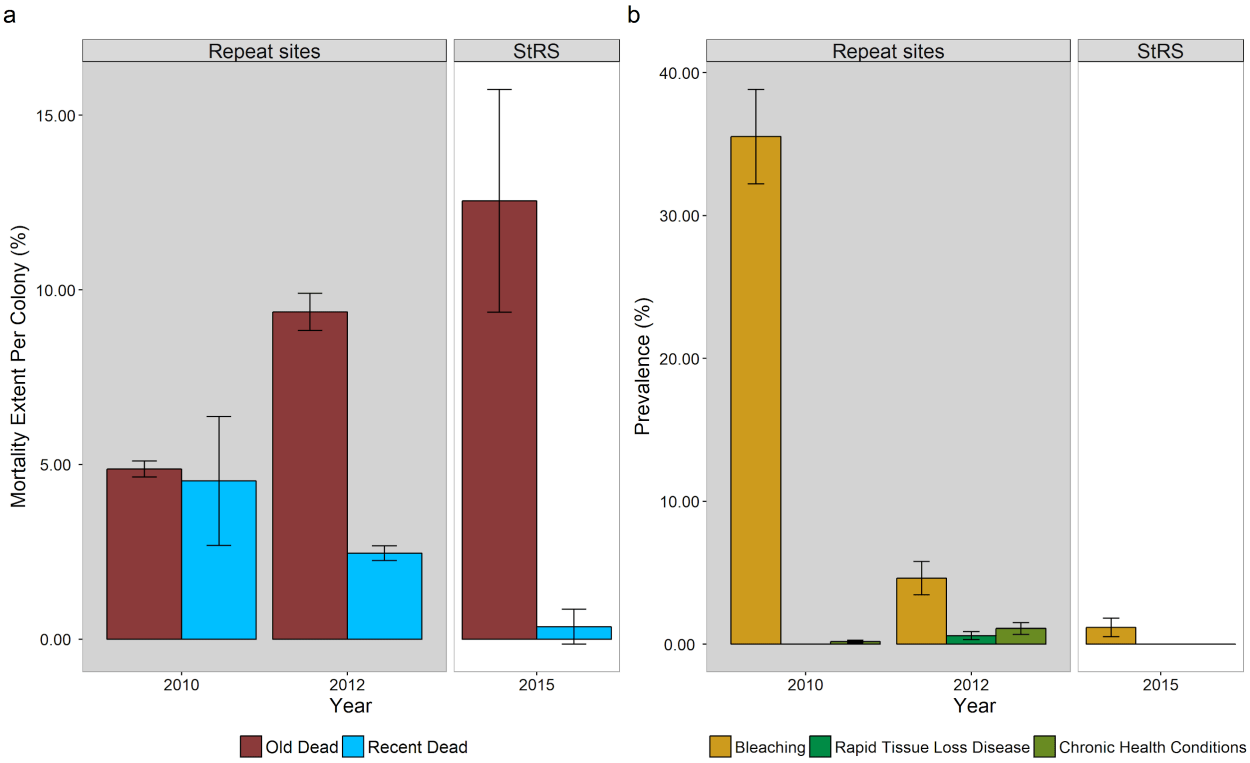

Figure 39. Time series of mean (± 1 SE) (a) percent partial mortality and (b) prevalence of bleaching, rapid tissue loss diseases, and chronic health conditions at Howland Island based on mid-depth (>6–18 m) strata Rapid Ecological Assessment surveys by survey design, repeat sites or stratified-random sampling (StRS), conducted from 2010 through 2015.

Old coral mortality at Howland Island increased during the study period, and those increases were proportional to the accumulated recent mortality from the previous year (Figure 39a). In other words, recently dead coral surfaces became "old dead" during the subsequent survey years. The two-fold increase in old mortality between 2010 and 2012 was the result of mass coral bleaching (Figure 39b) and consequent recent coral mortality associated with the 2009–2010 El Niño event and documented during the 2010 surveys (Vargas-Ángel et al. 2011). Notably, that two-fold surge in old mortality is underpinned by an approximately 20% decrease in coral cover detected on TDS between 2010 and 2012 (Figure 33). Later, between 2012 and 2015, old mortality increased again, commensurate to the amount of recent dead detected in 2012. Prevalence of bleaching, rapid tissue loss diseases, and chronic health conditions in 2012 amounted to approximately 6% (Figure 39b). Although plausible, it is not absolutely certain that these two drivers accounted for the increased old mortality between survey years. Subsequently, bleaching prevalence has remained at background levels (range ~1–5%).

Overall and across survey years, the prevalence of coral diseases was low. Rapid tissue loss diseases were only present in 2012, albeit at low levels of prevalence (mean = 0.6% ± 0.3). Additionally, the mean prevalence of chronic compromised health conditions also remained at low background levels, decreasing in recent years from 1.1% (0.4 SE) in 2012 to absent in 2015. While the difference in survey design necessitates caution when interpreting differences in data collected at repeat sites and StRS sites, excluding the 2010 bleaching event, low background

levels of coral disease suggest that in the recent past, corals at Howland Island have remained relatively disease-free.

Benthic Macroinvertebrates

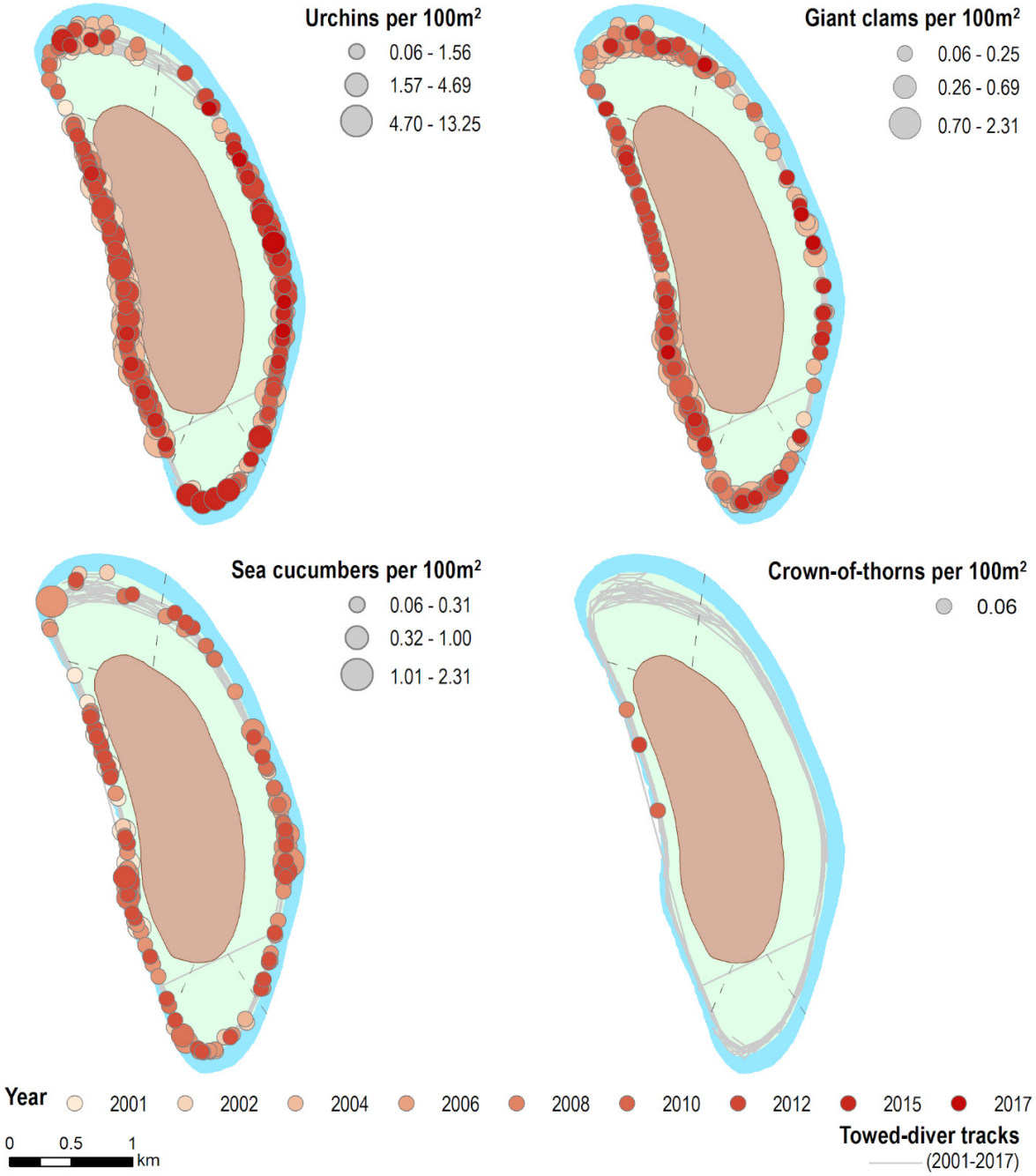

Figure 40. Density of conspicuous, ecologically- or economically-important macroinvertebrates (urchins, crown-of-thorns sea stars, giant clams, and sea cucumbers) observed per segment from benthic towed-diver surveys (TDS) conducted throughout all depth strata (>0–30 m) around Howland Island from 2001 through 2017. Sea cucumber observations were discontinued from TDS in 2014.

Urchins were observed in all survey years to be broadly and relatively homogeneously distributed spatially around Howland (Figure 40). There only a couple of focal absences of sea urchins at the boundary between the North and East georegions, as well as the western boundary of the South georegion. The highest densities of urchins per segment were observed in 2004, with a maximum density of 13 individuals per 100 m^2 found in the West georegion.

Giant clams—currently under status review (Federal Register 2017)—also had broad spatial distribution around Howland; however, they were most abundant in the South, West, and North georegions (Figure 40). While spatially ubiquitous, giant clam densities were low overall (<2.3 individuals per 100 m^2).

Crown-of-thorns sea star sightings around Howland were exceptionally rare, with only three individuals recorded during a total of 522 TDS segments since the inception of the monitoring surveys in 2001: one each in 2008, 2010, and 2012 (Figure 40).

Finally, while sea cucumber observations were discontinued from TDS in 2014, occurrences were recorded during each survey year except for 2001, with the highest densities recorded in 2008 (Figure 40). Sea cucumbers were broadly distributed around Howland, though the highest densities were observed in the West and East georegions. Individual segment densities peaked at 2.3 individuals per 100 m^2.

*A gray reef shark (*Carcharhinus amblyrhinchos*) cruises through a school of anthias (*Luzonichthys whitleyi*) and redtooth triggerfish (*Odonus niger*).*
Photo: Molly Timmers, NOAA Fisheries.

Microbiota

7.5 Microbiota

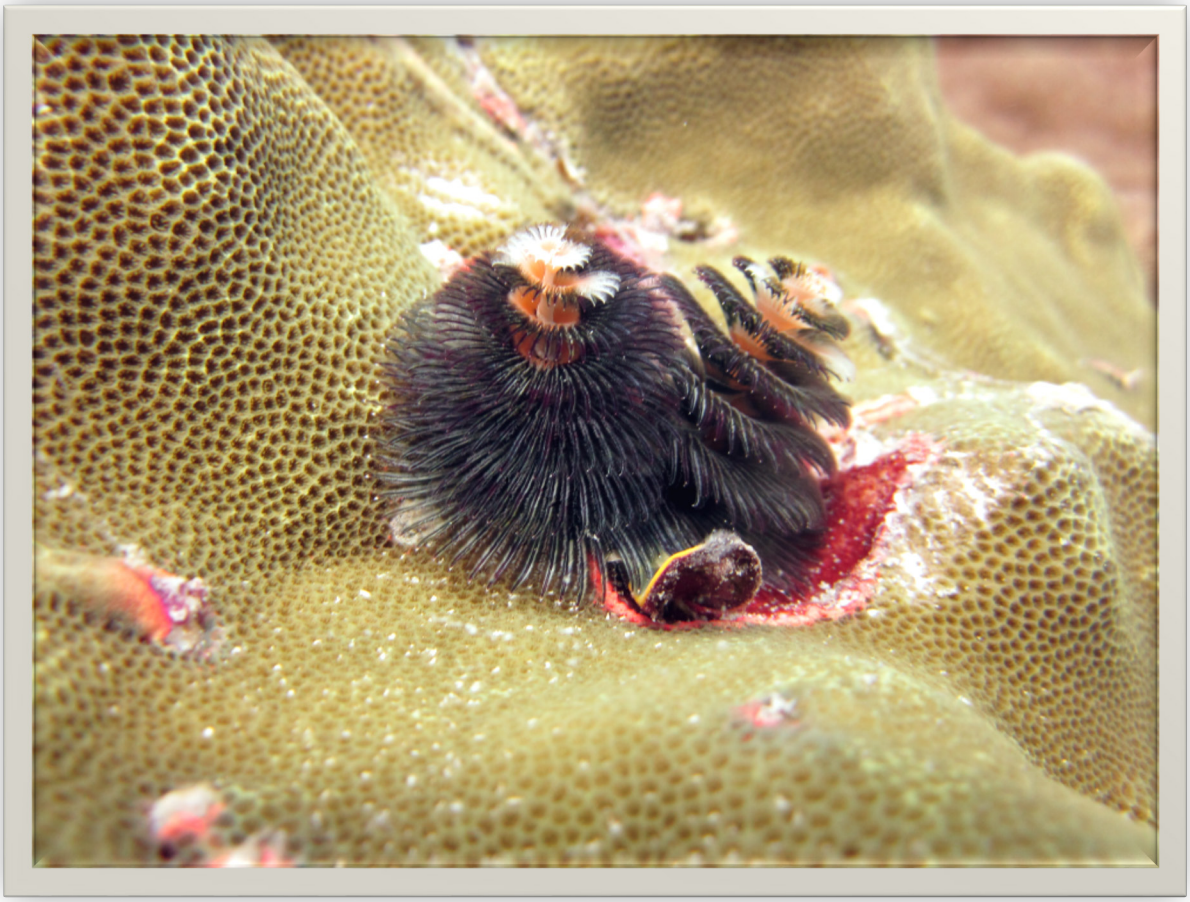

Christmas tree worms on coral at Howland Island.
Photo: NOAA Fisheries.

The reef microbiota facilitates the cycling of essential nutrients by breaking down organic materials released by photosynthetic picoplankton (e.g., cyanobacteria) and benthic macroorganisms (corals and macroalgae). Habitats dominated by reef-building organisms (i.e., stony corals and calcified algae), such as Howland Island, illustrate a functional role that suppresses the energetic losses through microbial catabolism and promotes trophic transfer of energetic resources, carbon and inorganic nutrients, into metazoan food webs. Reef water samples were collected from all RAMP sites across the U.S. Pacific Islands region beginning in 2008, with the first PRIMNM samples measured in 2009 (i.e., Wake and Johnston Atolls) and 2010 (i.e., Jarvis, Howland, and Baker Islands, Palmyra Atoll, and Kingman Reef). The assessment and monitoring of the reef microbiota paired with data collected on benthic and pelagic macro-biota across the entire U.S. Pacific Islands region allow for characterization of coral reefs from a molecular to an ecosystem scale.

Microbial Composition and Diversity

Microbial communities in reef waters were collected from RAMP sites across all U.S. Pacific Islands from 2012 to 2014. Reef water samples were processed for molecular identification of microbial populations using metagenomic sequencing. Microbial community composition at Howland Island is characterized by mid to higher than average community diversity (measured using the Shannon Index, a metric of both species richness and evenness) on average compared to other U.S. islands across the Pacific (Figure 41). The community structure of the microbes at Howland reflects the complex and nutrient-rich organic material released by coral-dominated systems and the enhanced niche space characteristic of intact reef habitats which promotes biodiversity across macro- and microbiota.

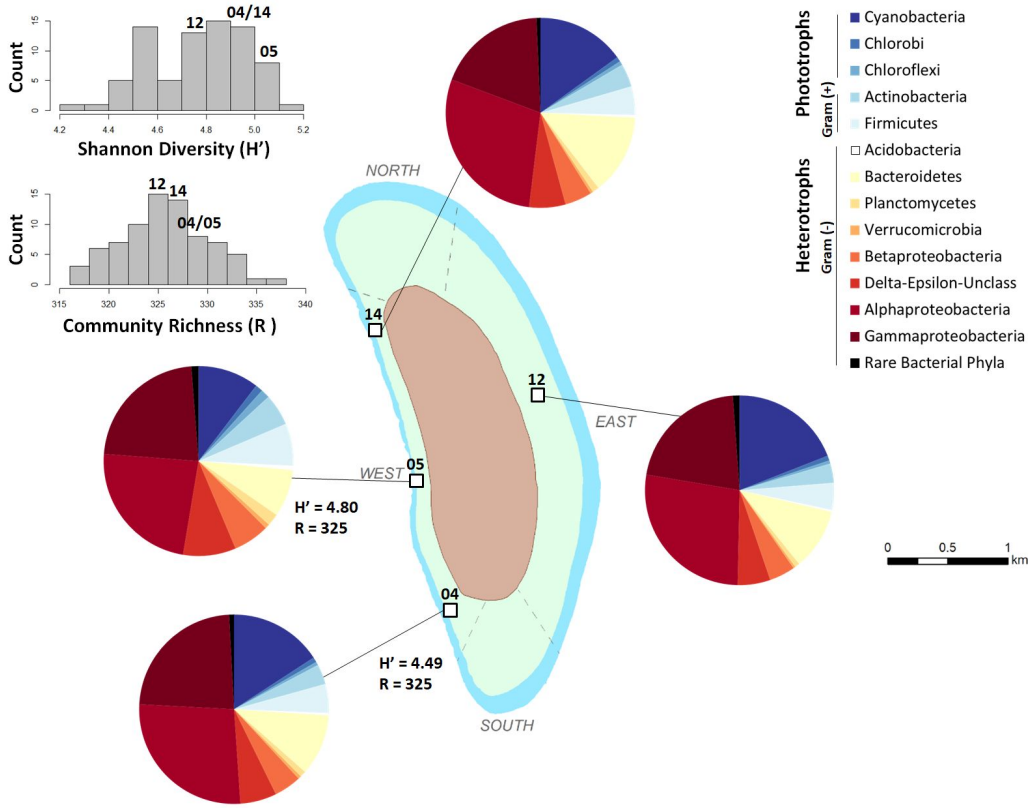

Figure 41. Microbial composition and diversity at Howland Island. The microbial taxonomic groups are shown at Phylum Level. Delta-Epsilon-Unclass, Deltaproteobacteria, Epsilonproteobacteria and Unclassified Proteobacteria are all combined. Community Richness and Diversity were calculated at the Genus Level. H', Shannon Index. R, Rarified Richness. Comparison of microbial diversity at four Howland reefs collected in 2012 (Sites 04, 05, 12, and 14) overlaid on a histogram of all Richness and Diversity observations across the U.S. Pacific islands collected between 2012 and 2014 (n = 77 reef sites).

Microbial Biomass on Reefs

Microbial biomass at Howland Island and other remote equatorial islands that experience equatorial and topographic upwelling (e.g., Baker and Jarvis), is higher than on remote atolls that do not experience strong upwelling (Figure 42). Reef degradation towards algae-dominated

states promotes greater cell biomass and higher proportions of fast growing heterotrophic taxa (as observed on the main Hawaiian Islands), which exhibit more microbial biomass in the overlying reef waters (i.e., Howland in 2015 = 32 mg m^{-3} and Oahu in 2008 = 153 mg m^{-3}, respectively). The associated changes in microbial community structure and growth strategies when benthic community composition shifts from corals to algae shunts much more of the energy produced by the system towards decomposition pathways with enhanced respiration of organic compounds to carbon dioxide. This phenomenon is referred to as microbialization.

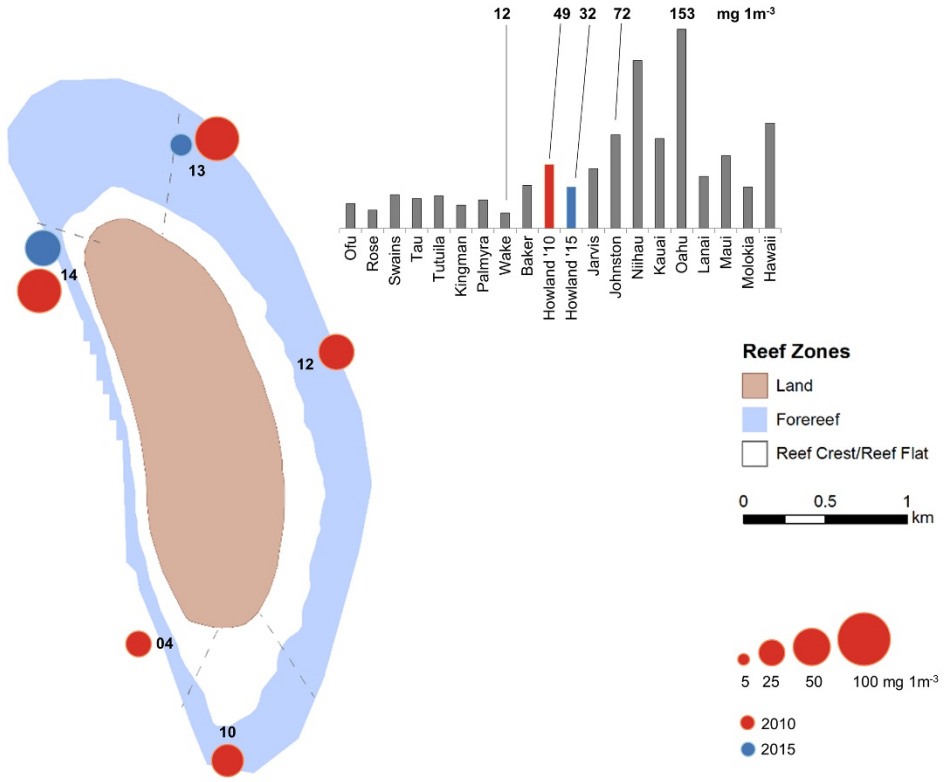

Figure 42. Microbial biomass collected at Howland in 2010 and 2015 (n = 8). Cell volume is estimated based on measurements of cell length and width and cell abundances enumerated using epi-fluorescent microscopy. Biomass is reported as milligrams per cubic meter (mg m^{-3}). The 2010 data were published in McDole et al. (2012).

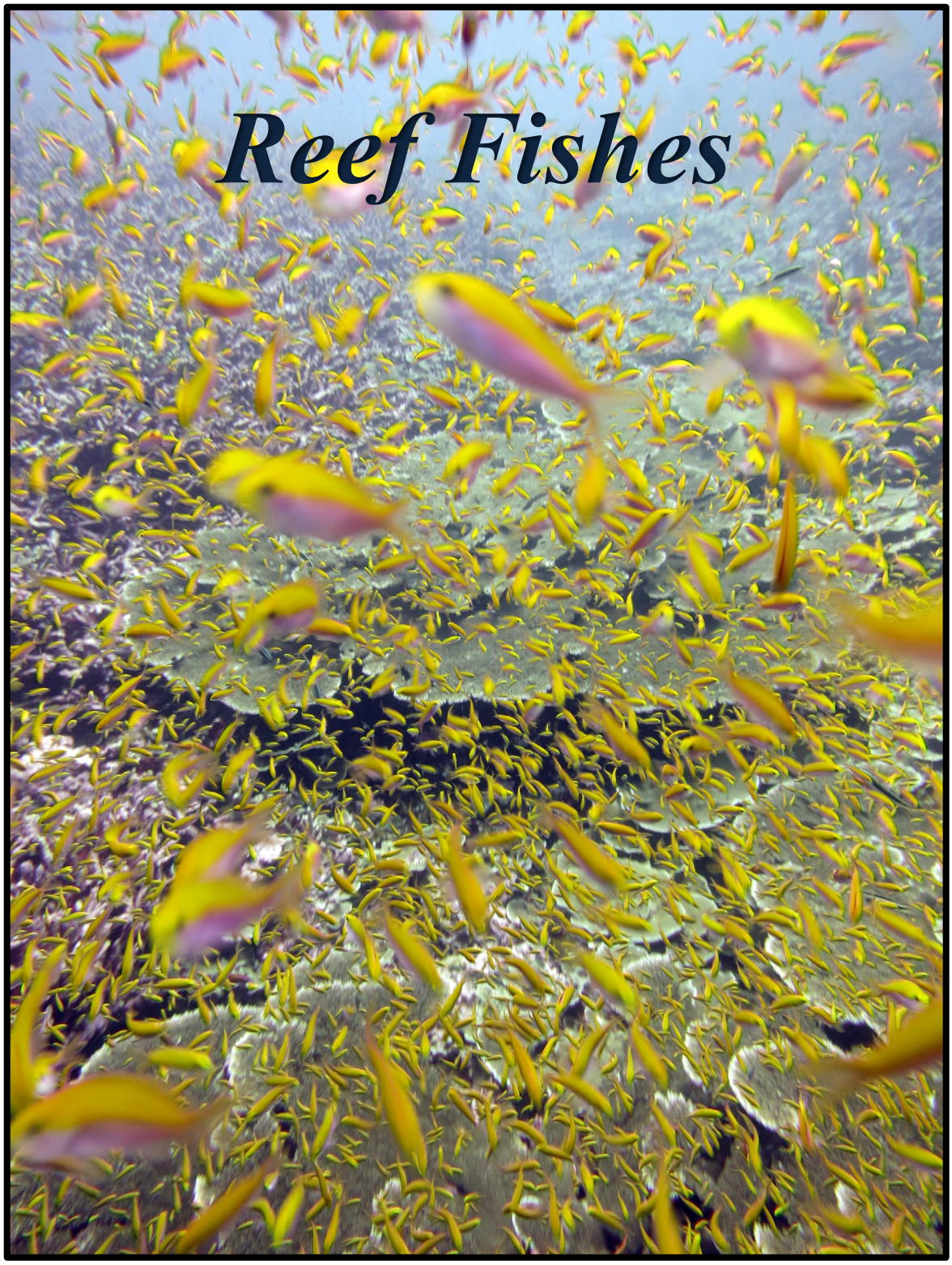

A school of anthias swarms over the reef at Howland Island.
Photo: Marie Ferguson, NOAA Fisheries.

7.6 Reef Fishes

A school of anthias swarms over the reef at Howland Island.
Photo: Kevin Lino, NOAA Fisheries.

Survey Effort and Site Information

Reef fishes were surveyed at Howland Island on eight occasions in the period 2001 through 2015, and to a limited degree in 2017 for a supplementary survey effort (Table 4). Reef fish surveys were a mix of comprehensive small-area surveys (belt-transect [BLT] or stationary point count [SPC]), and broad-scale (~2.2 km) towed-diver surveys (TDS) that focused on large-bodied fishes (>50 cm total length).

TDS were mostly conducted along forereef habitats approximately 10–20 m deep. BLTs, which were utilized between 2001 and 2008, were mostly conducted at haphazardly-located, typically mid-depth (~10–15 m) outer forereef sites, with the majority of sites on the west side of the island (Figure 42). In 2008, Pacific RAMP initiated the transition from BLT surveys to the current SPC survey method. In that year, SPC sites were all located on the west side of the island, but by 2010, the surveys had moved to a stratified-random design encompassing all hard-bottom habitats shallower than 30 m around Howland Island (Figure 25). Since that time, there have also been concerted efforts to increase the number of survey sites per visit, with 16 surveyed in 2010, 39 in 2012, and 35 in 2015, compared to 6 or fewer prior to 2008 (Table 4).

One consequence of the shift in survey design is that SPC sites have been much more widely spread around the island than BLT sites (Figure 43). Because of some inconsistency in the application of the BLT survey method in the program's earliest years, data from before 2003 were not used to generate quantitative estimates, such as density. Similarly, BLT data gathered at the time methods changed to the stratified-random design in 2008 cannot be meaningfully comparable with earlier BLT data gathered at fixed locations. Thus, the time series trends shown were built exclusively from TDS for the period 2001 through 2017, and the SPC surveys conducted for the period 2010 through 2015.

Table 4. **Reef fish survey effort at Howland Island. Data are number of surveys by year and method. Towed-diver surveys (TDS) were ~2 km long by 10 m wide transects (~20,000 m^2), typically in mid-depth forereef habitats in which divers counted only fishes >50 cm total length (TL). In contrast, during belt-transect (BLT) and stationary point count (SPC) surveys divers counted all fishes within small areas of reef (~350–600 m^2).**

	All Fishes		Large Fish (>50 cm TL)
Year	BLT	SPC	TDS
2001	6	–	2
2002	5	–	3
2004	5	–	8
2006	6	–	6
2008	10	10	7
2010	–	16	10
2012	–	39	9
2015	–	35	5
2017	–	–	5

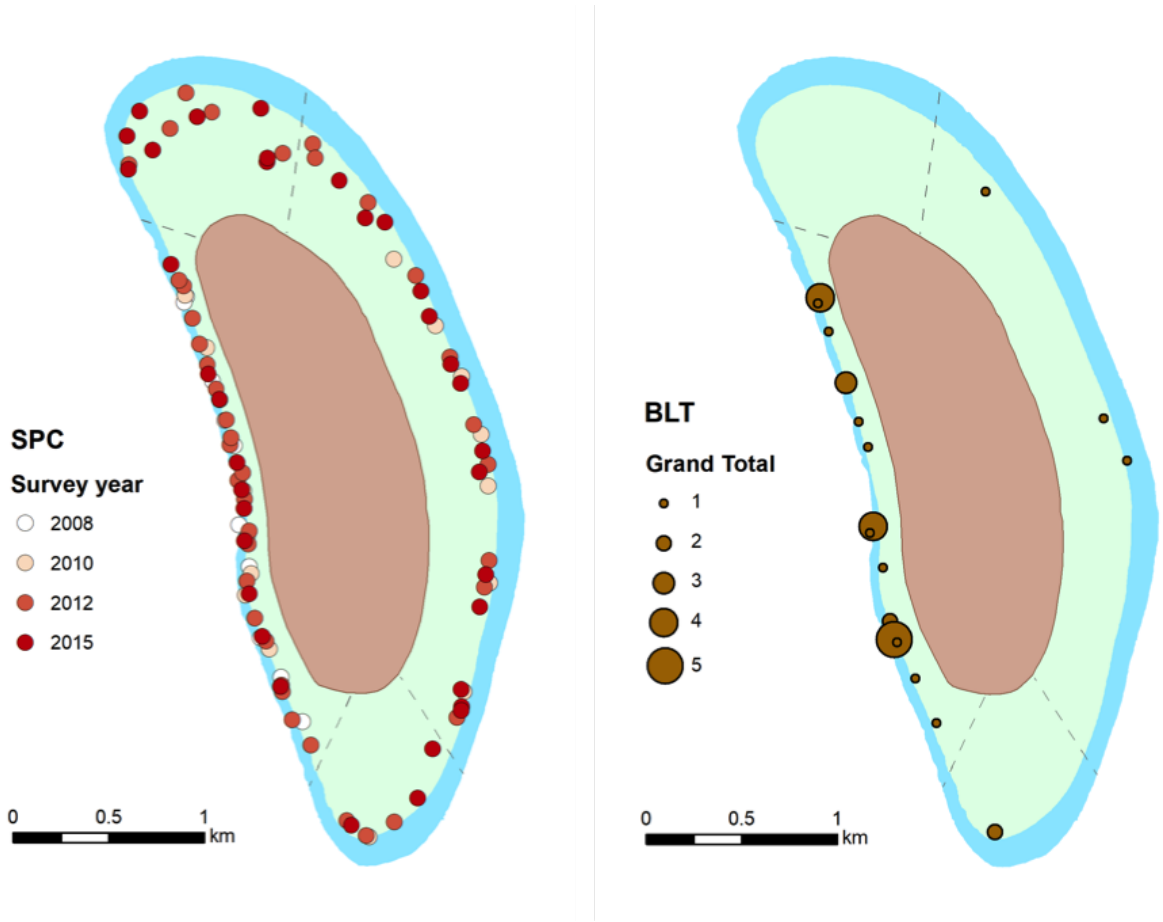

Figure 43. Location of belt-transect (BLT) and stationary point count (SPC) sites at Howland Island. SPC sites were not revisited, though the SPC survey year is distinguished by color. BLT survey sites were generally revisited during multiple survey years, and the total number of times each site was surveyed is indicated by the size of the bubble.

Distribution of Reef Fish Biomass and Abundance

Reef fish biomass was generally evenly distributed around Howland Island, with high biomass recorded at a large proportion of sites in all georegions (Figure 44). Mean total fish biomass was marginally higher in the South georegion than elsewhere, largely driven by high biomass of planktivores and piscivores (Figure 44). However, there were also few surveys in the South georegion—only 7 SPC sites in total—hence, the significance of that difference is unclear.

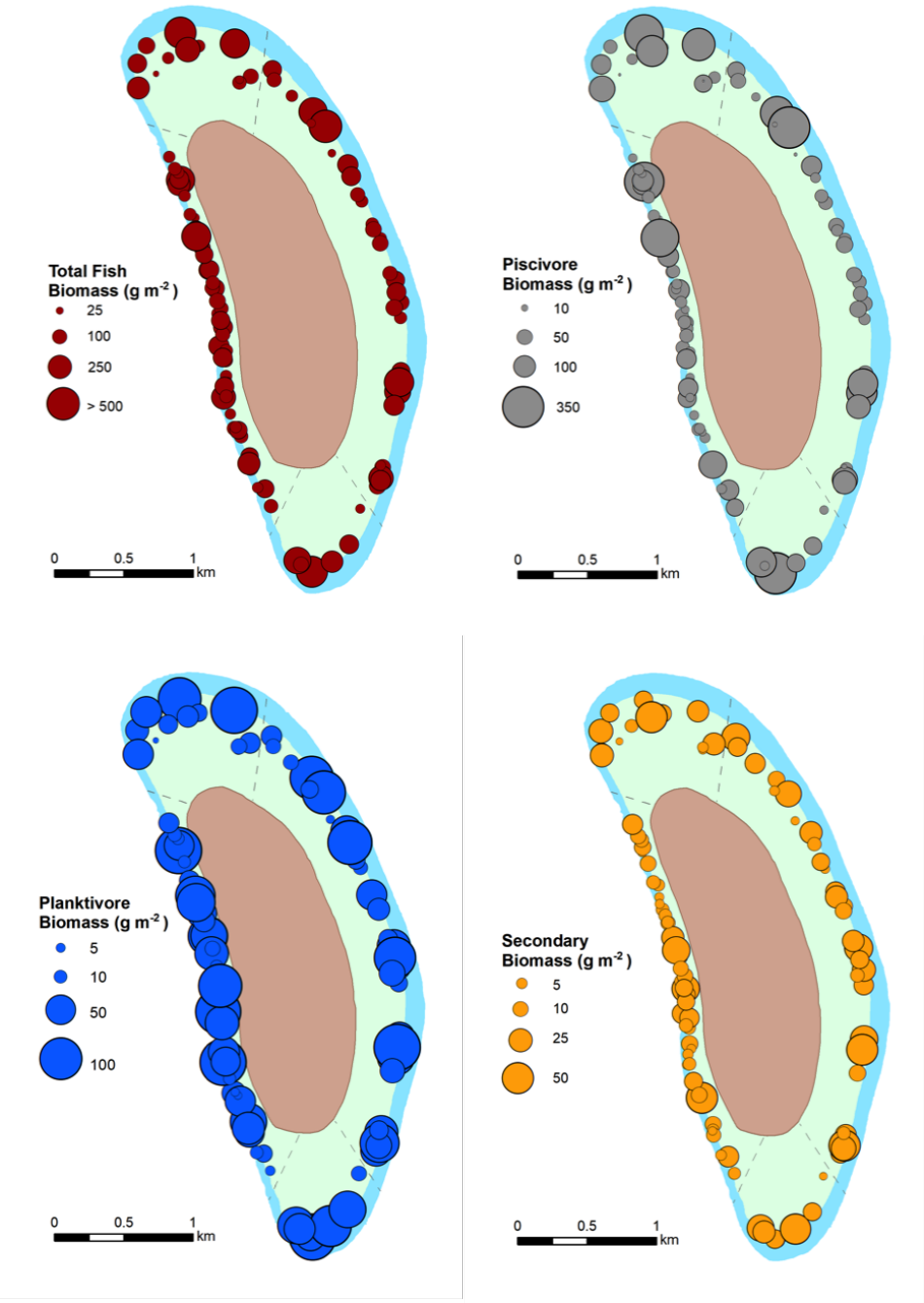

Figure 44. Biomass maps of Total fish, Planktivore, Piscivore and Secondary Consumer Groups around Howland Island from stationary point count over the period 2008 through 2015. Secondary consumers included omnivores and invertivores, comprising many abundant and generally small-bodied species.

Planktivorous fish biomass around all parts of the island was made up of a wide variety of species, including the sleek and bignose unicornfishes (*Naso hexacanthus, N. vlamingii*), the brick and blotcheye soldierfishes (*Myripristis berndti, M. amaena*), the dark-banded and yellow-and-blueback fusiliers (*Pterocaesio tile, Caesio teres*), as well as the superabundant, small-

bodied anthias (olive and Bartlett's, *Pseudanthias olivaceus* and *P. bartlettorum*) that were a highly conspicuous component of the reef fish assemblage at many sites.

Herbivorous fish biomass was also evenly distributed around the island, although tending to be higher in the West georegion (Figure 45). Herbivorous fish assemblages were diverse in all areas (i.e., not dominated by a few species). However, major contributors to biomass included the whitecheek and striped-fin surgeonfishes, as well as the orangespine unicornfish (*Acanthurus nigricans*, *Ctenochaetus marginatus*, *Naso lituratus*). Commonly observed parrotfishes included several large-bodied species: the redlip, tricolor, and bridled (*Scarus rubroviolaceus*, *S. tricolor*, *S. frenatus*).

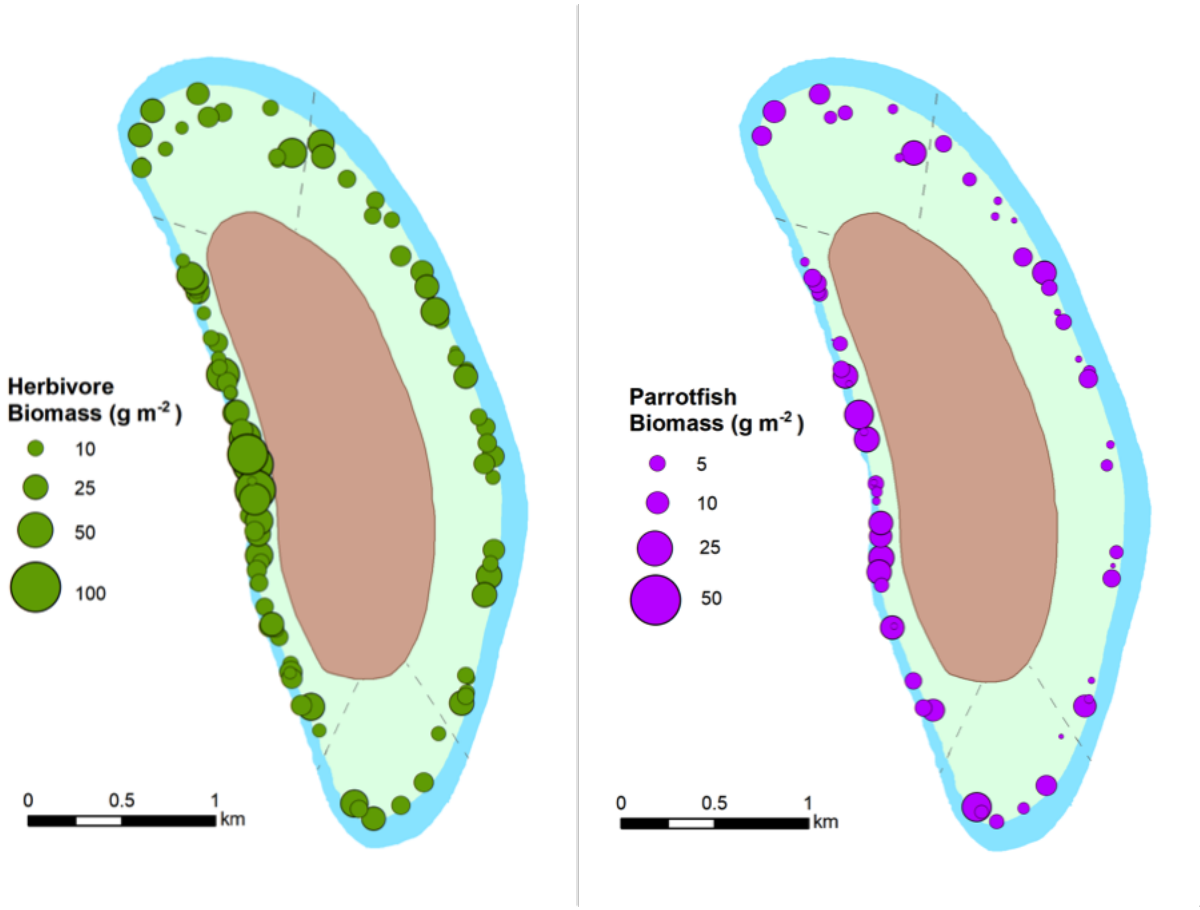

Figure 45. **Total herbivorous fish and parrotfish biomass from stationary point count surveys around Howland Island over the period 2008 through 2015.**

Gray reef sharks (*Carcharhinus amblyrhynchos*) were the most commonly observed shark species in all georegions, followed by blacktip reef sharks (*Carcharhinus melanopterus*). Overall, sharks were observed on 50% of all TDS segments (~220 m long sub-units of the survey), including nearly 80% of all segments in the South georegion where shark biomass was highest (Figure 46).

Biomass of other predatory species was more evenly distributed around the island, but also tended to be higher in the south, largely due to higher biomass of the two-spot snapper (*Lutjanus*

bohar) at sites there. That species was, however, common across all georegions, comprising the largest component of non-shark piscivorous fish biomass in all georegions. Other substantial components of piscivorous fish biomass included a diverse assemblage of groupers (Serranidae) and trevally jacks, particularly the bluefin and black (*Caranx melampygus, C. lugubris*). Infrequent encounters with schools of barracuda also added to total piscivore biomass.

Humphead wrasse (*Cheilinus undulatus*) have been very infrequently observed at Howland Island—there have only been 6 sightings in total across all the fish surveys conducted for Pacific RAMP, all of which were in the West and South georegions (Figure 46). Pacific RAMP survey divers have not recorded any observations of the bumphead parrotfish (*Bolbometopon muricatum*) at Howland.

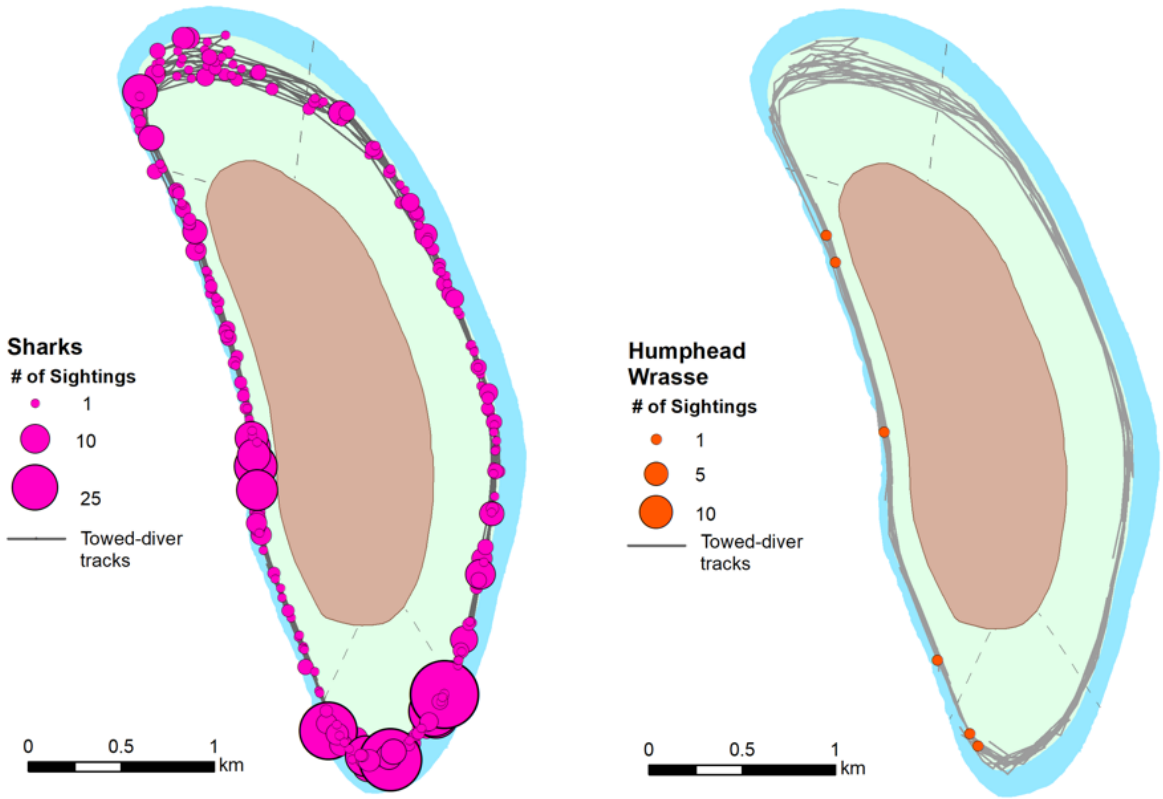

Figure 46. Towed-diver survey sightings of sharks and humphead wrasse around Howland Island during the period 2001 through 2017.

Distribution of Other Species of Interest

Manta rays (*Mobula* spp.) have been sighted during TDS at Howland Island during approximately 3% of all tow segments—most commonly in the West georegion (Figure 47). It is important to recognize that divers cannot readily and reliably distinguish between *Mobula birostris*, the giant manta, which is listed under the ESA, and the reef manta, *Mobula alfredi*, which is not.

Sea turtles were also commonly sighted during the TDS: green sea turtles (*Chelonia mydas*) have been recorded during approximately 16% of TDS segments, and hawksbill sea turtles (*Eretmochelys imbricata*) during approximately 1% of all segments. Both of those species are currently ESA listed. Green sea turtles were most frequently seen during TDS segments in the West and East georegions (27% and 16%, respectively, of segments there), but were rarely encountered in the North georegion (3% of segments, Figure 47).

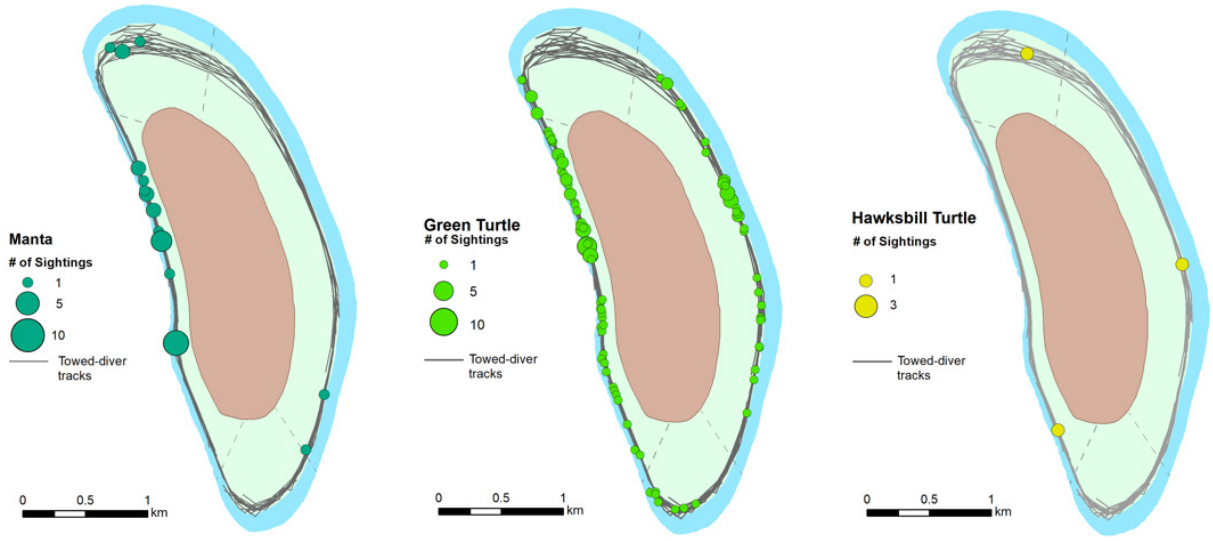

Figure 47. Towed-diver sightings of manta rays and sea turtles around Howland Island during the period 2001 through 2017. Green sea turtle sightings include observations recorded as (unspecified) sea turtle, as the great majority of sea turtles seen at Howland were green sea turtles.

Reef Fish Time Series

Time series of reef fish biomass, incorporating data from both BLT and SPC surveys, are shown in Figure 48. As is evident from the size of the confidence intervals in early years, there were generally insufficient data from earlier survey periods to identify clear patterns or changes. Based on the SPC data that were collected during the period 2010 through 2015, there are also no clear indications of change. Specifically, the scales of difference among years are small relative to the uncertainty in the data (represented by the errors bars). However, there are indications of lower biomass of parrotfishes in 2015, as well as small rises in planktivores and piscivores after 2010 (Figure 48).

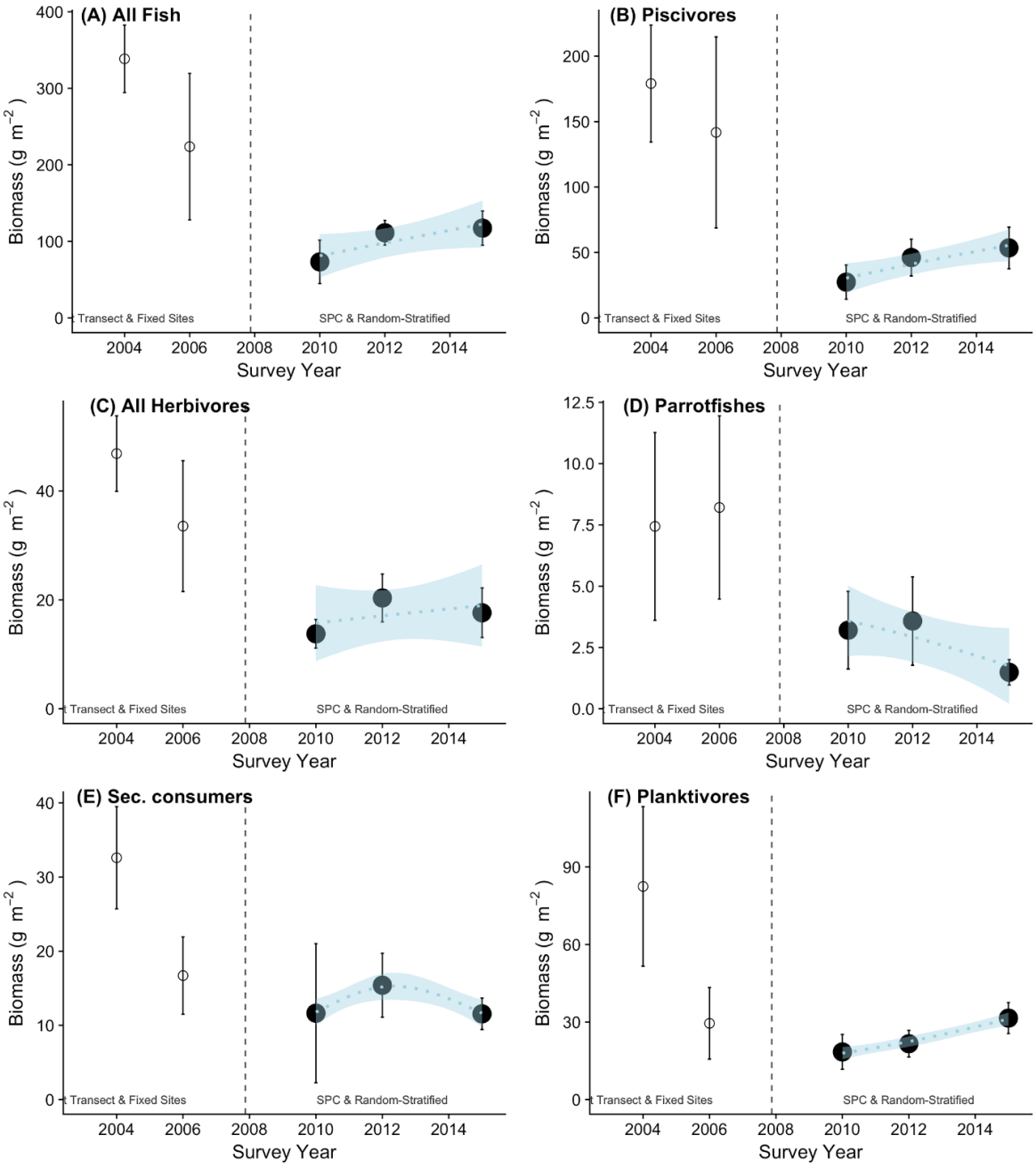

Figure 48. Time series of reef fish biomass at Howland Island. Data are shown for belt-transect surveys conducted at a limited number of mid-depth forereef sites in 2004 and 2006, and stationary point count (SPC) surveys conducted at randomly located sites encompassing all hard-bottom forereef in water depths <30 m over the time period 2010 through 2015. Circles indicate mean values and vertical bars represent standard error per time period. The light blue dotted trend line and 95% confidence intervals added for visualization purposes were derived from generalized additive models of biomass against survey year. Biomass values from the different periods cannot be directly compared due to differences in methods and survey locations.

Based on TDS data, there were no clear trends in overall shark or jack abundance at Howland Island (Figure 49). The peak of jack abundance, in 2004, occurred as a result of an encounter with a large school of bigeye trevally (*Caranx sexfasciatus*) in the South georegion, and the peaks in 2008, and to a lesser extent 2010, were largely related to encounters with schools of 100 or more rainbow runners (*Elagatis bipinnulata*) at a variety of locations around the island. Both species were also observed in other years, but not recorded in such large numbers. Somewhat higher counts of reef sharks in years from 2004 through 2008 were primarily driven by one or two encounters with large numbers (40–75 individuals) of gray reef sharks (*Carcharhinus amblyrhynchos*) in each of those years. Thus, the high variability in recorded abundance among years for both sharks and jacks was very likely due to inherent natural variability and extreme patchiness of several roving, predatory species, combined with relatively low sample size (i.e., between 6 and 10 TDS in each year).

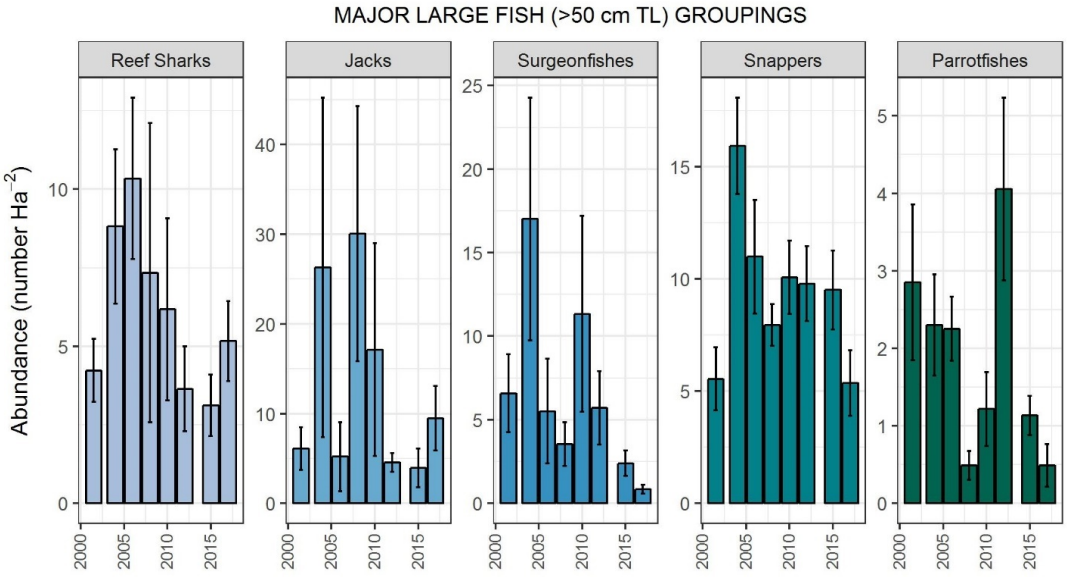

Figure 49. **Bar plots by year for reef sharks, jacks, surgeonfishes, snappers, and parrotfishes from towed-diver surveys (TDS) around Howland Island over the period 2001 through 2017. Data shown are mean and standard error. Note that 2001 and 2002 data are pooled due to low sample sizes in those years. In order to increase consistency among years, trends were derived only from TDS >500 m in length, which were conducted in forereef habitats between 10 and 20 m deep.**

Relatively few surgeonfishes are large enough to regularly be recorded during TDS (in which only fishes larger than 50 cm are counted). Therefore, variability in towed-diver counts for those groups (Figure 49) is not indicative of larger change for the majority of species in those families. Surgeonfish counts primarily reflect the frequency of encounters with schools of large-bodied unicornfish (*N. hexacanthus, N. vlamingii*), and thus have high natural variability. At Howland Island, the great majority of towed-diver observations of parrotfishes were of the redlip parrotfish (*Scarus rubroviolaceus*). In 2012, divers encountered 35 individuals of that species during a single TDS.

Species Lists, Encounter Rates and Diversity

Mean species richness of reef fishes around Howland Island was relatively high compared to other islands of the PRIMNM, averaging 33.8 species per survey. Richness was lower and evenness higher in 2010 than in later years, but there was no consistent trend in richness or evenness at Howland over the period 2010 through 2015 (Figure 50).

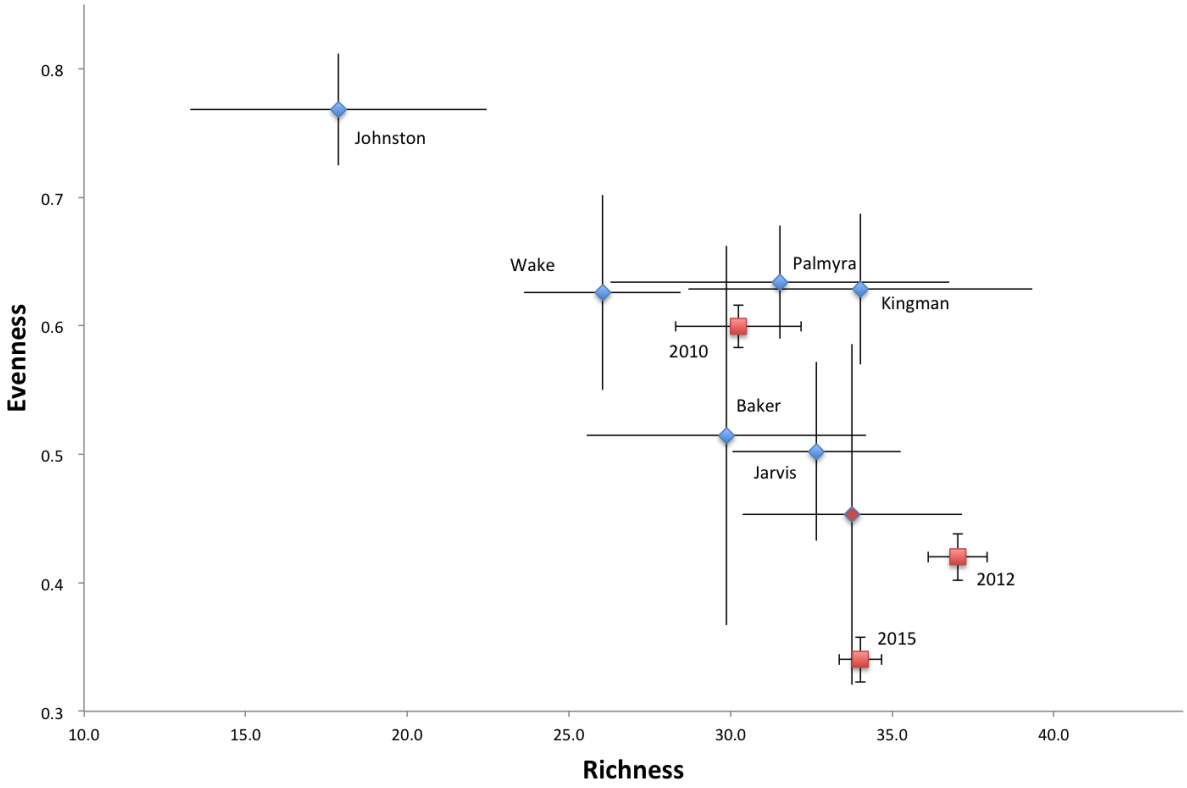

Figure 50. Richness vs. evenness. Red squares are species richness (the number of species encountered per survey) and evenness (how equally distributed the total fish abundance was among species) values (± SE) at Howland Island by year. Blue circles represent mean (± SD) of richness and evenness values for other islands in the Pacific Remote Islands Marine National Monument across all years. The single red dot represents the mean values of richness and evenness at Howland across all years. For consistency among locations, only data from forereef areas are included.

As noted above, the green sea turtle (*Chelonia mydas*) and hawksbill sea turtle (*Eretmochelys imbricata*) are ESA listed, as are the giant manta (*Mobula birostris*). Although divers have observed manta rays at Howland, it is not possible for divers to reliably distinguish between the giant manta and the reef manta (*Mobula alfredi*, which is not ESA listed) during most visual surveys. There have also been three observations during the Pacific RAMP surveys of ESA-listed scalloped hammerhead sharks (*Sphyrna lewini)* at Howland, one each in 2006, 2008, and 2012.

Eight species of fishes recorded during surveys at Howland Island are listed as endangered, vulnerable, or near threatened by the International Union for Conservation of Nature (IUCN) Red List (IUCN 2017). Three of those were frequently encountered by survey divers.

Carcharhinus amblyrhynchos and *C. melanopterus* were regularly observed during both towed-diver and SPC surveys around Howland. Although somewhat less common, manta rays *(Mobula* spp., both species of which are IUCN listed) were also routinely observed during towed-diver and SPC surveys. For example, those were observed by SPC divers in vicinity of survey sites in around one quarter of all such surveys (i.e., recorded by divers as "present" even if not counted during surveys). The spotted eagle ray, *Aetobatus narinari*, was occasionally observed by survey divers (e.g., at 3% of SPC sites). Another IUCN listed species, the Chevron butterflyfish, *Chaetodon trifascialis*, which was seen during 6% of SPC surveys, is very closely associated with table *Acropora* corals and thus highly unlikely to be observed except where those corals are present. Small numbers of humphead wrasse (*Cheilinus undulatus*)—one or two individuals per year—have been recorded during surveys at Howland in a number of years, with the most recent record in 2012. Clearly, they have not been abundant at Howland throughout the survey period. As noted above, scalloped hammerhead sharks (*Sphyrna lewini)* have been seen at Howland in some years. Divers have also reported seeing the great hammerhead shark (*Sphyrna mokarran)* in the vicinity of survey sites at Howland on a number of occasions, although they have never been recorded during surveys. Finally, there is one recorded observation from 2001 of a Galapagos shark (*Carcharhinus galapagensis*) at Howland. As it can be difficult to distinguish between Galapagos and gray reef sharks, and because this observation was early in the program's history, it seems likely that this represents a misidentification of the much more common gray reef shark. A complete list of fish species observed each year is given in Appendix B of "Chapter 9: Pacific Remote Islands Marine National Monument in the Pacific-wide Context."

Marine Debris

7.7 Marine Debris

Marine debris was noted sporadically at Howland Island during the period from 2001 through 2012 (Figure 51). In total, debris was recorded 7 times during the benthic TDS. This does not encompass all debris found at Howland, given that debris observations were not always included in the surveys. It is also possible that the same debris was noted in different survey years.

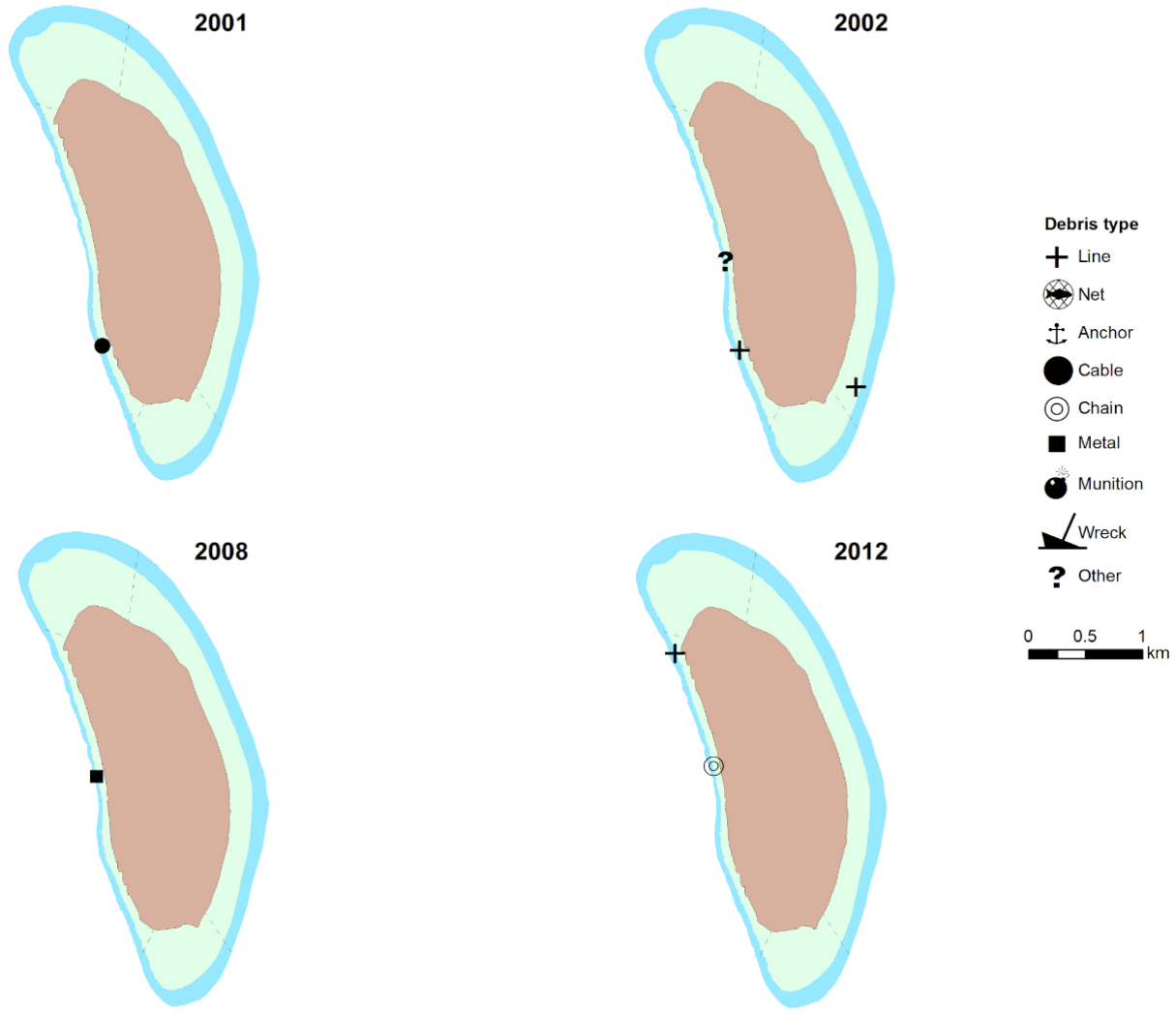

Figure 51. Marine debris sightings, including line, cable, metal, chain, and miscellaneous (other) debris observed around Howland Island from 2001 to 2012.

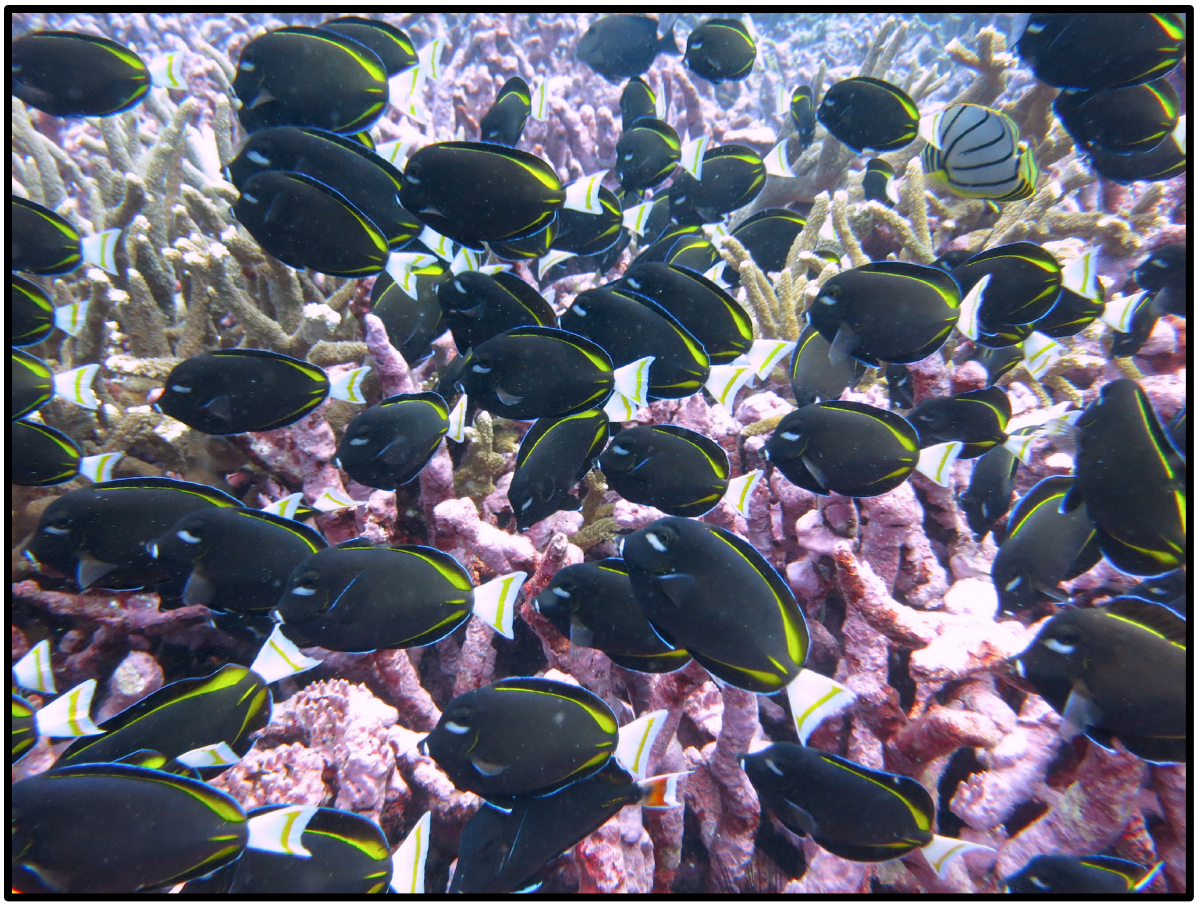

*Surgeonfish (*Acanthurus nigricans*) at Howland Island.*
Photo: Kelvin Gorospe, NOAA Fisheries.

Ecosystem Integration

7.8 Ecosystem Integration

*Photos left to right at Howland Island: Perspective view of Howland Island showing steep slopes on all sides; subsurface temperature recorder installed at coral reef, Photo: Noah Pomeroy; Amethyst anthias (*Pseudanthias pascalus*) school above the reef, Photo: Jeff Milisen; manta ray, Photo: Kevin Lino.*
All images courtesy NOAA Fisheries.

Oceanic Drivers of Benthic and Fish Populations

Located just north of the equator in the path of both the westward-flowing surface South Equatorial Current (SEC) and the eastward-flowing subsurface Equatorial Undercurrent (EUC), Howland Island is characterized by equatorial and topographic upwelling that varies in strength and intensity across years with ENSO cycles. During La Niña conditions, enhanced upwelling resulted in anomalously cool, nutrient-rich and biologically productive surface waters that were also lower in pH and aragonite saturation state. In contrast, the weakening of upwelling during El Niño events resulted in warmer temperatures and declines in chl-*a* concentrations as surface waters shifted toward lower productivity, though higher pH and saturation states are more favorable to calcification. Island-wide measures from 2002 to 2012 indicated hard coral cover had remained relatively high (~42–52%) and stable. Across survey years, forereef areas of Howland were also characterized by uniformly low macroalgal cover, low prevalence of coral diseases, microbial diversity and biomass similar to other remote islands, and exceptionally low abundances of corallivorous crown-of-thorns sea stars. The latter case was due perhaps to a lack of planktonic larval dispersal of the species to this remote and isolated island. Cover of macroalgae may have been maintained at low levels by an abundance of grazers, such as sea urchins and herbivorous fishes that were typically observed evenly distributed around the island. The ESA-listed hawksbill sea turtle (*Eretmochelys imbricata*) was sighted on only 1% of TDS, and opportunistic sightings have also revealed the presence of the ESA-listed scalloped hammerhead (*Sphyrna lewini*) at Howland.

Due to its location in the western portion of the central equatorial Pacific, oceanographic conditions characteristic of El Niño events tended to be milder in magnitude at Howland Island during events (including extreme ones) that took place in the Eastern Pacific. For instance, sea surface temperature anomalies and thermal stress at Howland were substantially less severe during the extreme 2015–2016 El Niño than at Jarvis Island located approximately 1,850 km (1,000 nm) to the east (Brainard et al. 2018). The composition of benthic cover before and after this particular bleaching event remained relatively stable, with patterns consistent through time in the size-class structure of live corals. The forereef of Howland, however, is not entirely immune to the thermal impacts of El Niño conditions, particularly during events in the Central Pacific region. Surveys revealed a 25% decrease in coral cover following a weak El Niño in 2006–2007 that unexpectedly resulted in a series of thermal anomalies in both surface and

subsurface temperatures at Howland. A moderate El Niño also occurred in 2009–2010, and surveys in 2012 indicated a subsequent two-fold increase in partial coral mortality, likely as a result of the coral bleaching (~30–40%) and consequent mortality that occurred during that event. Surveys of reef fishes over the period 2010–2015 suggested a possible increasing trend in biomass of piscivores and planktivores, whereas parrotfishes (a subgroup of herbivores) appeared to have declined in biomass between 2012 and 2015. Importantly, if and to what extent these patterns in fish abundance were related to El Niño events and subsequent levels of coral bleaching remains unclear.

Spatial Variation within the Island

Although the East and West georegions of Howland Island are both characterized by forereef areas with very steep slopes, the defining oceanographic conditions differ substantially between them. Prevailing trade wind-driven waves and the surface SEC both approach Howland from the east, whereas localized topographic upwelling occurs along the leeward west side of the island as the eastward-flowing subsurface EUC encounters the steep western slope, resulting in cool, nutrient-rich surface waters. Benthic cover of both coral and CCA were typically higher in the East georegion, but some of the greatest declines in coral cover were also evident in these forereef areas. Across depth strata, the overall density of hard corals decreased with increasing depth, with shallow- and mid-depth strata composed mostly of *Porites* spp., *Montipora* spp., and *Acropora* spp., whereas *Pavona* spp. and *Pocillopora* spp. dominated the deep-depth stratum.

Sightings of giant clams and sea cucumbers were slightly less dense in the East georegion, and all three instances of crown-of-thorns-sea star sightings occurred in the West georegion. The biomass of herbivorous fishes and sightings of ESA-listed green sea turtles (*Chelonia mydas*) were both greater in the West georegion, yet macroalgal cover remained uniformly low around the entire island. Sightings of manta rays (*Mobula* spp., potentially ESA-listed *M. birostris*) were also elevated in the West georegion, perhaps due to movement patterns and foraging activity related to high-current areas with intermittent periods of upwelling. Lastly, forereef areas in the North and South georegions experienced high currents as the prevailing westward-flowing SEC accelerated around these island corners, which coincided with areas greater in piscivore biomass. Sighting of sharks were especially prevalent in the South georegion.

7.9 References

Bak R, Meesters E (1998) Coral population structure:the hidden information of colony size-frequency distributions. Mar Ecol Prog Ser 162:301–306. doi: 10.3354/meps162301

Brainard RE, Oliver T, McPhaden MJ, Cohen A, Venegas R, Heenan A, Vargas-Ángel B, Rotjan R, Mangubhai S, Flint E, Hunter SA (2018) Ecological Impacts of the 2015/16 El Niño in the Central Equatorial Pacific. Bull Am Meteorol Soc 99:S21–S26. doi: 10.1175/BAMS-D-17-0128.1

Clark SJ, Oliver T Incident Wave Swath: A new approach to quantifying coastal wave exposure in regions with remotely generated waves.

Federal Register (2009) Establishment of the Pacific Remote Islands Marine National Monument. Fed. Regist. 74:1565–1575.

Federal Register (2017) Endangered and Threatened Wildlife; 90-Day Finding on a Petition To List 10 Species of Giant Clams as Threatened or Endangered Under the Endangered Species Act. In: Fed. Regist. https://www.federalregister.gov/documents/2017/06/26/2017-13275/endangered-and-threatened-wildlife-90-day-finding-on-a-petition-to-list-10-species-of-giant-clams-as.

Hein JR, McIntyre BR, Piper DZ (2005) Marine Mineral Resources of Pacific Islands—A Review of the Exclusive Economic Zones of Islands of U.S. Affiliation, Excluding the State of Hawaii. Reston

IUCN (2017) The IUCN Red List of Threatened Species. In: Version 2017-3. http://www.iucnredlist.org.

Jimenez W (2018) Spatial and temporal patterns of coral community structure at Baker and Howland Islands. University of Hawaii

Kamehameha Schools (2014) 1930's The New Kapalama Campus. In: Kamehameha Sch. Kapalama Museum Arch. http://blogs.ksbe.edu/archives/timelines/1930s-the-new-kapalama-campus/. Accessed 12 Apr 2018

Maragos J, Miller J, Gove J, De Martini E, Friedlander AM, Godwin S, Musburger C, Timmers M, Tsuda R, Vroom P, Flint E, Lundblad E, Weiss J, Ayotte P, Sala E, Sandin S, McTee S, Wass T, Siciliano D, Brainard R, Obura D, Ferguson S, Mundy B (2008) US Coral Reefs in the Line and Phoenix Islands, Central Pacific Ocean: History, Geology, Oceanography, and Biology. In: Coral Reefs of the USA. Springer Netherlands, Dordrecht, pp 595–641

McDole T, Nulton J, Barott KL, Felts B, Hand C, Hatay M, Lee H, Nadon MO, Nosrat B, Salamon P, Bailey B, Sandin S a., Vargas-Angel B, Youle M, Zgliczynski BJ, Brainard RE, Rohwer F (2012) Assessing Coral Reefs on a Pacific-Wide Scale Using the Microbialization Score. PLoS One 7:e43233. doi: 10.1371/journal.pone.0043233

National Oceanic and Atmospheric Administration (2005) U.S. Distributions of the 15 ESA-

listed Indo-Pacific Coral Species. In: Pacific Islands Reg. Off.

Pandolfi JM, Connolly SR, Marshall DJ, Cohen AL (2011) Projecting Coral Reef Futures Under Global Warming and Ocean Acidification. Science (80-) 333:418–422. doi: 10.1126/science.1204794

US Fish and Wildlife Service (2018) Howland Island. In: U.S. Fish Wildl. Serv. https://www.fws.gov/refuge/howland_island/. Accessed 12 Apr 2018

Vargas-Ángel B (2010) Crustose coralline algal diseases in the U.S.-Affiliated Pacific Islands. Coral Reefs 29:943–956. doi: 10.1007/s00338-010-0646-x

Vargas-Ángel B, Looney EE, Vetter OJ, Coccagna EF (2011) Severe, Widespread El Niño–Associated Coral Bleaching in the US Phoenix Islands. Bull Mar Sci 87:623–638. doi: 10.5343/bms.2010.1095

NOAA

NATIONAL OCEANIC AND ATMOSPHERIC ADMINISTRATION

U.S. DEPARTMENT OF COMMERCE

NOAA FISHERIES